POLITECNICO DI MILANO

Scuola di Ingegneria Civile ed Ambientale

Corso di Studi in Ingegneria per l'Ambiente e il Territorio

EFFECTS OF NUTRIENTS VARIABILITY ON GREEN MICROALGAE KINETICS IN A CONTINUOS FLOW PHOTOBIOREACTOR

Relatore: Prof.ssa Elena Ficara

Correlatori: Benedek G. Plósz e Dorottya S. Wágner

Tesi di laurea di:

Clarissa Cazzaniga

Matr. 837548

Anno accademico 2015/2016

Acknowledgements

I would like to thank to all the people who has been part of my university experience along the last 5 years.

Thanks to my supervisor at DTU Benedek Gy. Plósz for allowing me to work on this project and for encouraging me along these months.

Thanks to my co-supervisor at DTU Dorottya S. Wágner for having followed me step by step along the way.

Thanks to my supervisor at Politecnico di Milano Elena Ficara for having helped me in the final stages of this experience.

Thanks to my family for believing in me and for having supported me in every situation.

Thanks especially to my dad Gilberto for allowing me to pursue my aspirations and my desires.

Thanks to my friends: to the old ones and to the new ones, to whom I spent few days and to whom I spent years. I want you to know that each of you has been essential for me and I won't easily forget you.

Thanks to Andrea for the time we spent together studying (and we only know how much!), laughing, crying, rejoicing, despairing ...Without you, I do not think I would make it.

Thanks to Alessio for being with me the last two years and for never having abandoned the ship, despite all the difficulties.

So, thanks to everyone has crossed my path over the past 5 long and intense years.

Ringraziamenti

Vorrei ringraziare tutte le persone che mi hanno accompagnato nella mia esperienza universitaria negli ultimi 5 anni.
Grazie al mio relatore della DTU Benedek Gy. Plósz per avermi permesso di lavorare a questo progetto e per avermi sempre incoraggiato.
Grazie alla mia correlatrice della DTU Dorottya S. Wágner per avermi seguito passo dopo passo in questo percorso.
Grazie alla mia relatrice del Politecnico di Milano per avermi aiutato nell'atto finale di questa esperienza.
Grazie alla mia famiglia per aver creduto in me e per avermi supportato (e sopportato!) in ogni momento.
Grazie soprattutto a mio papà Gilberto per avermi permesso di inseguire le mie aspirazioni e i miei desideri.
Grazie ai mie amici: a quelli vecchi e a quelli nuovi, a quelli con cui ho passato pochi giorni e a quelli con cui ho passato anni. Voglio che sappiate che ognuno di voi è stato essenziale per me e che non vi dimenticherò facilmente.
Grazie ad Andrea per il tempo passato insieme studiando (e solo noi sappiamo quanto!), ridendo, piangendo, gioendo, disperando, ...senza di te, non credo ce l'avrei potuta fare.
Grazie ad Alessio per essere stato con me negli scorsi due anni e per non aver mai abbandonato la nave nonostante tutte le difficoltà.
Insomma grazie a chiunque abbia incrociato la mia strada negli ultimi 5 lunghi e intensi anni.

Summary

Recently, different studies have suggested the application of green microalgae for wastewater treatment, highlighting their ability to take up nitrogen and phosphorus producing valuable biomass. Among the others, Valverde-Pérez (2015) proposed an innovative full biochemical resource recovery process (TRENS), where the tertiary treatment is done through the cultivation of microalgae in photobioreactors.

This thesis aims to take forward Valverde-Pérez (2015) work, focusing on the understanding of the effects of the influent wastewater variation on the photobioreactors operation. In particular, the consequences caused by the variation of the influent N-to-P ratio are investigated studying green microalgae culture stability in terms of composition and contamination and the effects on the kinetics of the processes involved. With this aim, laboratory experiments were carried out and a model-based approach was used to analyze the experimental data.

From the results, green microalgae seem to be not greatly affected by the variation of the N-to-P ratio in the influent and no relevant effects of the culture history on the kinetics have been underlined. However, the overall removal of nitrogen results enhanced by 20%, which means that there may be a possibility to increase the efficiency of the treatment by subjecting green microalgae to cycles of nutrients limitation.

Finally, a new images analysis method to quantify the microbial community is also described.

Table of contents

List of Figures

List of Tables

Abbreviations

AD	Anaerobic Digester
ATP	Adenosine Triphosphate
CANR	Completely Autotrophic Nitrogen Removal
COD	Chemical Oxygen Demand
CFS	Continuous Flow reactor
EBPR	Enhanced Biological Phosphorus Removal
EBP2R	Enhanced Biological Phosphorus Removal and Recovery
H	Reactor Depth
HRT	Hydraulic Retention Time
IL	Inlet Light
LHSS	Latin Hypercube Sampling based Simplex
LP	Light Parameter
OD	Optical Density
PAO	Polyphosphate Accumulating Organisms
PBR	Photobioreactor
PHA	Polyhydroxialcanoates
RMSNE	Root Mean Square Normalized Error
SBR	Sequencing Batch Reactor
R1	Reactor 1 of Continuous Flow PBR Experiment (Reference)
R2	Reactor 2 of Continuous Flow PBR Experiment
sCOD	Soluble Chemical Oxygen Demand
SRT	Solid Retention Time
TP	Total Phosphorus
TN	Total Nitrogen
TSN	Total Soluble Nitrogen
TSS	Total Suspended Solid
WW	Wastewatater
WWTP	Wastewater Treatment Plant

Chapter 1

BACKGROUND AND MOTIVATIONS

1.1 Resource shortages and their increasing demand

The future of human population and Earth's capacity to support people are highly unpredictable, since they depend on both natural constraints and human choices (Cohen, 1995). Recent previsions suggest that, although the growth rate of the world population seems to be decreasing, the total number of living humans on Earth is expected to rise by 50% over the course of this century, reaching 11 billion of people (Ortiz-Ospina & Roser, 2016). Even if these predictions do not come true, improving standard of life, urbanization, industrialization and climate change could put a constrain on global growth. This means that we will have to find more and more resources as food, water, raw materials and energy in a world where they seem already scarce and where our environmental impact is at the threshold. The traditional "take, make, waste" of the linear economy approach to managing resources is no longer sustainable; subsequently, the interest in optimized uses of natural resources and in their recovery from waste streams is growing encouraging the shifting to a circular economy approach (Christensen & Hauggaard-Nielsen, 2015) (Figure 1-1).

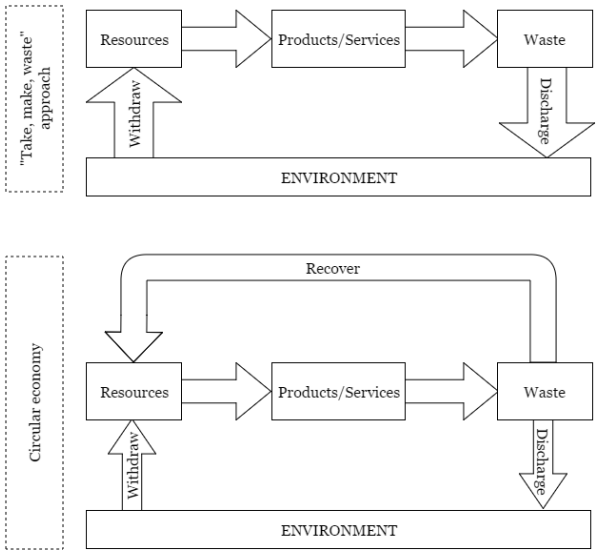

Figure 1-1 "Take, make, waste" approach flows vs Circular economy

Currently, one of the most concerning problem is the global water and food security vulnerability, which has brought in the last 35 years to a worldwide excessive withdraw of fresh water and an intense use of cropland and their rapid expansion (Brown, 1981).
While impressive results are being achieved regarding food production, the environment has been overexploited. In order to double the global agricultural food production, a massive withdraw of fresh water for irrigation was carried out together with an unsustainable resources consumption and a widespread dispersion of nutrients.

1961 2011

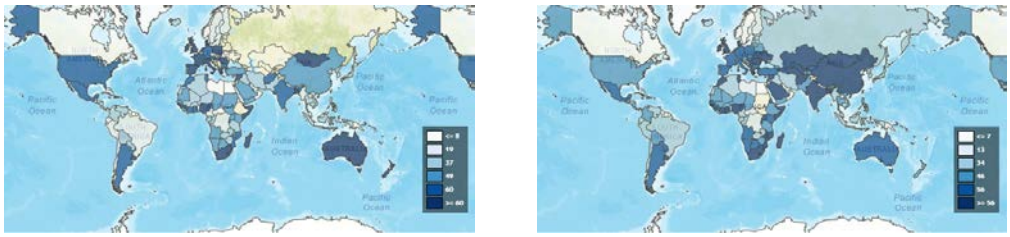

Figure 1-2 Distribution of % agricultural area of total land area in 1961 and 2011 (FAO, 2016)

For instance, Asia is one of the continents that has been more affected by this phenomenon. To face the extremely high request of food, from 1700 to 1980, the total area designed for agricultural land in South and Southeast Asia has increased respectively by 296% and 1275% and its management, in terms of maintenance of soil fertility by chemical fertilization and irrigation, has intensified. From 1962 to 2002, in this region, irrigated croplands have increased roughly by 115% and fertilizer use has increased by 1900% (Zhao, et al., 2006). This has resulted in critical consequences for the environment and, although the number of

malnourished people in the last 20 years decreased by 30%, about 563 million of people have to deal with the lack of food. To definitively defeat this problem, a more sustainable way has to be found.

1.2 A new solution: Resources recovery from waste streams – Circular Economy

One solution to the contemporary lack of resources and environment pollution seems to be the recovery of hidden resources in waste streams.

Over the years many countries have tried to apply this idea to the solid waste. In Europe every year, about 250 million of tons of municipal solid waste are produced and large part of these are products with a relatively short life and a high resources and energy demanding production (Ispra, 2014). Thus, different resource recovery system were developed. Recent studies of ISPRA about the fate of wasted packaging report that, in 2011, 63.3% were recycled and 13,7% were sent to incineration plants for energy recovery (Ispra, 2014). This has allowed to considerably reduce new resources withdraw from the environment and to limit the consumption of energy. Since good results are being achieved in the solid waste field, it is desirable to expand this policy to other fields, such as the wastewater field.

Indeed wastewater is a resource of renewable energy, nutrients, such as nitrogen and phosphorus, and fresh water. However, nowadays conventional wastewater treatment plants are focused on the destruction of organic and inorganic pollutants, instead of on the recovery of these precious resources. Moreover, most of the traditional wastewater treatment plants are great resource consumers (CSS, 2015). Means (2004) estimated the about 4% of the public energy use of a municipality in US is spent for WWTPs. Mo & Zhang (2012) reported that they also require such a large amount of materials over their lifetime, that the indirect energy embodied in those materials accounts for almost two thirds of the energy directly consumed in the WWTPs.

Therefore, research is pushing towards the development of new technologies, which should revolutionize the wastewater treatment.

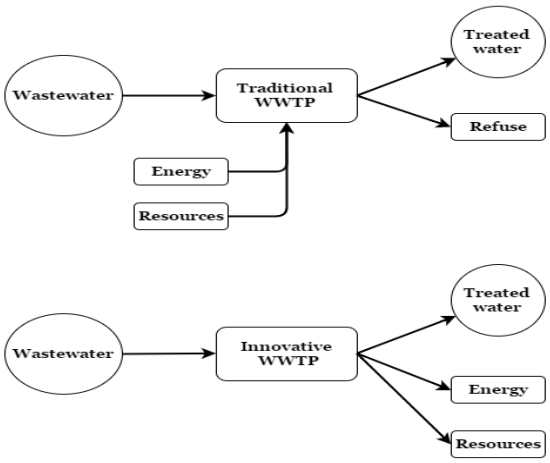

Figure 1-3 Main flows in a traditional WWTP and in an innovative WWTP

Recently new technologies for resources recovery have been studied and the proposed solutions head towards a redefinition of the conventional wastewater treatment plants. Nonetheless, if these solutions seem efficient and able to reclaim most of the resources from wastewater, most of them lead to such an high environmental impact, due to the intensive use of energy and chemicals, that sometimes it switches them into a counter-productive solution that on the whole are less sustainable than the traditional wastewater treatment plant. This may be the limiting factor for the diffusion and the full-scale application of this new approach. As alternative, Valverde-Pérez (2015) proposed an innovative full biochemical resource recovery process (TRENS) that consists of an enhanced biological phosphorous removal and recovery (EBP2R) combined with green microalgal cultivation in a photobioreactor (PBR) and an anaerobic digester(AD). Innovative, because it is one of the few that uses only biological treatment and that recovers efficiently water, energy and nutrients from wastewater. This means that it could be a competitive and feasible option to meet the needs above discussed.
This thesis reconsiders Valverde-Pérez's work and resumes it, investigating thoroughly the PBR operation starting from the reported uncertainties and problems. In the next chapter, TRENS system and the main related problems are described.

1.3 TRENS System

TRENS system is a completely biochemical resource recovery process, which was developed as alternative to the current resource recovery strategies characterized by an high environmental impact due to the high energy demand and chemicals consumption. TRENS allows to recover large part of the hidden resources in wastewater, converting them in high value products, such as methane for energy production and microalgae biomass combined with water for slow leaching fertilization. Therefore, through TRENS one of the most

problematic waste stream of the society can be converted into a solution to several current problems. Indeed, the outputs of TRENS can benefit society by providing a clean source of energy and by remediating the lack of nutrients and the scarcity of fresh water for crop irrigation.

In this chapter, the description of the structure and the processes involved in TRENS is reported, followed by the analysis of the obtained results and the observed problems.

1.3.1 Structure

TRENS consists of an enhanced biological phosphorus removal and recovery (EBP2R) and a photobioreactor (PBR) combined with an anaerobic digester and a completely autotrophic nitrogen removal system (CANR). In Figure 1-4 the structure of the system is represented, focusing on the outflows.

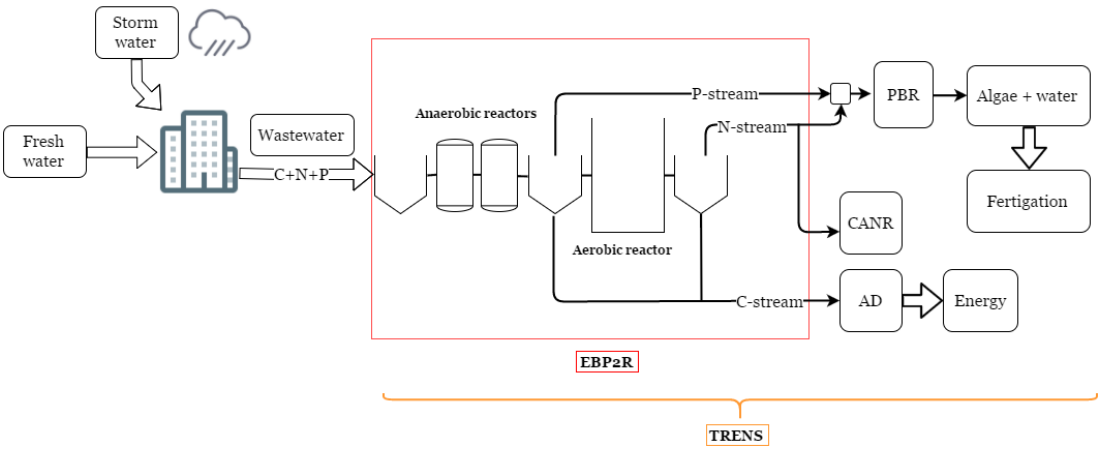

Figure 1-4 TRENS system structure

As shown in Figure 1-4, the collected wastewater rich in carbon, nitrogen and phosphorous enters in TRENS as input for the EBP2R system, which aim is to produce three different output streams using bacterial based technologies. The three streams, here called C-stream, N-stream and P-stream, are respectively rich in carbon, nitrogen and phosphorous. C-stream is directed to the anaerobic digester, where it is used as primary element for methane production. N-stream and P-stream are mixed properly to produce an optimum medium for algal cultivation. In case of relatively high content of nitrogen in the medium, CANR should help to remove the excess. While in case of low N-to-P ratio, the P-stream flow rate can be slightly decrease without affecting the operation of the system. In PBR, microalgae grow accumulating nutrients in their cells, thus the final output of TRENS results innocuous for the environment avoiding soil pollution and eutrophication of groundwater, when it is used for fertigation.

The next paragraphs describe the main technologies implemented in TRENS.

EBP2R

EBP2R idea arises from the need to adapt the traditional wastewater treatment to the stricter regulations on the emission of wastewater in the reservoirs and the increasing consumption with consequent release of water and nutrients, which are limited resources.

EBP2R is based on the traditional Enhanced Biological Phosphorous Removal System (EBPR) for phosphorous removal, which was developed in the late 50s as response to the increasing concern on eutrophication of aquatic environment due to the release of untreated wastewater. A complete description of the EBPR system may be found elsewhere, for instance in Metcalf&Eddy(2014). Nevertheless, differently from EBPR, as its own name suggests, EBP2R not only aims to remove the nutrients from the incoming wastewater, but it is also proposed to recover these nutrients in order to reuse them in other applications.

As mentioned in the previous paragraph, EBP2R has the objective to produce three different output streams, each one rich in a different nutrient (carbon, nitrogen or phosphorous) to guarantee constant inputs to the following technologies in TRENS.

Layouts and processes

Two different layouts for EBP2R were proposed and studied: a continuous flow system, referred as CFS, and a sequencing batch reactor. Anyhow, the objectives of this work are based on the issues related to the first layout, therefore only the CFS is considered and described in this paragraph.

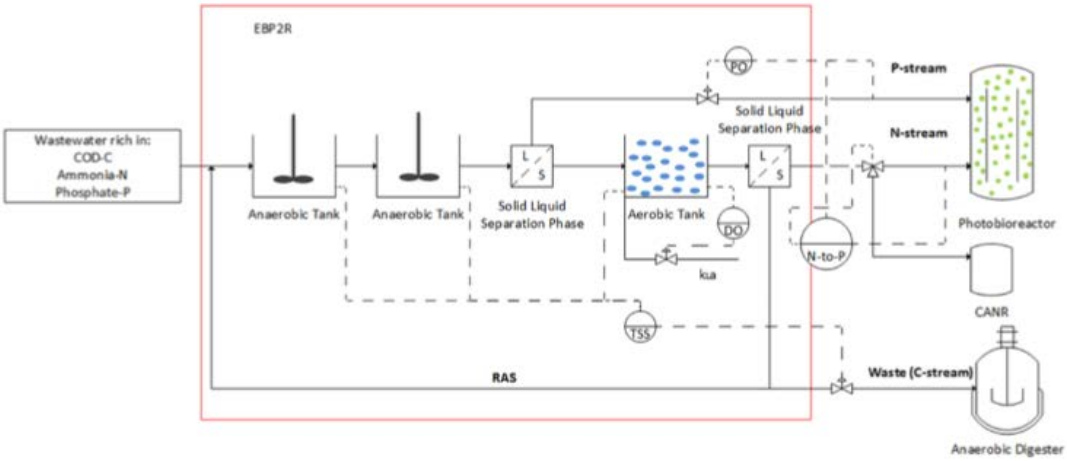

Figure 1-5 EBP2R in the Continuous Flow System layout (CFS) (Valverde Perez, 2015)

Although the CFS layout is similar to the traditional EBPR system, as shown in Figure 1-5, the following expedients need to be applied to the system to achieve the desired results:

- The EBP2R is operated at relatively short SRT (around 5 days) to achieve two different goals. First, at low SRT, carbon oxidation is minimized and thus the recovery of carbon can occur through the sludge. Indeed, carbon is concentrated in the sludge thanks to bioflocculation and microbial assimilation and storage of PHA and glycogen, depending on the type of bacteria. Second, at low SRT, nitrifying bacteria are washed out of the system, which implies lower energy demand for aeration and ammonia is left in the N-stream as main nitrogen component, which is also the green microalgae preferred nitrogen source over nitrate and nitrite (Cai, et al., 2013);
- The biomass is recycled from both aerobic and anaerobic reactors, thus promoting PAOs growth (Mino, et al., 1998);
- An additional solid-liquid separation unit, downstream to the anaerobic reactors, collects the P-stream. Indeed, the liquid outflow from the anaerobic reactors is rich in phosphorous released by PAOs during the anaerobic phase;
- The N-stream is collected by the traditional solid-liquid separation unit downstream to the aerobic reactor. In fact, the liquid outflow from the aerobic reactor is rich in ammonia and it is low in phosphorus. During the aerobic phase, PAOs uptake phosphorus and consequently P is recirculated with the sludge.

Further information and details could be found in Valverde-Pérez (2015).

Process control system

As previously reported, the primary objective of EBP2R is to produce an optimal medium for the downstream algae cultivation in the PBR, therefore N-stream and P-stream have to be mixed to maintain a certain N-to-P ratio in input to the PBR. Indeed, the algae culture is kept stable and the effluent inorganic nutrients content is minimized, only fulfilling the needs of the selected algal species. The secondary objective of the EPB2R system is to maximize the resource recovery with focus on the phosphorus, since it is produced from a non-renewable resource. To guarantee these goals, control actions have been defined:

1) In case the maximum phosphorus recovery leads to a relatively high N-to-P ratio, part of the nitrogen is removed via CANR;
2) In case the maximum phosphorus recovery leads to a relatively low N-to-P ratio, less phosphorus is recover reducing the P-stream flow rate (Q_P).

To manage the control actions, a process control system was needed. Therefore, as described in Valverde Pérez et al. (2016), it was design, tested and evaluated using the plant-wide

procedure by Larsson & Skogestad (2000). This procedure consists in six step summarized in Figure 1-6 and briefly described in the next paragraphs for the CFS case.

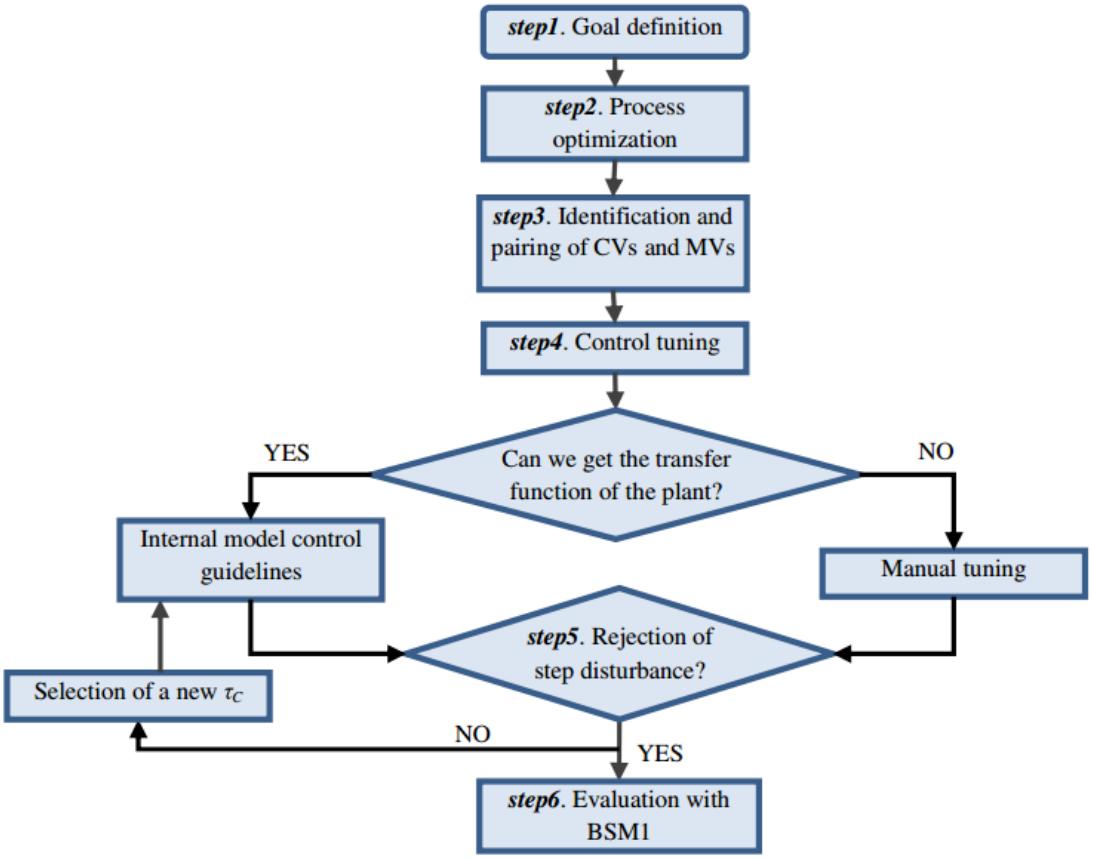

Figure 1-6 Control structure design methodology (Valverde Pérez, et al., 2016)

Step 1: Goal definition

The goal set for the system is to reach the highest phosphorus recovery at the optimal N-to-P ratio for the downstream algal cultivation.

Step 2: Process optimization

The process optimization in this study was done trying to find the pair of values for SRT and P-stream flow rate (Q_P), which allows to reach the goal. The chosen values are SRT=4,5 day and Q_P=30% of the influent flow rate, that lead to recover 65% of the influent phosphorus.

Step 3: Identification and paring of CVs and MVs

The controlled variables (CVs) are DO level, phosphorus load conveyed to the PBR, SRT and N-to-P ratio, while the manipulated variable (MVs) are three different flow rates, represented

in Figure 1-5 as valves: P-stream flow rate ($Q_{P)}$, wastage flow rate (Q_W) and N-stream flow rate ($Q_{N)}$. From the pairing of these variables it results that the SRT is controlled by $Q_{W,}$ the phosphorus load conveyed to the PBR is controlled by Q_P and the N-to-P ratio is controlled by the $Q_{N.}$ Indeed, regarding the DO level in the aerobic tank, air supply is used to keep the oxygen level at 1,5 mg/l.

Step 4: Controller tuning

Controller tuning refers to the selection of tuning parameters to ensure the best response of the controller. In this case, the controllers were modeled as Proportional Integral (PI) controllers and they were either tuned following the internal model control (IMC) rules or manual tuned, when the transfer function cannot be obtained (Sebog, et al., 2004; Skogestad, 2003).

Step 5: Rejection of step disturbances?

The system was subjected to step disturbances in the influent quality to assess the ability of the control system to keep the system stable. In case of failure, the procedure re-started from Step 4. During this phase, only one factor at time was changed and the step was introduced in steady state conditions on day 50 of 100 days of simulation. In Table 1-1 the average values of the factors with the relative step change magnitude are reported.

Table 1-1 Average values and step change magnitude for each factor of the influent

Factor	Average value	Step change magnitude (Metcalf&Eddy, et al., 2014)
TCOD	712 mgCOD/l	±20%
TN	54 mgN/l	±30%
TP	9 mgP/l	±20%

Subjected to these disturbance, the system performed well in terms of phosphorus recovery and N-to-P ratio fed to the PBR.

Step 6: Evaluation with BSM1

The system was simulated under dynamic conditions with variations in the influent TCOD, TN, TP and flow rate as represented in Figure 1-7. In Figure 1-8 the results are showed.

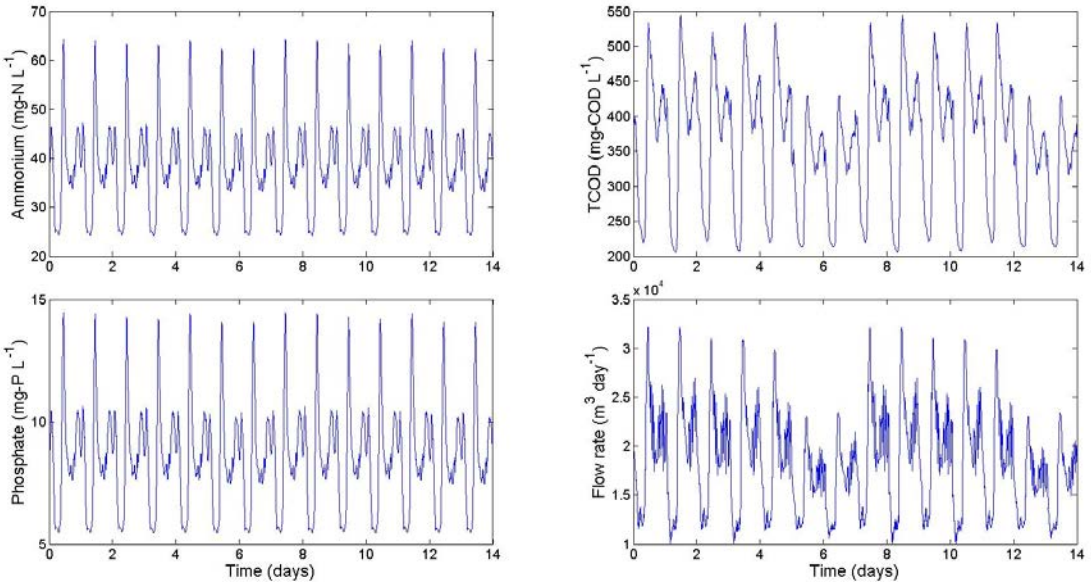

Figure 1-7 Influent to the EBP2R (Valverde Pérez, et al., 2016)

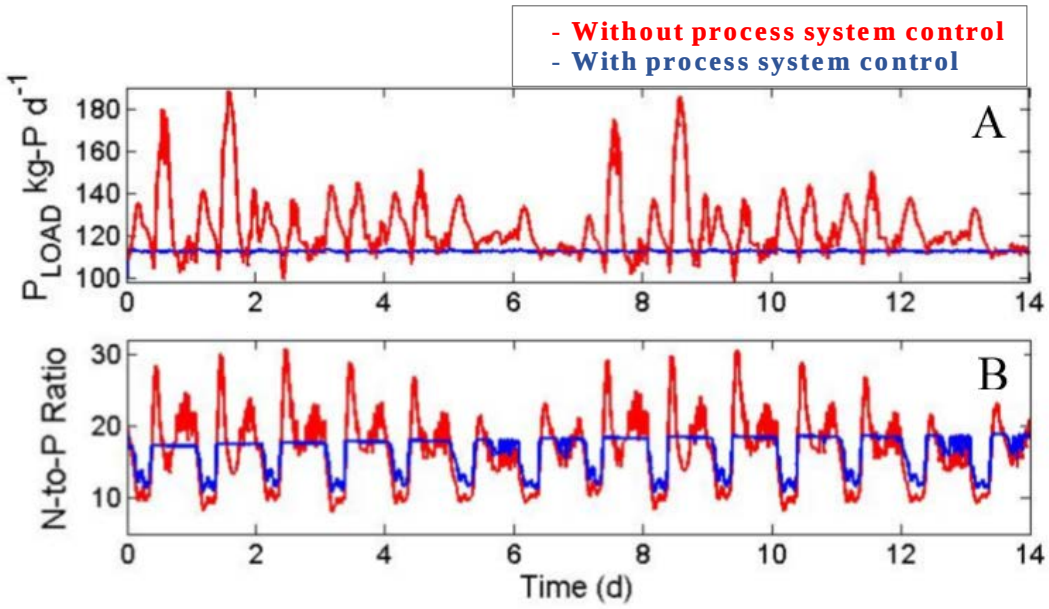

Figure 1-8 Phosphorus load and N-to-P ratio in input to the PBR under dynamic condition in the CFS case (Valverde-Pérez, 2015).

The results show that if the control system is mainly able to smooth variation of P-load, it is not able to keep the N-to-P ratio at a setpoint level (17 molN/molP). Although the peaks of N-to-P ratio, shown by the open loop system, are toned down, the N-to-P ratio regularly falls under the optimum value.

PBR

The optimal cultivation medium produced in the previous step is sent to the PBR, where the selected microalgae culture is spurred to grow using the incoming nutrients together with light and CO2 that have to be supplied to the system. Carbon dioxide may be delivered through a gaseous flow rich in CO2 originated from the biogas combustion in the cogeneration units, that potentially could follow the anaerobic digester (Napan, et al., 2015). At the same time, this flow can also guarantee a proper mixing in the reactor.

In these optimal conditions, the growth medium is optimized and nutrients are encapsulated inside algae biomass, thus the effluent from PBR is composed by algal biomass suspended in the treated water with a low inorganic nutrients load. To avoid harvesting costs, which are one of the main problem related to the latest microalgae based technologies (Liu & Vyverman, 2015), the effluent can be directly applied to the land for crops fertigation (Wilkie & Mulbry, 2002). Indeed, microalgae had shown good properties as natural fertilizer (Mulbry, et al., 2005) and the risk of soil pollution and ground water eutrophication is minimized thanks to the low concentration of pollutants in the treated water. Through drip irrigation, the effluent can reach directly the roots area in the cropland. When the algae biomass in suspension in the effluent reaches the ground, it settles and, according to Mulbry et al. (2005), it starts to release nutrients in an available form for crops uptake. The water instead accumulates in the soil until the field capacity is reached. Afterwards, it starts to leach towards the groundwater. If it reaches the aquifer, it does not represent a problem, because, as it was explained previously, the concentration of pollutants in the water is minimal, thus the risk of contamination of the ground water is minimized. This is a great advantage over using raw wastewater or treated wastewater from a traditional wastewater treatment plant as irrigation water (Figure 1-9). Indeed, they can potentially compromise the groundwater quality and therefore its withdraw for other purposes.

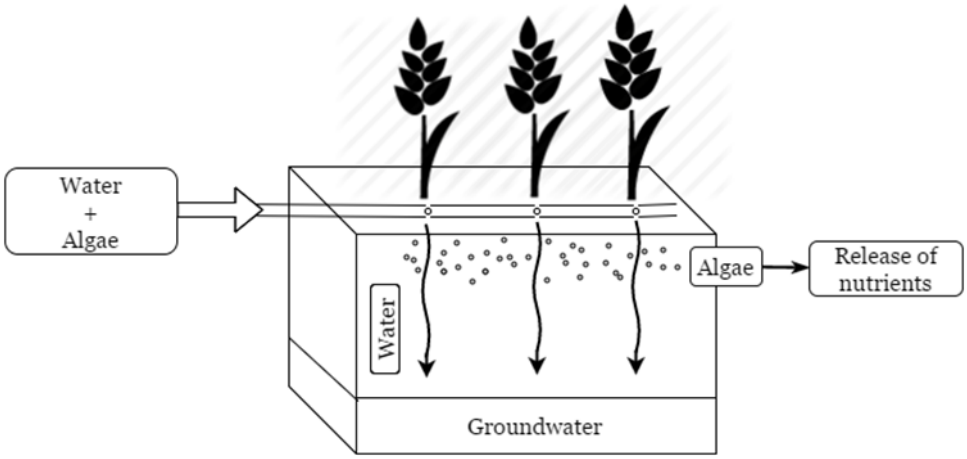

Figure 1-9 TRENS effluent application in fertigation

Anaerobic digester

As previously specified, the third stream produced by EBP2R is rich in carbon and thus organic matter, which is the main component required in input at the anaerobic digester for methane production. The anaerobic digestion of waste activated sludge is a technology relatively well established, which has been studied and developed to give a solution to the costly disposal of this waste. Indeed, not only it has the abilities to destroy most of the pathogens present in the sludge and to limit the odor problems related to the residual putrescible matter, but it also transforms the residual organic matter into biogas with an average content of methane about 55%vol-75%vol (De Mes, et al., 2003). This means that from the C- stream a further recovery of resources is possible through the production of energy from biogas (Apples et al., 2008). More information about anaerobic digestion may be found elsewhere (Apples, et al., 2008) (Carballa, et al., 2015).

CANR

In case of relatively high content of nitrogen in the wastewater, which could lead to an N-to-P ratio higher than the set one, to meet the request of the PBR the process control system send part of the N-stream to the CANR. CANR is a new biological nitrogen removal process based on a partial nitrification and anoxic oxidation of ammonia. Therefore, it almost completely converts the ammonia presents in the N-stream into dinitrogen gas. The process works properly with the N-stream from EBP2R, since it can treat wastewater that contains low amounts of organic material. However, this process has not been fully tested yet and it is still in the experimental phase. More information about CANR may be found elsewhere (Khin & Annachhatre, 2004; Mutlu, et al., 2013).

1.3.2 Results: achievements and limitations

Valverde-Pérez (2015) has demonstrated the efficiency of EBP2R in separation and recovery of phosphorus and nitrogen from municipal wastewater via model-based studies. The continuous EBP2R allows to recover 65% maximum of the influent phosphorus through P-stream. Nevertheless, phosphorus recovery was found to be limited by EBP2R SRT and nitrate presence in the anaerobic reactors. Indeed, anoxic enviroments can appear promoting denitrification over phosphorus release. Moreover, in the continuous EBP2R, PAOs growth can be limited by phosphorus availability in the aerobic reactor.

The control system has been tested using dynamic input disturbance scenarios and it results to be able to keep constant the P load in input to the PBR, but it fails to limit the variation of the N-to-P ratio when the influent nitrogen to the EBP2R becomes limiting. Even if the variations from the optimal N-to-P ratio are not severe, some aspects need to be studied. For

instance, the effects on the PBR effluent quality and the green microalgae culture stability. Indeed, according to Beuckles, et al. (2015), N-to-P ratio seems to drive competition between algal species in algae consortia. Moreover, it could weaken the culture facilitating contaminations.

Another aspect underlined by Valverde-Pérez (2015) is the culture history effect on maximum nitrate uptake rate. Indeed, during laboratory experiment, where the design allowed to distinguish between the impact of culture history and the impact of substrate availability, the maximum nitrate uptake results higher after a period of supplied nitrogen limitation, which could occur when the supply N-to-P ratio to the PBR drops from circa 17molN/molP to circa 10molN/molP.

TRENS system's strengths and weaknesses have been studied by a life cycle assessment (Fang, et al., 2015). Environmental benefits of nutrients recycling through fertigation were highlighted, even if they may be compromised by the discharge of heavy metal on land. Micropollutants are also an important aspect, since the low SRT in the EBP2R doesn't facilitate their removal (Polesel, et al., 2015) and legislations are moving towards the recognition of those substances as harmful to the environment (Plosz & Polesel, 2015).

1.4 Thesis objectives

The aim of this thesis is to investigate the consequences in the PBR of the variation of the N-to-P ratio in the supplied influent.

In particular, this thesis is focused on:

1. The assessment of the green microalgae culture stability in terms of composition and contamination;
2. The evaluation of the influence of the green microalgae culture history on the uptake and storage of nitrogen and phosphorus, studying the kinetics of the processes involved in the PBR;
3. The development of a new images analysis method to quantify the microbial community.

Chapter 2
STATE OF ART

The term *algae* was first introduced by Linnaeus in 1753 to refer to a group of plants, which are known since ancient civilization. It refers to a wide group of unicellular and multicellular organisms present worldwide in different habitats, that can grow photoautotrophically, heterotrophically and even mixotrophically (Van Wagenen, et al., 2015), depending on the different environmental conditions.

Phototrophic microalgae are unicellular microorganisms capable of efficiently converting CO2, sunlight and some basic nutrients into high valuable and energy-rich products. They cover indispensable roles: not only they are the base for aquatic food chain, but they are responsible for the production of more than 75% of oxygen consumed by animals and humans (Posten & Walter, 2012). Although this may seem implausible, given the small size of the microalgae, it became possible due to microalgae abundance and diversification. Indeed, thanks to the singular evolution, that has affected microalgae history, their biodiversity became remarkable and innumerable species of microalgae were found all over the world. Even if the number of known species is already vast, around 35.000, it was estimated that undiscovered species may exceed known species by a factor of four to eight (Norton, et al., 1996). Since microalgae evolutionary history is uncertain and their characteristics are various, a consistent classification for microalgae, as well as a deep understanding of their biology, is still in progress and it needs improvement.

In the great biodiversity of this group, main groups of microalgae were established, for instance the so-called green microalgae, which is the group of particular relevance for this work. This group was studied and investigated due to their potential applications in several fields and guidelines for their cultivation have been identified.

In the first part of the chapter, the processes involved in green microalgae cultivation are described and analyzed with focus on the main influent factors on green microalgae growth and nutrients uptake and storage. A deepening on green microalgae cultivation in wastewater and the relative issues is also reported. Finally, a literature review about the studies conducted to understand the effects of nutrients variation in the medium on microalgae growth is reported.
In the second part of the chapter, a brief literature review on the modeling applied to microalgae is presented, followed by the description of the ASM-A model and its relative parameters estimation procedure, which were used in this work.

2.1 Green microalgae cultivation

As previously mentioned, algae are present worldwide and they have adapted to live in several environments under different conditions. Nevertheless, some factors are required to ensure an optimal growth. For green microalgae, the most relevant factors are light and nutrients, which are carbon, nitrogen and phosphorus. According to the Liebig's law of the minimum, the deficiency of one of those elements could deeply compromise algal growth. As reported in Spaargaren (1996), each essential element has to be present in adequate quantity, in appropriate ratio and in the bioavailable chemical form in the cultivation medium, so that microalgae growth will not be limited.
It is important to underline that the chemical form of nutrients in the cultivation medium, in particular of carbon, and the need of light vary depending on the type of growth used by green microalgae. Indeed, as mentioned before, algae are able to grow in three different ways: photoautotrophically, heterotrophically and mixotrophically.
Photoautotrophic green microalgae metabolism is driven by photosynthesis. Through photosynthesis, green microalgae are able to use light as energy source to assimilate water, inorganic carbon and nutrients and to produce new biomass compounds and oxygen (Figure 2-1).

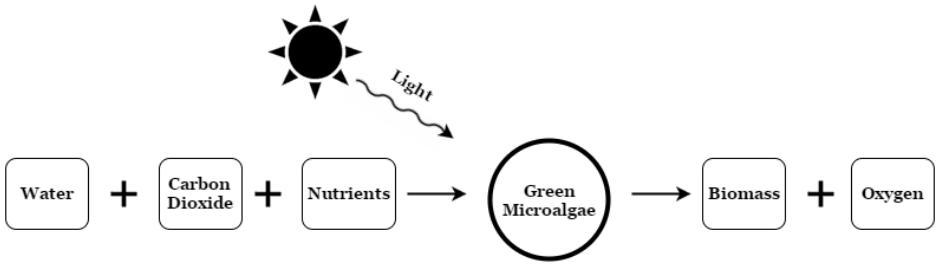

Figure 2-1 Green microalgae photosynthesis

Heterotrophic green microalgae, instead, are able to grow in complete darkness, if oxygen and an organic carbon source are supplied.
Mixotrophic green microalgae represent a particular case, since in presence of light and organic carbon, they are able to simultaneously photosynthesize while assimilating and metabolizing organic carbon. (Van Wagenen, et al., 2015; Smith, et al., 2015).

Table 2-1 Type of carbon source and light presence for each type of growth

Type of growth	Type of carbon source	Presence of light
Photoautotrophic	Inorganic	yes
Heterotrophic	Organic	no
Mixotrophic	Inorganic + Organic	yes

Light

Light is the energy source used by green microalgae during the photosynthesis. Therefore, light is one of the most important factors in green microalgal cultivation and it must be considered during the optimization of the PBR performance (Grognard, et al., 2014). In particular, to maximize algal productivity, attention must be payed to the light attenuation along the PBR due to self-shading.
Even if the impact of light depends on the specie of the cultivated green microalgae, some general aspects are recognizable. Generally, light type and intensity greatly affect both algal growth and biomass composition. Indeed algal growth rate has the tendency to increase with light intensity until a maximum is reached. This maximum coincides with the intensity where green microalgae cannot utilize more photons for photosynthesis and all the extra energy is converted to heat. Instead, if the light intensity is too high algal growth rate may decrease due to light inhibition (Sorokin & Krauss, 1958). Regarding algal composition, different effects were found. For instance, Seyfabadi, et al. (2011) reported that at high light intensity green microalgae have the tendency to produce more pigments for light protection. Instead, at low light intensity, Van Wagenen, et al.(2012) has shown that the relative abundance of unsaturated fatty acids increases.

Carbon

Up to 65% of dry weight of green microalgae is made of carbon, indeed, it contributes to all organic compounds in the cells (Markou, et al., 2014).
Green microalgae are able to assimilate both inorganic and organic carbon, depending on the type of growth they have developed to live in a particular environment.

When they grow *phototrophically*, carbon is taken up in inorganic form ($CO_{2)}$. since the majority of microalgae live in aquatic environment, CO_2 has to be dissolved in water to be taken up. When CO_2 dissolves in water, it reacts with H_2O and the equilibrium described by Equation 2-1 occurs.

$$CO_{2(aq)} + H_2O \overset{pK1\approx3,6}{\longleftrightarrow} H_2CO_3 \overset{pK2\approx6,3}{\longleftrightarrow} HCO_3^- + H^+ \overset{pK3\approx10,3}{\longleftrightarrow} CO_3^{2-} + 2H^+$$

Equation 2-1 Carbon dioxide equilibrium in water (Markou, et al., 2014)

Depending on pH, salinity, pressure and temperature of the solution, different dissolved inorganic carbon species are available for the algal uptake. Those species are carbon dioxide, bicarbonate and carbonate. Thus, since the form and the quantity of the different dissolved inorganic carbon depend on several factors, green microalgae have developed different affinities. According to Decostere et al. (2013) green microalgae have higher affinity for carbon dioxide then for bicarbonate, while according to Yeh et al. (2010) they have the lowest affinity for carbonate.

$$CO_{2(aq)} > HCO_3^- > CO_3^{2-}$$

Equation 2-2 General green microalgae affinity for inorganic carbon sources

CO2 can be provided in different forms, e.g. by pumping air, concentrated CO2, a mixture of the previous ones or by dosing bicarbonate salts. In general, bubbling gaseous flow rich in CO2 is preferred. Especially since numerous studies have reported the possibility to reuse CO2 rich gas flow from other processes as: anaerobic digestion (Travieso, et al., 1993),
alcoholic fermentation (Bezzera, et al., 2013) or pre-treated flue gases (Kadam, 1997). Moreover, in this case the dissolution of CO2 in water the pH decreases, but the contemporary consumption of carbon dioxide by algal biomass increases it keeping pH at neutral values (Azov, 1982). Instead, when bicarbonate salts are used, the pH tends to reach high values, therefore it can be used only with green microalgae species, which tolerate high pH (Chi, et al., 2011).

When green microalgae grow *heterotrophically*, they use organic carbon as energy and carbon source. The most used organic carbon sources are monosaccharides (glucose, fructose etc.), volatile fatty acids (acetic acid), glycerol and urea (Markou, et al., 2014). According to Mühling et al. (2015) the utilization of organic molecules depends on algae species and strains. This characteristic is interesting when green microalgae are used to treat media already rich in organic carbon molecules.

When green microalgae grow *mixotrophically*, they consume inorganic and organic carbon sources (Van Wagenen, et al., 2015). Therefore, what has been reported for photoautotrophic and heterotrophic growth is applicable to this case.

Nitrogen

From 1% to 14% of dry weight of green microalgae is made of nitrogen. Indeed, it is used to build many essential compounds, such as nucleic acids, amino acids and pigments (Markou, et al., 2014).
Green microalgae can use both inorganic and organic nitrogen form. The most commonly reported forms are, in affinity order: ammonia, nitrate, nitrite and urea (Valverde-Pérez, et al., 2015).

Ammonia/ammonium is the preferred nitrogen source, because its uptake and assimilation is less energy demanding than the other forms of nitrogen. (Pérez-Garcia, et al., 2011) Moreover, it can be directly converted to biomolecules (Cai, et al., 2013). Nevertheless, free ammonia has detrimental effects on green microalgae at relative low concentration (Azov & Goldman, 1982). Therefore, pH and temperature have to be controlled to unbalance the equilibrium between ammonia and ammonium (Equation 2-3) towards ammonium, which in general has significant less toxicity (Källqvist & Svenson, 2003).

$$NH_4^+ + OH^- \overset{pK \approx 9{,}25}{\longleftrightarrow} NH_3 + H_2O$$

Equation 2-3 Ammonia/ammonium equilibrium in water (Markou, et al., 2014)

During ammonia uptake protons are released into the medium, therefore pH tends to decrease (Podevin, et al., 2015).

Nitrate uptake is more energy demanding than ammonium uptake, because it is taken up by active mechanisms and, once in the cell, it has to be converted to ammonia by nitrate reductase (Graham & Wilcox, 2000). Nevertheless, it does not show toxic effects to cells up to very high concentration (Jeanfils, et al., 1993) and it does not compromise microalgae growth. Indeed, according to Boussiba (1989) and Park et al. (2010) the growth rate using nitrate as nitrogen source is similar as when ammonia/ammonium is used.
During nitrate uptake, pH tends to increase (Podevin, et al., 2015).

Nitrite is taken up through both activate transportation and diffusion (Flores, et al., 1987; Fuggi, 1993) and it is also produced as intermediate during the reduction of nitrate to ammonia. Since nitrate uptake is a constant process and nitrite reduction into ammonia takes

place only when light is available, under light limitation, nitrite can accumulate in the cells (Brussaard, et al., 1998) and thus, it may be released in the medium due to its toxic effect at high concentration (Malerba, et al., 2012). Moreover, if nitrate concentration is too high, nitrite can accumulate in the cells even in non-light limitation condition, inhibiting microalgae growth (Jeanfils, et al., 1993).

Urea and some amino acids are taken up actively and are metabolized in the cells (Pérez-Garcia, et al., 2011; Flores & Herrero, 2005). Some green microalgae seem not only to be able to use organic nitrogen, but, when they use these molecules, their growth rate are similar or higher than when they use other inorganic forms of nitrogen. However, the possibility to use organic nitrogen compounds as nitrogen resource is species dependent (Flores & Herrero, 2005).

It has to be noted that, when different nitrogen sources are simultaneously present in the medium, green microalgae firstly uptake the more affine depleting it, then they uptake the others (Boussiba & Gibson, 1991).

Phosphorus

From 0,05% to 3,3% of dry weight of green microalgae is made of phosphorus. Indeed, it is used to build several essential compounds, such nucleic acids, membrane phospholipids and ATP (Markou, et al., 2014).

Phosphorus is taken up actively by green microalgae when it is in orthophosphate form. Organic forms of phosphorus can also be used once they are mineralized extracellularly by phosphatase enzymes (Dyhrman & Ruttenberg, 2006).

Nutrients limitation

In natural environments algae may be exposed to nutrients limitation, therefore they had developed different strategies to manage these non-optimal conditions enabling adaptation across a wide range of environments (Loladze & Elser, 2011)
They can either encapsulate excess quantities of nutrients in period of nutrients abundance (Eixler, et al., 2006) or grow with lower quantity of nutrients, changing their internal composition.
In fact, green microalgae had shown the so-called *luxury uptake* of nutrients, which is the capacity to accumulate intracellular phosphorus and nitrogen reserves (Powell, et al., 2009; Pueschel & Korb, 2001). This storage can be used by algae under starving conditions. Until it

is depleted, algal activity it is not affected by the environmental conditions as well as growth rate and the algal biomass composition (Beuckles, et al., 2015; Ruitz-Martinez, et al., 2014). When the internal reserves of nutrients are not available, green microalgae adapt their biomass in response. Indeed, the algal biomass is generally mainly made of biochemical compounds rich in N and P, but, when N and P became limited, algae are able to change their internal composition (Beuckels et al, 2015; Choi & Lee, 2015), increasing the internal percentage of carbon-rich compounds, as carbohydrates and lipids.

N-to-P ratio

In 1934 Alfred Redfield first proposed the theory that marine phytoplankton, i.e. unicellular microalgae and cyanobacteria, has relatively constrained elemental ratios. It means that there is a relationship between organisms' growth and internal composition and the ratio of the elements in the surrounding environment. In particular, nitrogen and phosphorus have been recognized to be highly influential factors. Therefore, their singular and relative availability in the growth medium is crucial. In 1958 Redfield concluded that the optimal ratio for marine phytoplankton for those nutrients was 16 molN/molP, which coincides with the average N-to-P ratio found in the studied organisms. However, as mentioned before, the internal algal N-to-P ratio may vary in relation to the surrounding conditions. Several studies have been carried out to investigate the effective N-to-P ratio in microalgae composition, its variability and the critical medium N-to-P ratio, that determines changing in microalgae behavior.

Variability of internal N-to-P ratio and critical medium N-to-P ratio (Geider & La Roche, 2002)

In 2002, Geider and La Roche had tried to determine the range of the variability of the N-to-P ratio for different species of algae and cyanobacteria using a compilation of data on the elemental composition of marine phytoplankton. The traditional Redfield's N-to-P ratio is used as criterion to distinguish N-limitation from P-limitation assuming that a N-to-P ratio lower than 16 molN/molP corresponds to a nitrogen limitation and a N-to-P ratio higher than 16 molN/molP corresponds to a phosphorus limitation. Instead, in their study, it is shown that the internal N-to-P ratio can vary within different ranges in relation to the condition where organisms are growing. In nutrient-limited cells the N-to-P ratio is very plastic and can vary from < 5 molN/molP, when nitrogen is greatly limited, to >100 molN/molP, when nitrogen is present in large excess. The cellular N-to-P ratio is more constrained when the concentration of inorganic nutrients in solution is several-fold greater than the half saturation constants for nutrients assimilation (from 0,001 to 15 gN/m3 for NH_4^+ and NO_3^-; from 0,001 to 5 gP/m3 for PO_4^{3-}). In fact, it ranges from 5molN/molP to 19 molN/molP.

Table 2-2 Ranges of internal N-to-P ratio in nutrients limited condition and optimal nutrient condition proposed by Geider & La Roche (2002)

	Internal N-to-P ratio	
	Lower boundary	Upper boundary
	[molN/molP]	[molN/molP]
Nutrients limited condition	<5	>100
Optimal nutrients condition	5	19

The critical N-to-P ratio, that marks the transition between N-limitation and P-limitation, was found to lie in a range between 15 molN/molP and 30 molN/molP.

2.2 Microalgae cultivation in wastewater

Over 50 years ago in the U.S., Oswald & Gotaas (1957) had proposed the biological treatment of wastewater with algae to remove nutrients such as nitrogen and phosphorus. This idea has since been intensively tested all over the world, together with the study of the potential utilizations the algal biomass (Abdel-Raouf, et al., 2012).

The application of microalgae in the wastewater treatment has several advantages, i.e. the removal of coliform bacteria (Moawad, 1968; Sebastian & Nair, 1984), the reduction of both chemical and biochemical oxygen demand (Colak & Kaya, 1988), the removal of nitrogen and phosphorus (Talbot & De la Noue, 1993) and also the removal of heavy metals (Rai, et al., 1981). This may help to avoid secondary pollution in reservoirs due to the residual nutrients, which can lead to eutrophication, uncontrolled spread of certain aquatic macrophytes, oxygen depletion, loss of key species and degradation of fresh water ecosystems (Wang, et al., 2010; Doria, et al., 2012). Moreover, through photosynthesis microalgae convert solar energy into useful and valuable biomass requiring less land than a traditional crop (Liu & Vyverman, 2015).

Microalgae perform well, in terms of nutrients removal and biomass production, treating different wastewater: municipal wastewater (Li, et al., 2011; Shelef, et al., 1980; Chi, et al., 2011), livestock wastes (Lincon & Hill, 1980), agro-industrial wastes (Mulbry, et al., 2009; Mulbry, et al., 2008) and industrial wastes (Markou & Georgakakis, 2011).

Microalgae have been proposed to be applicable in the secondary (Tam & Wong, 1989), tertiary (Lavoie & De la Noue, 1985; Martin, et al., 1985a; Evonne & Tang, 1997) and higher treatments (Oswald, 1988b). In general, their application in tertiary treatment and higher treatment seems to be less cost and energy demanding than other technologies (Abdel-Raouf, et al., 2012).

Hence, microalgae cultivation seems to be a good alternative as a biological treatment method for wastewater (Cai , et al., 2013).

2.2.1 Nutrients variation in wastewater

Wastewater has been shown to be a suitable medium for algal growth, because it can provide most of the necessary nutrients (Renuka, et al., 2013).
As mentioned before, algae can grow in wastewater from different origins. Nevertheless, its composition vary with sources and many other variables (Cai , et al., 2013).
For instance, municipal wastewater is mostly composed by discharged water from residential areas, commercial and institutional facilities and industries and potentially stormwater. Therefore, its quantity and quality undergo substantial variations in time (in short term and in long term) and in space (Henze & Comeau, 2008).
This variability can represent an obstacle to the application of microalgae in wastewater treatment. Indeed, nutrient components greatly affect the microalgae growth rate, the uptake and storage of nutrients and the biomass composition. In particular, the key elements for microalgae cultivation are nitrogen and phosphorus. As reported Table 2-3, the ranges of variation of these components have been found to be very wide (Henze & Comeau, 2008; Cai, et al., 2013; Muttamara, 1996; Carey & Migliaccio, 2009) and consequently the N-to-P ratio. Indeed, it can vary from 1,33 molN/molP to 55 molN/molP.

Table 2-3 Range of variation of TN and TP in municipal wastewater

	Range
TN [mgN/l]	15-100
TP [mgP/l]	4-25

Since according to Geider & La Roche (2002), the critical N-to-P ratio in the growth medium can vary between 15 molN/molP and 30 molN/molP in order to guarantee an optimal algal cultivation, the variability of the raw municipal wastewater here reported is too large and it may compromise the process.

Effects of medium N-to-P ratio

To understand the effects of the medium N-to-P ratio and its variation on the culture, a deepened review of studies reported in literature was carried out. Most of the studies, found in literature about N-to-P ratio implications, were conducted in batch reactors and only few report experiments in other reactor configurations(semi-continuous reactor). Therefore, it has been decided to study articles where batch reactor experiments were performed. In some

studies, the N-to-P ratio was controlled changing only one nutrient (either P or N), in others changing both with the idea to test the limitation of one nutrient by time. In the selected articles, it was possible to find a relation between the N-to-P ratio in the medium and the N- and P-uptake and growth rate. In Table 2-4 the summary of these studies is reported.

Table 2-4 N-to-P ratios influence on microalgae metabolism from literature.

S= Synthetic Medium; WW = Wastewater; W=Freshwater.

Article	**Algae specie**	**Medium**	**N-to-P ratio [molN/molP]**	**N range [mgN/l]**	**P range [mgP/l]**	**Results on N- and P- uptake**	**Results on growth rate**
Liu & Vyverman (2015)	*Cladophora sp.* *Klebsormidium sp.* P*seudanabaena sp.*	S	1-20	5	0,5 - 10	P-Uptake directly ∝ N-to-P ratio; N-Uptake independent of N-to-P ratio	N-to-P ratio affects the growth rate, but the effect is species-specific
Whitton, et al. (2016)	*Chlorella vulgaris* *Scenedesmus obliquus*	WW	1.1 – 22.1	6,77 - 14	31 – 1,5	P-uptake directly ∝ N-to-P ratio; N-uptake inversely ∝ N-to-P ratio	N-to-P ratio affects the growth rate (no more info)
Choi & Lee (2015)	*Chlorella vulgaris*	WW	1-80 (changing both P and N)	-	-	P-Uptake directly ∝ N-to-P ratio; N-Uptake independent of N-to-P ratio	Growth rate is highly dependent on the N-to-P ratio. It increases until N-to-P=10 then gradually decreases reaching a minimum at N-to-P=30
Seung-Hoon, et al. (2013)	Consortium	WW	120 and 31	7,04	0,13 and 0,5	N- and P-uptake higher at 31 N-to-P ratio	N-to-P ratio affects the growth rate (no more info)

Arbib, et al. (2013)	*Scenedesmus obliquus*	WW	1 -35	22,77 – 92,77	5,69 - 40	P-uptake directly ∝ N-to-P ratio; N-Uptake independent of N-to-P ratio	No significant influence of N-to-P ratio on growth rate except a slight reduction for N-to-P ratio = 35
Suttle & Harrison (1988)	Consortium	W +S	5 -45	35 - 10	2 – 0,5	P-uptake directly ∝ N-to-P ratio; N-uptake inversely ∝ N-to-P ratio	-
Rhee (1978)	*Scenedesmus sp.*	S	5-80	0,21 – 3,36	0,093	N-uptake inversely ∝ N-to-P ratio;	Growth rate increases linearly with N-to-P until 30, then levels off -> N limitation before 30
Li, et al. (2010)	*Scenedesmus sp.*	S	2-100	2,5 - 25	0,1 - 2	P-uptake independent of N-to-P ratio; N-uptake inversely ∝ N-to-P ratio	Growth rate is independent of N-to-P, until N or P becomes limiting

These studies generally show a dependency of microalgae metabolism on nutrients availability and the N-to-P ratio in the medium. For instance, the growth rate seems to be affected by the N-to-P ratio and it is sensitive to the depletion of nutrients.

Nevertheless, it was hard to find other trends among the studies. The results about the relation between N-to-P ratio and nutrients uptake seem to be contradictory and not consistent with each other. This may be caused by the differences between the studies and the amount of variable involved in the processes. In particular, not only the N-to-P ratio has effects on microalgae metabolism, but also the singular concentrations of nitrogen and phosphorus have an impact on it. Indeed, the same N-to-P ratio may be obtained starting from different levels of nutrients, thus one of them could be either limiting or in abundance implying different responses by microalgae. Moreover, these studies were conducted using different microalgae species. Comparing the results, it was pointed out that each microalgae specie has different behaviors when subjected to the same environmental conditions due to their internal N-to-P ratio.

Therefore, from this literature review it emerges that most of the studies published so far are not easily comparable, even if they study the same phenomena. It may be interesting to conduct studies more coordinated, reducing the number of variables involved.

Effects of culture history

So far, little attention has been paid to the effects of culture history on microalgae metabolisms and physiology. Only few studies about the effects of starvation periods have been found in literature. Generally, the starvation periods were induced suspending the supply of one nutrient (nitrogen or phosphorus) or both. The experiments found in literature correspond to three different methods (Figure 2-2):

1) The nutrients condition in the culture medium is switched three times: from nutrient-rich conditions to starvation and then again to nutrient-rich conditions (Hernandez, et al., 2006; Young & Beardall, 2003);
2) The nutrients condition in the culture medium is switched two times: from nutrient-rich conditions to starvation (Mujtaba, et al., 2012; El-Sheek & Rady, 1995);
3) The nutrients condition in the culture medium is switched two times: from starvation to nutrient-rich conditions (Hernandez, et al., 2006; Brussaard, et al., 1998).

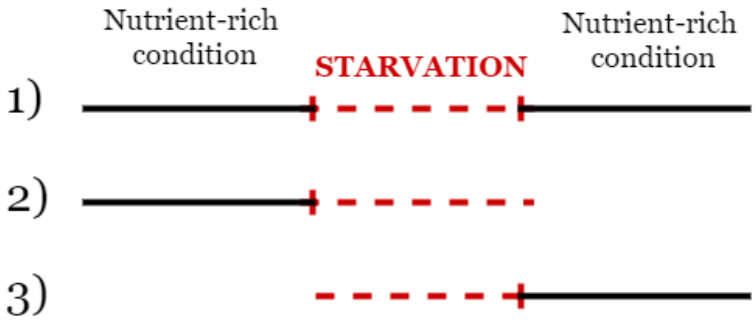

Figure 2-2 Experiments methods used in literature

Moreover, the studies were more focused on the effects on microalgae internal composition and the production of valuable compounds, i.e. lipids and proteins, which production appears to be enhanced by nutrient starvation, than on the kinetics of the processes.

As previously said in *Background and Motivations - Thesis objectives*, this work has been focused on the effects of the exposure to different N-to-P ratio in the medium on microalgae culture stability and the kinetics of the processes involved. As reported in *Materials and methods*, the concentrations of nitrogen and phosphorus used in the experiment have never lead to deep starvation of the culture. However, no papers about this kind of investigation were found in literature.

2.3 Microalgae modelling

To improve our knowledge on the phenomena involve in green microalgae growth a model based approach is commonly used. Many models were developed for modeling microalgae processes. The modeling approaches found in literature are various and range in complexity. Some of them consider only one variable on microalgae growth, such as light intensity (Grima, et al., 1994), others combined the influence of several variables, such as light intensity, nutrient availability, temperature and pH (Wolf, et al., 2007; Broekhuizen, et al., 2012; Ambrose, 2006; Fachet, et al., 2014). Although, the latter group of models has a high complexity, in some cases they lack important aspects for the evaluation of the application of microalgae on the water management. For instance, the model proposed by Wolf et al. (2007), even if consider growth of heterotrophs, nitrifies and microalgae on inorganic carbon, light and nitrogen, do not consider the phosphorus, which is a fundamental aspect for the application of algae in the water management. Another example is the model proposed by Broekhuizen et al. (2012). It considers the effects of light, inorganic carbon, oxygen, nitrogen, phosphate and pH on microalgae growth, but nutrient uptake and microalgae growth are directly coupled and therefore the storage of nutrients and the growth on the stored nutrients are neglected. Consequently, the growth under multiple substrate limitations is not modeled. Nevertheless,

in 1973, Droop proposed a model, which describes the uptake and storage of nutrients and the growth on the stored nutrients as two different processed. Consequently Droop's model can describe the microalgae growth in absence of nitrogen and/or phosphorus in the medium using the internal storage of nutrients. When the external nutrient are absented, the minimum internal nutrient quota is gradually reached and the growth rate converge to zero. Vice versa, when the medium is rich in nutrients, the maximum internal quota is reached, and the growth rate converges to the maximum. In this condition the microalgae growth becomes independent from the availability of nutrients in the medium (Bernard, 2011). This model may remedy the lack of Broekhuizen work, indeed it has been successfully applied in other models (Ambrose, 2006; Fachet, et al., 2014).
However, none of the above mentioned models consider the growth of algae on different organic substrates, even if it is well documented, as described in *State of art - Green microalgae cultivation*.

Among the others, the so called the ASM-A model presented by Wágner et al. (2016) was selected to be used in this work. It was developed to remedy to the issues briefly described above. Since it has been recently introduced, in the next pages, it is described together with the Latin Hypercube Sampling based Simplex (LHSS), i.e. the parameters estimations procedure applied in this work. For more information it is strongly advised to read Wágner et al. (2016).

2.3.1 ASM-A model

ASM-A was developed as an extension of the well-known Activated Sludge Model ASM-2d (Henze, et al., 2000). ASM-A only considers green microalgae's biochemical processes. The considered processes catalyzed by green microalgae are presented in the Gujer matrix reported in Table 2-5 and later explained in terms of modeling choices.

Table 2-5 The Gujer matrix of ASM-A model (Wágner et al., 2016)

Component	**NH_4**	**NO_3**	**Internal quota N**	**PO_4**	**Internal quota P**	**Inorg. carbon**	**Acetate**	**O_2**	**Algal Biomass**	**Inert Particulates**	**Slowly biodegradable Particulate**	**Rate**
Symbol Unit	**S_{NH4}** gN/m^3	**S_{NO}** gN/m^3	**$X_{Alg,N}$** gN/m^3	**S_{PO4}** gP/m^3	**$X_{Alg,PP}$** gP/m^3	**S_{Alk}** $g\ C/m^3$	**S_A** $gCOD/m^3$	**S_{O2}** $gCOD/m^3$	**X_{Alg}** $gCOD/m^3$	**X_I** $gCOD/m^3$	**X_S** $gCOD/m^3$	
Process	**Stoichiometric Matrix**											
Uptake and storage of nitrogen from NH4	**-1**		**1**									**R1**
Uptake and storage of nitrogen from NO3		**-1**	**1**									**R2**
Uptake and Storage of PO4				**-1**	**1**							**R3**
Autotrophic growth			**$-iN_{Xalg}$**		**$-iP_{Xalg}$**	**$-1/Y_{Xalg,SAlk}$**		**$2.67/Y_{Xalg,SAlk}$**	**1**			**R4**
Heterotrophic growth			**$-iN_{Xalg}$**		**$-iP_{Xalg}$**	**$0.4/Y_{Ac}$**	**$-1/Y_{Ac}$**	**$1-1/Y_{Ac}$**	**1**			**R5**
Decay	**iN_{Xalg} $-fX_I.iN_{XalgI}$ $-(1-fX_I).iN_{XalgS}$**			**iP_{Xalg} $-fX_I.iP_{XalgI}$ $-(1-fX_I).iP_{XalgS}$**				**$-(1-fX_I)$**	**-1**	**fX_I**	**$1-fX_I$**	**R6**

Table 2-6 Process rates of the ASM-A model (Wágner et al., 2016)

Process rates	
R1 [g N m^{-3} d^{-1}]	$k_{NH4} \cdot \frac{S_{NH4}}{S_{NH4} + K_{NH4,Alg}} \cdot \frac{X_{Alg,Nmax} \cdot X_{Alg} - X_{Alg,N}}{X_{Alg,Nmax} \cdot X_{Alg}} \cdot X_{Alg}$
R2 [g N m^{-3} d^{-1}]	$k_{NO} \cdot \frac{S_{NO}}{S_{NO} + K_{NO,Alg}} \cdot \frac{K_{NH4,Alg}}{K_{NH4,Alg} + S_{NH4}} \cdot \frac{X_{Alg,Nmax} \cdot X_{Alg} - X_{Alg,N}}{X_{Alg,Nmax} \cdot X_{Alg}} \cdot X_{Alg}$
R3 [g P m^{-3} d^{-1}]	$k_{PO4} \cdot \frac{S_{PO4}}{S_{PO4} + K_{PO4,Alg}} \cdot \frac{X_{Alg,PPmax} \cdot X_{Alg} - X_{Alg,PP}}{X_{Alg,PPmax} \cdot X_{Alg}} \cdot X_{Alg}$
R4 [g COD m^{-3} d^{-1}]	$\mu_{A,max} \cdot (1 - \frac{X_{Alg,Nmin} X_{Alg}}{X_{Alg,N}}) \cdot (1 - \frac{X_{Alg,PPmin} X_{Alg}}{X_{Alg,PP}}) \cdot \frac{S_{Alk}}{S_{Alk} + K_{Alk}} \cdot \frac{I_{Av}}{I_S} \cdot e^{1 - \frac{I_{Av}}{I_S}} \cdot X_{Alg}$
R5 [g COD m^{-3} d^{-1}]	$\mu_{H,max} \cdot (1 - \frac{X_{Alg,Nmin} X_{Alg}}{X_{Alg,N}}) \cdot (1 - \frac{X_{Alg,PPmin} X_{Alg}}{X_{Alg,PP}}) \cdot \frac{S_A}{S_A + K_A} \cdot \frac{S_{O2}}{S_{O2} + K_{O2}} \cdot \frac{K_I}{K_I + I_{Av}} \cdot X_{Alg}$
R6 [g COD m^{-3} d^{-1}]	$b_{Xalg} \cdot X_{Alg}$

Table 2-7 State variables of ASM-A model (Wágner et al., 2016)

State variables	Description	Unit
S_{NH4}	Soluble ammonium nitrogen concentration in the bulk liquid	g N· m^{-3}
S_{NO}	Soluble nitrate plus nitrite nitrogen concentration in the bulk liquid	g N· m^{-3}
S_{PO4}	Inorganic soluble P as ortho-phosphate concentration in the bulk liquid	g P· m^{-3}
$X_{Alg,N}$	Internal cell quota of N	g N · m^{-3}
$X_{Alg,PP}$	Internal cell quota of P	g P · m^{-3}
S_{Alk}	Alkalinity consumed via photoautotrophic growth	g C· m^{-3}
S_{O2}	Dissolved oxygen, produced during photoautotrophic growth and consumed during heterotrophic growth	g COD· m^{-3}
S_A	Fermentation products serving as carbon source for heterotrophic growth (acetate)	g COD· m^{-3}
X_{Alg}	Algal biomass, produced through growth processes	g COD· m^{-3}
X_I	Non - biodegradable inert particulate organic matter	g COD· m^{-3}
X_S	Slowly biodegradable particulate organic matter	g COD· m^{-3}

Table 2-8 Stoichiometric parameters and conversion factors with the initial values used in this study (Wágner et al., 2016)

Stoichiometric parameters and conversion factors	Description	Unit	Initial values
$Y_{Xalg,SAlk}$	Yield of biomass on alkalinity	g COD·g^{-1}C	2,69
Y_{Ac}	Yield of biomass on acetate	g COD·g^{-1}COD	0,42
iP_{Xalg}	P content in biomass	g P ·g^{-1}COD	0,0021
iN_{Xalg}	N content in biomass	g N· g^{-1}COD	0,00936
fX_I	Fraction of inert biomass	g COD·g^{-1}COD	0,1
iN_{XalgI}	N content of inert particulate COD	g N·g^{-1}COD	0,00431
iN_{XalgS}	N content of slowly biodegradable substrate	g N·g^{-1}COD	0,00495
iP_{XalgI}	P content of inert particulate COD	g P·g^{-1}COD	0,00101
iP_{XalgS}	P content of slowly biodegradable substrate	g P·g^{-1}COD	0,00109

Table 2-9 Kinetic parameters of ASM-A model with the initial values used in this study (Wágner, 2016)

Kinetic parameters	Description	Unit	Initial values
$\mu_{A,max}$	Maximum specific photoautotrophic growth rate	d^{-1}	4,12
$\mu_{H,max}$	Maximum specific heterotrophic growth rate	d^{-1}	4,5
I_s	Light saturation intensity	µmol m^{-2} s^{-1}	758,2
$X_{Alg,PPmin}$	Minimum P cell quota	g P·g^{-1}COD	0,0021
$X_{Alg,Nmin}$	Minimum N cell quota	g N· g^{-1}COD	0,00936
$X_{Alg,PPmax}$	Maximum P cell quota	g P· g^{-1}COD	0,016
$X_{Alg,Nmax}$	Maximum N cell quota	g N· g^{-1}COD	0,13
$K_{NO,Alg}$	Half-saturation coefficient of NO_3	g N·m^{-3}	12,61
$K_{NH4,Alg}$	Half-saturation coefficient of NH_4	g N·m^{-3}	7,87
$K_{PO4,Alg}$	Half-saturation coefficient of PO_4	g P·m^{-3}	4,49
$k_{NH4,Alg}$	Maximum specific uptake rate of NO_3	g N·g^{-1}COD·d^{-1}	0,036
$k_{NO,Alg}$	Maximum specific uptake rate of NH_4	g N·g^{-1}COD·d^{-1}	0,043
$k_{PO4,Alg}$	Maximum specific uptake rate of PO_4	g P·g^{-1}COD·d^{-1}	0,16
K_{Alk}	Alkalinity half-saturation coefficient	g C·m^{-3}	3
K_A	Half-saturation coefficient of acetate	gCOD·m^{-3}	6,3
K_I	Inhibiting light intensity	µmol $m^{-2}s^{-1}$	331
K_O	Half-saturation coefficient for oxygen	gCOD m^{-3}	2
b_{Xalg}	Decay rate	d^{-1}	0,21

Uptake and storage of nitrogen (R1 and R2)

Green microalgae can uptake and store nitrogen from both soluble ammonia (R1) and soluble nitrate (R2). In both cases the uptake and storage of nitrogen depends on the availability of nitrogen in the medium (S_{NH4} or S_{NO}), which is modeled with a Monod kinetic, and on the

internal cell quota of nitrogen (X_{AlgN}), which limits the nitrogen uptake when it approaches the maximum internal cell quota ($X_{Alg,Nmax}$). Moreover, according to Cai, et al. (2013) and Markuo et al. (2014) green microalgae prefer ammonia over nitrate. Therefore, in the nitrate uptake process rate, a competitive inhibition term is added.

Uptake and storage of phosphorus (R3)

The uptake and storage of phosphorus (R3) depends on the availability of phosphorus as soluble orthophosphate in the medium (S_{PO4}), which is modeled with a Monod kinetic, and on the internal cell quota of phosphorus (X_{AlgP}), which limits the phosphorus uptake when it approaches the maximum internal cell quota ($X_{Alg,PPmax}$).

Photoautotrophic growth (R4)

Green microalgae photoautotrophic growth (R4) is based on the availability of internal nutrients storage, soluble inorganic carbon and light. Thus, the specific growth rate decreases when the internal cell quota of nitrogen or phosphorus approaches the minimum ($X_{Alg,Nmin}$ or $X_{Alg,PPmin}$) and it is modeled according to Droop (1973). The consumption of inorganic carbon (S_{Alk}) is modeled using Monod kinetics. The light limitation is modeled using the Steele equation (Steele, 1962).

Heterotrophic algal growth (R5)

Green microalgae heterotrophic growth (R5) is based on the availability of internal nutrients storage, soluble organic carbon and oxygen. Thus, Monod kinetics are used to model the heterotrophic growth as function of the organic carbon substrate concentration, i.e. acetate (S_A), and the terminal electron acceptor, i.e. oxygen (S_{O2}). As describe for the photoautotrophic growth, the specific growth rate decreases when the internal cell quota of nitrogen or phosphorus approaches the minimum ($X_{Alg,Nmin}$ or $X_{Alg,PPmin}$). Light limits the heterotrophic growth, thus it is modeled using a competitive inhibition term.

Alga decay (R6)

The algal decay includes several processes: internal resources used for maintenance, biomass decreasing during dark respiration, death, lysis, loss of biomass due to predators grazing on the algal biomass. According to Van Loosdrecht & Henze (1999) the decay process is modeled following the dead-regeneration principle, which entails the availability of part of the decay products for microbial growth.

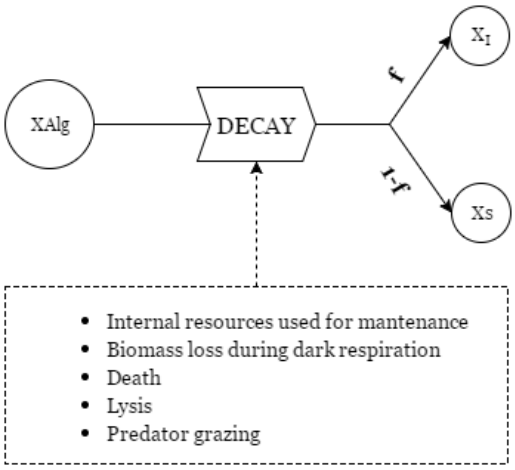

Figure 2-3 Decay process and its causes. Parameter f is the fraction of algal biomass converted in inert particulate.

Average light intensity

The average light in the reactor was calculated for each time step of the simulation based on (Benson, et al., 2007), thus integrating the Lambert-Beer equation over the reactor depth. As shown in Equation 2-4, inlet light (IL), reactor depth (H) and TSS measurement, as indication of the density of the culture, were considered in the calculation.

$$AL\left[\frac{\mu m}{m*s}\right] = IL\left[\frac{\mu m}{m*s}\right] * \frac{1 - e^{-LP1*TSS\left[\frac{mgTSS}{L}\right]*H[m]*e^{-LP2*TSS\left[\frac{mgTSS}{L}\right]}}}{TSS\left[\frac{mgTSS}{L}\right]*H[m]*LP1*e^{-LP2*TSS\left[\frac{mgTSS}{L}\right]}}$$

Equation 2-4 Beer-Lambert law for Average Light

Where:

$LP1 = Light\ parameter\ 1 = 0{,}161\ \frac{L}{mgTSS*m}$

$LP2 = Light\ parameter\ 2 = 0{,}0016\frac{L}{mgTSS}$

The light parameters used in the equation are attenuation coefficients and their estimation process is presented by Wàgner et al. (2014).

2.3.2 Parameters estimation for the ASM-A model

In the work presented by Wàgner et al. (2016) a procedure for parameters estimation and for identifiability assessment was implemented and tested. The developed methodology is referred to as the Latin Hypercube Sampling based Simplex (LHSS) and it was adapted from literature. It is composed of 3 parts with a total of 5 modular steps, which are later described and represented in Figure 2-4.

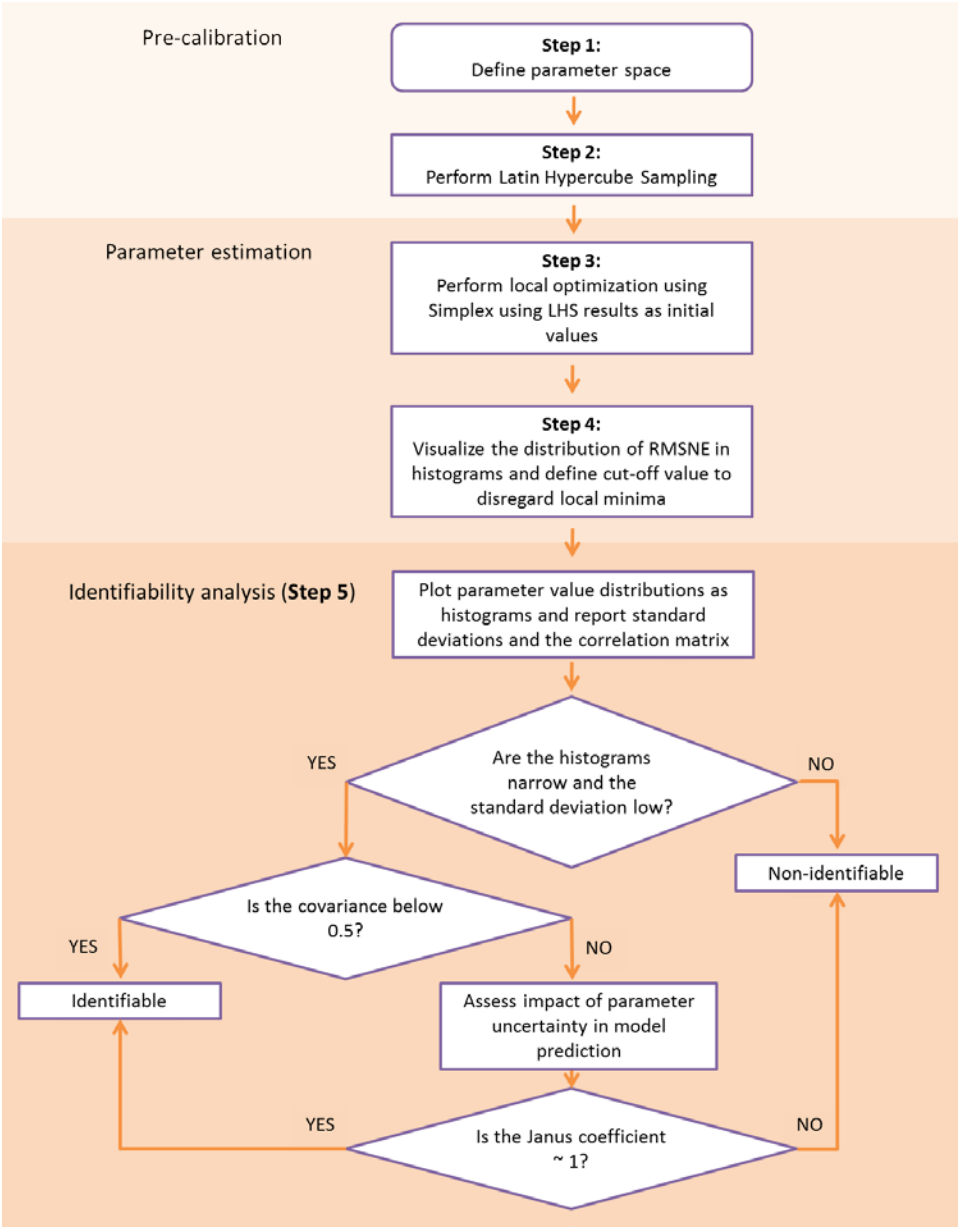

Figure 2-4 Scheme of the LHSS method proposed for parameter estimation and identifiability assessment (Wágner, 2016)

Pre-Calibration

Step 1

Based on a wide literature review in Wágner et al. (2016) a range of possible values for each parameter was defined. Table 2-10 reports the upper and lower boundaries that define the ranges for the parameters of interest for this work.

Table 2-10 Upper and lower bounds, that define the ranges used during the LHSS calibration process (Wágner, 2016)

Parameter	Lower bound	Upper bound
$\mu_{A,max}$ (d^{-1})	2.5	6.5
$K_{NO,Alg}$ ($gN \cdot m^{-3}$)	0.001	15
$K_{PO4,Alg}$ ($gP \cdot m^{-3}$)	0.001	5
$k_{NO,Alg}$ ($gN \cdot g^{1}COD \cdot d^{-1}$)	0.001	5
$k_{PO4,Alg}$ ($gP \cdot g^{-1}COD \cdot d^{-1}$)	0.001	5
b_{Alg} (d^{-1})	0.01	0.5

Step 2

The first parameters set is selected from the given ranges (Table 2-10) using the Latin Hypercube Sampling (Helton & Davis, 2003). In this work, 500 first parameters sets were identified.

Parameter estimation

Step 3

Each parameters set identified in Step 2 is the *a priori* values used for Simplex (Nelder & Mead, 1965), i.e. local optimization algorithm. It identifies the optimal parameters set, minimizing the root mean square normalized error (RMSNE) relative to the measured value.

$$RMSNE = \sqrt{\frac{1}{n}\sum_{i=1}^{n}\left(\frac{y_m - y}{y_m}\right)^2}$$

Equation 2-5 RMSNE Equation

Where:

$n = number\ of\ measurament\ points$

$y_m = measured\ value$

$y = predicted\ values$

At the end of this operation, 500 optimal parameters sets are defined (one for each *a priori* parameters set).

Step 4

The RMSNE distribution is plotted. Considering the minimum error of the distribution a cut-off value is defined increasing it by the 10%. All the results above the cut-off value is disregarded. With the remaining sets, the distribution of each parameter is plotted using histograms. Consequently, for each parameter the mean values and the standard deviations are calculated. In this way the optimal parameters set is defined.

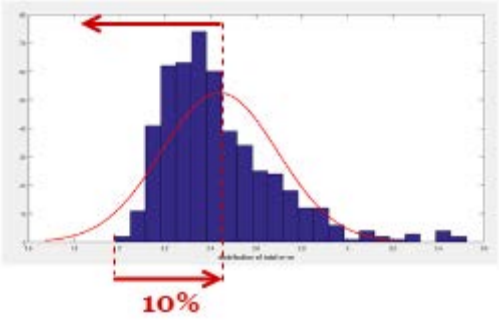

Figure 2-5 Example of the definition of the cut of value

Identifiability analysis

Step 5

To define the parameters identifiability the following elements are used:

- the distribution of the optimal parameter set values plotted as histograms
- the average parameter values
- the standard deviation
- the correlation matrix

According to Van Daele et al. (2015) the histograms of the optimal parameters set values obtained are interpreted according to their wideness and the standard deviation is consider as well for a first assessment of the parameter identifiability. If the histograms are too wide and the standard deviation relatively too high, the parameter is classified as non-identifiable. Otherwise, as suggested by Sin et al.(2010), the covariance is checked. If it is comparably low, the parameter is classified as identifiable. In the opposite case, the parameter identifiability is assessed by analyzing the difference in the simulation output by setting the parameter to its minimum and maximum boundaries defined by the standard deviation (Figure 2-6). As suggest by Sin et al.(2010), to assess the differences in the model predictions the Janus

coefficient is used. It describes the accuracy of the model prediction. When its value is close to 1 the model prediction is accurate and thus, the studied parameter is identifiable. Otherwise, the predictions are worse or better than the original model approximations obtained through parameter estimation and thus the studied parameter is non-identifiable.

$$Janus\ coefficient = \frac{RMSNE\_boundary}{RMSNE\_mean}$$

Equation 2-6 Janus coefficient equation

Where:

RMSNE_boundary = RMSNE calculated on the simulation with the parameter value at the boundary

RMSNE_mean= RMSNE calculated on the simulation with the mean parameter value

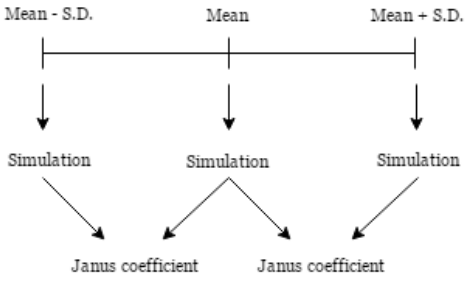

Figure 2-6 Diagram of the final process for the identifiability of the parameters

Chapter 3
MATERIALS AND METHODS

3.1 Laboratory experiments

3.1.1 Green microalgae culture

The mixed green microalgal culture used in these experiments was originally isolated in a natural pond in contact with wastewater. At that time, the culture mainly consisted of *Chlorella sp.* and *Scenedesmus sp.*. The algal culture grew strictly in suspension, without significant biofilm or aggregate formation (Wágner, 2016). The mixed culture was cultivated using the MWC+Se synthetic medium (Guillard & Lorenzen, 1972). Over time, the mixed culture selected to *Chlorella sp*. naturally. Therefore, the experiments were carried out with a monoculture of *Chlorella sp*..

3.1.2 Experimental design and reactors description

EBRP system

A laboratory scale EBPR system was used to treat wastewater.
The system was originally built as EBP2R system and later converted to a traditional EBPR system. The system was designed according to the empirical guidelines established by Randall et al. (1998) for EBPR system. It was built as a sequence of anaerobic-aerobic reactors for a

total of two anaerobic reactors, one aerobic reactor and one clarifier. The layout of the plant is reported in Figure 3-2 while pictures of each reactor can be seen in Figure 3-1.

1. The anaerobic phase was divided into two reactors setup in two glass cylinders with a working volume of 1,25L and a cap to close the reactor in order to limit oxygen transfer from air to the liquid phase. A rotational stirrer working at 60 rpm provided mixing. Differently from the traditional EBPR system, the anaerobic volume was divided in two different reactor to enhance phosphorus release in the anaerobic phase and thus to recover more phosphorus from the P-stream in the EBP2R (Valverde-Pérez, 2015). This feature wasn't changed when the system has been converted to EBPR.

2. The aerobic phase consisted of a 5.8L glass cylinder. Air was provided from the bottom of the reactor by an air diffuser and a rotational stirrer working at 85 rpm provided mixing.
3. The clarifier was a 2L glass reactor with a cylinder part for settling and a hopper in the bottom.

1. Anaerobic reactors 2. Aerobic reactor 3. Clarifier

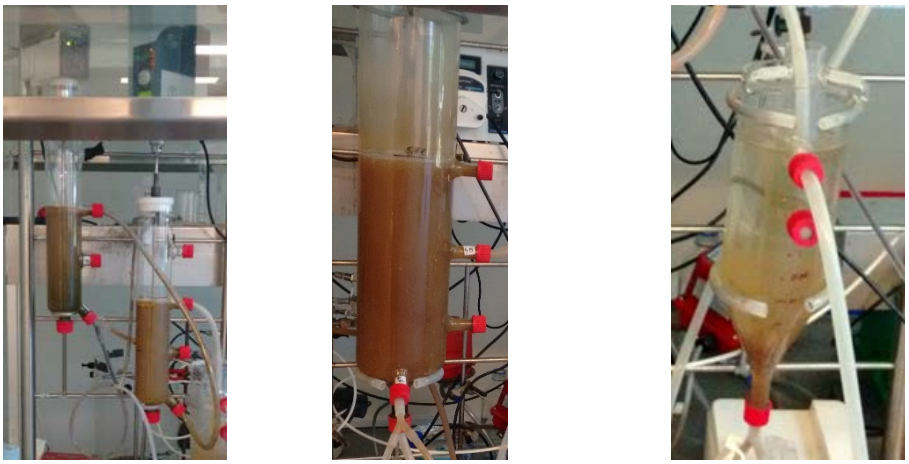

Figure 3-1 Pictures of the main components of the laboratory scale EBPR system

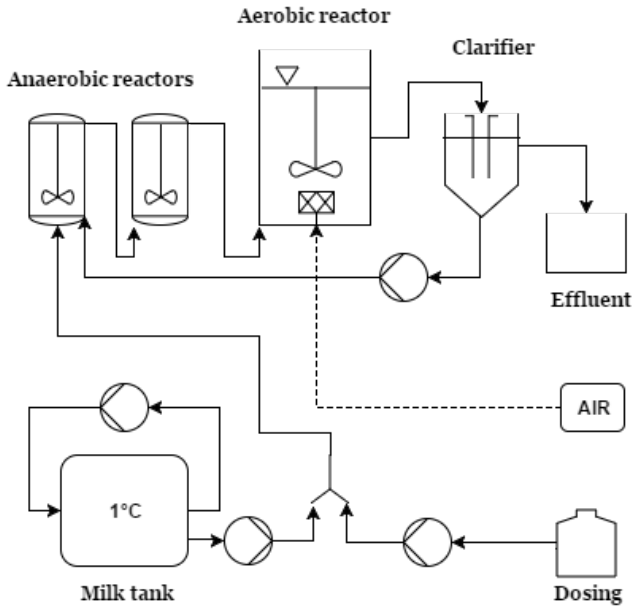

Figure 3-2 EBPR system layout

The system was fed with domestic wastewater from Lundtofte wastewater treatment plant (Denmark). This facility receives 28800 m3/d of wastewater on average. The average values of the quality parameters in input to the plant are reported in Table 3-1 (Valverde-Pérez, 2015).

Table 3-1 Lundtofte influent wastewater nutrients concentration

Parameter	Value	Unit of measure
COD	712	mgCOD/L
TN	54	mgN/L
TP	9	mgP/L

The wastewater collected for the experimentation was withdrawn after the preliminary clarification, therefore part of the nutrients in input to the plant were removed with the settled material. Once in the laboratory, the wastewater was stored in a refrigerated milk tank (Nutriservice© Srl, Italy)(Figure 3-3) working at 1°C with 180L of working volume, equipped by mixing and internal recirculation.

Figure 3-3 Milk tank used for the storage of the incoming wastewater

The influent to the system was obtained by mixing the wastewater with a synthetic solution, in order to keep the quality of the influent stable in terms of COD and nutrients (N and P).

Figure 3-4 Tank for the storage of the synthetic solution

Twice a week the synthetic solution was prepared based on the wastewater composition using Sodium-Propionate (abcr GmbH©, Germany), NA_2HPO_4 (Sigma-Aldrich Co.©, Germany) and NH_4HCO_3 (Th. Geyer GmbH & Co. KG.©, Germany). In Table 3-2 the desired influent nutrients concentrations to the EBPR are reported.

Table 3-2 Desired influent nutrients concentrations

Component	Value	Unit of measure
COD	500	mgCOD/L
NH_4^+	40	mgN/L
PO_4^{3-}	9	mgP/L

The HRT in the system was kept to 13,8h with an inflow of 11,1L/day. As a traditional EBPR system, recirculation of sludge from the clarifier to the first anaerobic reactor was provided. Moreover part of the sludge was daily discharged from the aerobic reactor, thus total SRT was kept at 16 days. Peristaltic pumps were used to maintain the flows in the system.

Continuous flow PBRs

Two PBRs were run in parallel downstream to the laboratory scale EPBR system. They were setup using two glass cylinders with a working volume of 1,4 L (Figure 3-5). The system was built under a fume hood to reduce risk of unwanted contamination and to keep surrounding environmental conditions stable (T~20°C).

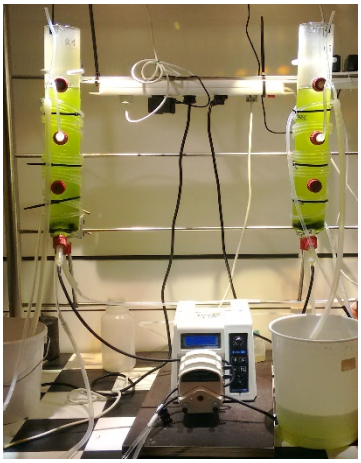

Figure 3-5 Picture of the two parallel photobioreactors

Continuous lighting was provided by a custom-built lamp, providing an average of 1250 µmol photons m^{-2} s^{-1}, with one metal-halide light bulb (OSRAM©, Germany), which simulates the solar spectrum, from the top of the reactor and a black sheet was used to cover the lateral surface of the cylinder, so it received light only from the top (Figure 3-6).

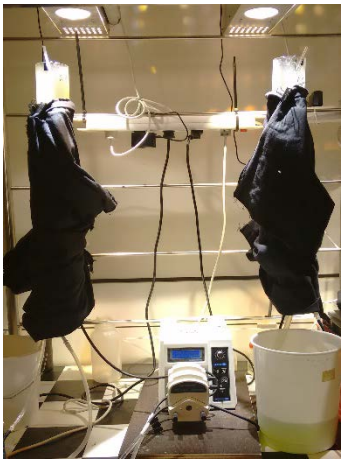

Figure 3-6 Picture of the two parallel photobioreactors covered with a black sheet and the lamps on the top

CO2 enriched airflow was supplied from the bottom of the reactor by an air hose diffuser to guarantee CO2 supply and full mixing. Mixing allowed maintaining homogeneous conditions along the reactor and equal light exposure to algae. CO2 dissolution was used to keep pH inside the reactor at neutral values (range 6,10-7,9). For this purpose, the airflow and the %vol of CO2 were manually adjusted every day(30%±10 for the %vol of CO2). Inlet light and pH were monitored using LI-1400 Data Logger with LI-193 Spherical Underwater Quantum Sensor (2016LI-COR©, USA)(Figure 3-7) and Multi 3430 Digital pH meter for pH-Electrode Sentix 940 sensor (2016 WTW Wissenschaftlich-Technische Werkstätten GmbH. ©, Germany), respectively.

Figure 3-7 Light sensor

Influent streams were provided from the bottom of the reactors by a peristaltic pump (BT100-1F) with two pump head (Longer Precision Pump Co., China), which guarantee 243 μm/min flow to each reactor. Thus the SRT=HRT was kept at 3,5 days. Each pump heads withdrew the

influents from a dedicated containers. The 2L polyethylene containers were maintained at 5°C in a FrigoMix Cooling Water Bath (2016 B.Braun©, Denmark), so the quality of the influents could be conserved(Figure 3-8).

Figure 3-8 Cool system for influent storage

The influents were prepared collecting EBPR effluent and adjusting the pH to 7 and spiking N and P to reach the desired nutrient content. $NaNO_3$ solution with 10mgN/ml and KH_2PO_4 solution with 1,55mgP/ml were used to reach the chosen nutrient conditions. PO_4^{3-} concentration was always kept constant at about 4 mgP/l spiking the KH_2PO_4 solution. Instead, NO_3^- concentration varied depending on the chosen N-to-P ratio. Since NH_4^+ concentration in the EBPR system effluent is under half saturation constant for NH_4^+, NO_3^- was used as the main N-source for microalgae.

One of the reactors, referred to as R1, was selected as reference reactor and it was always fed with 17 N-to-P ratio. The other one, referred to as R2, was exposed to different N-to-P ratio circa every 3 SRT, thus steady state condition were reached, for a total of 3 periods as reported in Table 3-3.

Table 3-3 N-to-P ratio in R2 influent

Period	N-to-P ratio (mol/mol)
1	17
2	10
3	17

Two different points of extraction of the effluent were tested. The first experiment was setup with the effluent extraction point from the top of the reactor, the second one was setup with

the effluent extraction point from the half height of the reactor. As explained in *Results and Discussion - System layout: the problem and the solution* the second layout, represented in Figure 3-9 , was chosen.

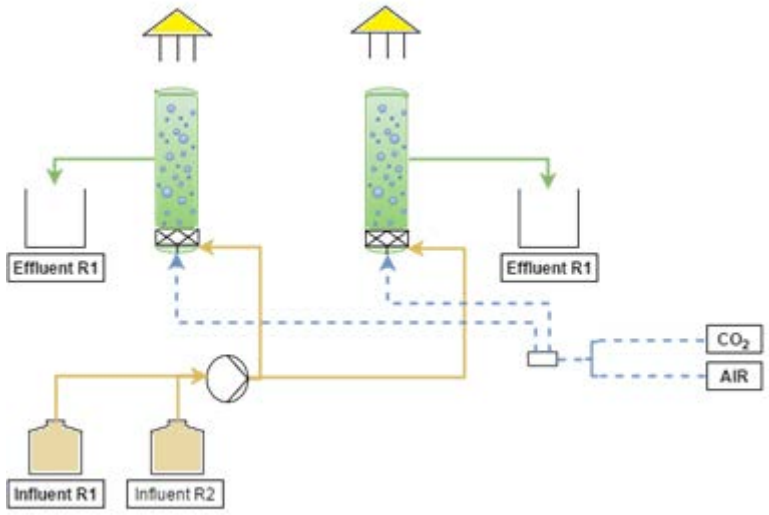

Figure 3-9 Layout of continuous flow PBRs system

1-L Batch experiment

One batch experiment was set up with 1-L wide-neck glass bottle (2014Duran©, Germany) equipped by a multi-port system (Figure 3-10), allowing for sample extraction and aeration with 10 L/h CO_2 enriched air (5% CO2), which guarantees CO2 supply. Mixing was provided by a magnetic stirrer at 180 rpm to maintain equal conditions along the reactor and equal light exposure to algae. Continuous lighting was radiated by one 80-W GroLux fluorescent lamp (2013 Osram Sylvania©, USA), which simulates the solar spectrum, located on one side of the reactor, which provided an average light intensity of 150 μmol/(m^2*s). The temperature of the environment was maintained at 20°C thanks to the air conditioning system implemented in the laboratory where the experiment was carried out. pH remained around neutral values.

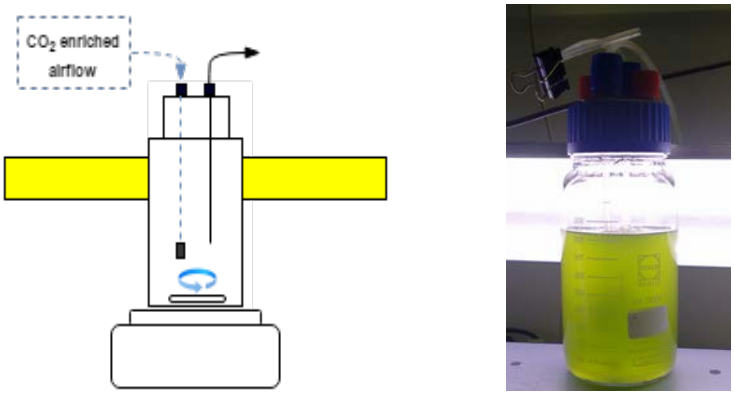

Figure 3-10 Batch experiment layout and photo

The batch was prepared using 800ml of effluent from the pilot scale EBPR system and 200 ml of *Chlorella sp*. culture. The experiment was run with an initial N-to-P ratio of about 17 mol/mol and an initial concentration of $PO3^-$ of about 4 mgP/L . This condition was reached spiking NH_4KCO_3 solution and KH2PO4 solution (1,55 gP/ml). In Table 3-4 the initial concentration of nutrients and total suspend solids are reported.

Table 3-4 Initial condition in 1-L Batch experiment

$NH4^+$	**$NO3^-$**	**$NO2^-$**	**$PO4^{3-}$**	**TSS**
[mgN/l]	[mgN/l]	[mgN/l]	[mgP/l]	[g/l]
14,8	11,2	0,42	3,07	0,057

It is important to notice that, at starting point, there were two main N-source available for the culture, $NH4^+$ and $NO3^-$. This will have an effect on the uptake of nutrients, which will be describe in *Results and Discussion - Implication on N-source.*
The experiment was run until stable concentration for $NH4^+$, $NO3^-$ and $PO4^{3-}$ were reached.

1.2 L batch experiments

Two batch experiments were setup using a glass cylinder with a working volume of 1,2 L (Figure 3-11). A black sheet was used to cover the lateral surface of the cylinder, so it received light only from the top. Continuous lighting was provided by one custom-built lamp with one metal-halide light bulbs (2016 OSRAM©, Germany), which simulates the solar spectrum, from the top of the reactor with an average ligth intensity of 1000 µmol/(m^2*s). CO2 enriched airflow was supplied from the bottom of the reactor by an air hose diffuser to guarantee CO2 supply and full mixing. Mixing allowed maintaining equal conditions along the reactor and equal light exposure to algae. Moreover, CO2 dissolution was used to keep pH at neutral values between 6.5 and 7.5. For this purpose, the airflow and the %vol of CO2 were manually adjusted

every day(30%±10 for the %vol of CO2). The system was built under a fume hood to reduce risk of unwanted contamination and to keep surrounding environmental conditions stable (T~20). Incoming light intensity and pH were monitored using LI-1400 Data Logger with LI-193 Spherical Underwater Quantum Sensor (2016 LI-COR©, USA) and Multi 3430 Digital pH meter for pH-Electrode Sentix 940 sensor (2016 WTW Wissenschaftlich-Technische Werkstätten GmbH. ©, Germany), respectively.

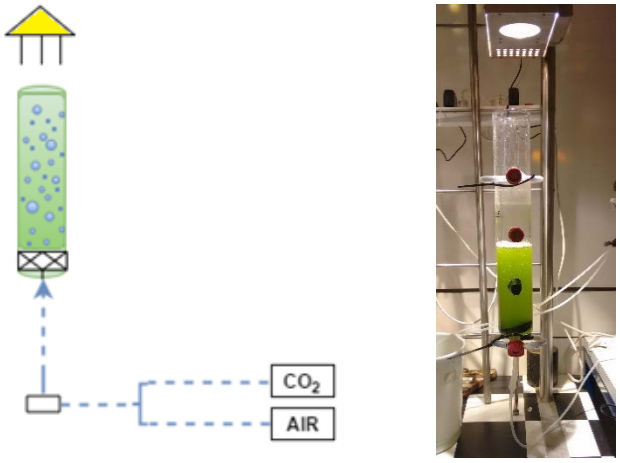

Figure 3-11 Batch experiment layout and photo

The batch was prepared using 1 L of effluent from the pilot scale EBPR system and 200 ml of effluent from the second PBR containing *Chlorella sp*. culture. Both experiments were run with an initial N-to-P ratio of 17 mol/mol and an initial concentration of $PO3^-$ of about 4 mgP/L. This condition was reached spiking $NaNO_3$ solution (10mgN/ml) and KH2PO4 solution (1,55 mgP/ml). The difference between the two experiments was the history of the culture. The first batch was prepared using the effluent of the second PBR (R2) collected during the first period, thus the *Chlorella sp*. culture was exposed for a long period to 17 mol/mol N-to-P ratio circa. Instead, the second batch was prepared using the effluent of the second PBR collected during the second period, thus the *Chlorella sp*. culture was exposed for a long period to 10 mol/mol N-to-P ratio circa.
The two experiments were run until nutrients concentrations ($NO3^-$, $PO4^{3-}$) were depleted.

3.1.3 Analytical methods

Biomass

Biomass in the reactors was analysed by total suspended solids measurement (TSS) and by measuring the optical density (OD) at 750 nm.
TSS was measured filtering the suspension using glass fiber filter Advantec® GA-55 with pore size of 0.6 µm (Frisenette ApS, Denmark) and drying them following the standard methods.
OD was measured using microtiter plates filled with 2mL of sample and analysing them with SynergyMX Multi-Mode Microplate Reader (2016 BioTek Instruments Inc. ©, Winooski) (Figure 3-12).

Figure 3-12 SynergyMX Multi-MOde Microplate Reader (©2016 BioTek Instruments Inc.)

Nutrients and COD

Total nitrogen (TN), total phosphorus (TP) and chemical oxygen demand (COD) were measured in algal suspension using commercial test kits (Hach-Lange©, USA).
Ammonium (N_{NH4^+}), nitrate (N_{NO3^-}), nitrite (N_{NO2^-}) and phosphate ($P_{PO4^{3-}}$) concentrations were measured in filtered samples using test kits supplied by Merck© (USA).
Total soluble nitrogen (TSN) and soluble chemical oxygen demand (sCOD) were measured in filtered samples using commercial test kits (Hach-Lange©, USA).
Filtration was carried out using glass fiber filter Advantec® GA-55 with pore size of 0.6 µm (Frisenette ApS, Denmark) followed by a second filtration with 0.2 µm Minisart® NML disposable filter (©2016 Th. Geyer GmbH & CO- KG., Germany).
The algal biomass was calculated converting TSS units in to COD using a conversion factor of 0,89 gTSS/gCOD estimated from the data collection for the studied microalgae culture.

$$AlgaeBiomass\ \left[\frac{gCOD}{L}\right] = \frac{TSS\left[\frac{gTSS}{L}\right]}{0{,}89\ \left[\frac{gTSS}{gCOD}\right]}$$

Equation 3-1 : Algae Biomass

The internal cell quota of nitrogen was calculated based on the difference of total nitrogen and total soluble nitrogen divided by the algal biomass.

$$Internal\_N\_Quota[\frac{mgN}{gCOD}] = \frac{(TN\left[\frac{mgN}{L}\right] - TSN\left[\frac{mgN}{L}\right])}{AlgaeBiomass\left[\frac{gCOD}{L}\right]}$$

Equation 3-2 Internal Nitrogen Quota

The internal cell quota of phosphorus was obtained by the difference of total phosphorus and soluble phosphate divided by the algal biomass.

$$Internal\_P\_Quota[\frac{mgP}{gCOD}] = \frac{(TP\left[\frac{mgP}{L}\right] - P_{PO4^{3-}}\left[\frac{mgP}{L}\right])}{AlgaeBiomass\left[\frac{gCOD}{L}\right]}$$

Equation 3-3 : Internal Phosphorus Quota

Microscopy and image analysis

The microalgae culture was monitored approximately every second day using a novel image analysis method developed during this study and described in *Results and Discussion - Development of a new images analysis method.*

Imaging was performed using a Motic AE31 microscope with a magnification of 20x and the image analysis software Image pro plus 7 3D suite (USA) was used to automate the processes of identification and quantification of the different types of algae based on their morphology.

To develop the method, 2 different algae culture were used. One mixed culture containing mostly *Chlorella sp.* and *Scenedesmus sp.* and monoculture containing uniquely *Chlorella sp.*.

3.2 Microalgae modelling and parameters estimation

All the data collected through the laboratory experiments were used in the ASM-A model presented by Wágner et al. (2016) to assess the goodness of the fit obtained with the parameter values by Wágner et al. (2016) and to estimate the most significant parameters for this study. In order to work with the model and the parameters estimation procedure, MATLAB® and Simulink were used.

The parameters chosen for the estimation are reported in Table 3-5. They were chosen because they were considered the critical ones, which should show the effect on the green microalgae kinetics sought in this work.

Table 3-5 Parameters chosen to be estimated in this work

Parameters	Description	Unit
$\mu_{A,max}$ (d^{-1})	Maximum specific photoautotrophic growth rate	d^{-1}
$K_{NO,Alg}$ ($gN \cdot m^{-3}$)	Half-saturation coefficient of NO_3	g $N \cdot m^{-3}$
$K_{PO4,Alg}$ ($gP \cdot m^{-3}$)	Half-saturation coefficient of PO_4	g $P \cdot m^{-3}$
$k_{NO,Alg}$ ($gN \cdot g^{1}COD \cdot d^{-1}$)	Maximum specific uptake rate of NH_4	g $N \cdot g^{-1}COD \cdot d^{-1}$
$k_{PO4,Alg}$ ($gP \cdot g^{-1}COD \cdot d^{-1}$)	Maximum specific uptake rate of PO_4	g $P \cdot g^{-1}COD \cdot d^{-1}$
b_{Alg} (d^{-1})	Decay rate	d^{-1}

Chapter 4
RESULTS AND DISCUSSION

The experiments and the analysis described in this chapter were carried out at the department of Environmental Engineering at Technical University of Denmark. The experimental setup described in *Materials and methods - Laboratory experiments* was used to study the impact of changes in nutrients content in the photobioreactor's influent on the green microalgae culture, on the processes involved and on the efficiency in terms of nutrients removal.

4.1 EBPR system: wastewater pre-treatment

In order to use the wastewater from Lundtofte WWTP for the experiments, it was necessary to treat it. Indeed, the water used for experiments should resemble as much as possible the inlet water to the PBR in TRENS. A laboratory scale EBPR system was used for this purpose. It was already working when the laboratory activities for this study began and it was run for the entire period of work, i.e. around 130 days.

As reported in *Materials and methods - EBRP system*, the nutrients concentrations in input to the system were regulated adding a synthetic solution containing Sodium-Propionate NA_2HPO_4 and NH_4HCO_3. In the following charts (Figure 4-1,Figure 4-2 and Figure 4-3) the weekly concentrations of COD, $NH4^+$ and $PO4^{3-}$ are reported and compared to the target concentrations in input to the EBPR system.

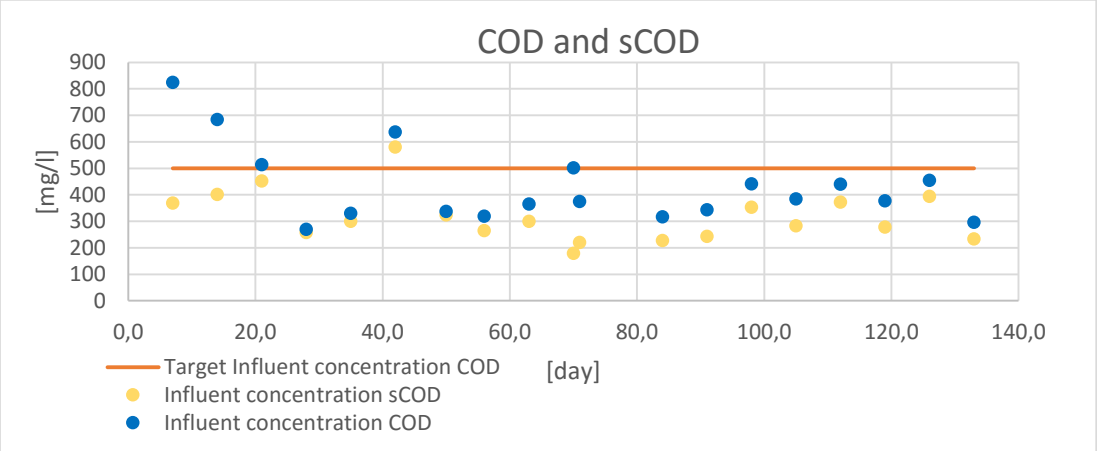

Figure 4-1 Measured COD and sCOD influent concentrations

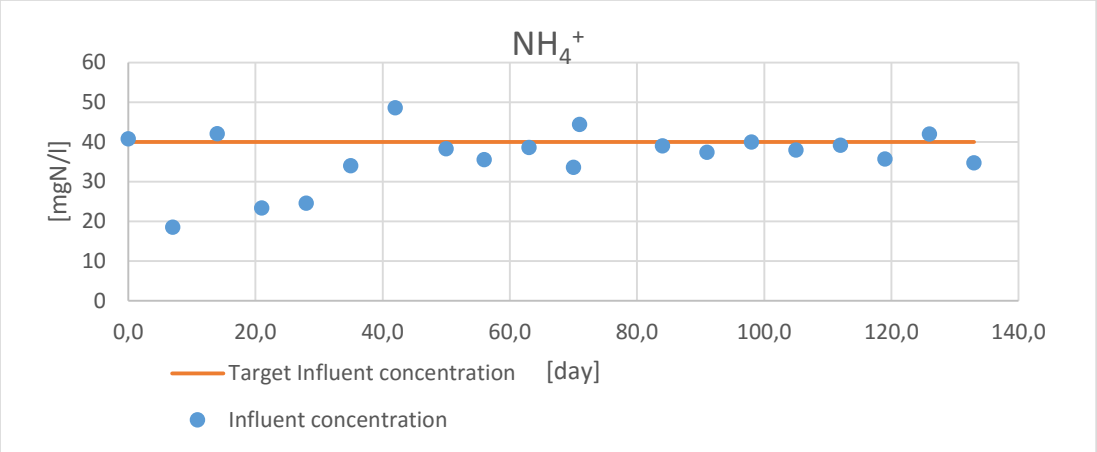

Figure 4-2 Actual NH4⁺ influent concentration

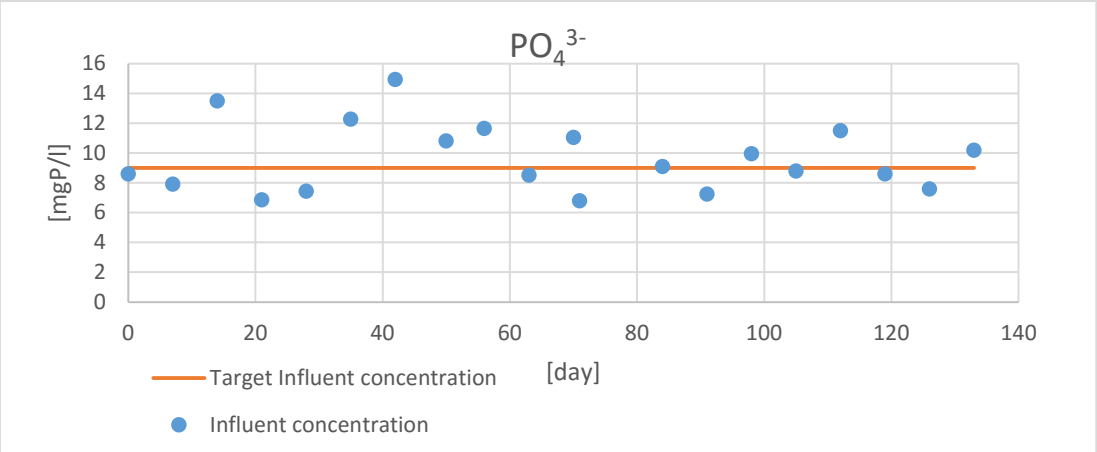

Figure 4-3 Actual PO4³⁻ influent concentration

From the charts it is possible to see that the input concentrations were kept almost constant and at the level of the target concentrations. Only the COD shows higher deviation from the desired target concentration. This is probably resulting from the fact that, to prepare the synthetic solution, the COD present in the wastewater taken form the WWTP of Lundtofte was not measured, but it was assumed to be 280 mg/l. Therefore, the correction with the synthetic solution may have been occasionally incorrect.

Nevertheless, the operation of the system has never been deeply compromised.

The main consequence found was the increasing of the phosphate concentration in the effluent of the system in response to the lower concentration of COD supplied in input, due to the lack of carbon source that limits PAOs activity. But this activity was recovered once the COD of the influent was recovered.

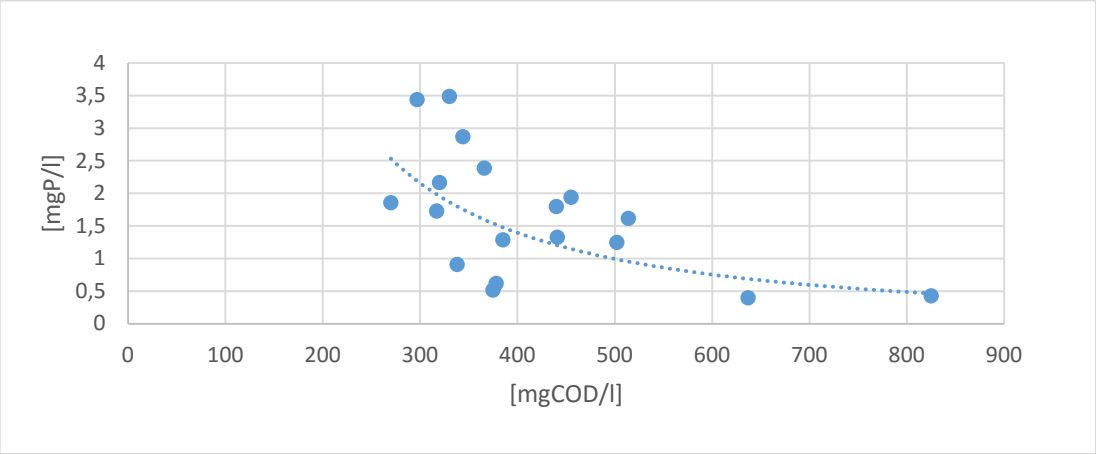

Figure 4-4 Dependence of phosphorus effluent concentration on the influent concentration of COD

The average efficiencies of the system in the removal of COD, inorganic soluble nitrogen and phosphate were respectively 93,7%, 66,4% and 81,1%. In Table 4-1 the average nutrients concentrations in the effluent are reported.

These values are relevant, because they characterize the water used in the experiment with green microalgae.

Table 4-1 Nutrients concentration in EBPR system effluent

Component	Average	Standard deviation	Unit of measure
COD	28,4	2,3	mgCOD/l
PO_4^{3-}	1,9	1	mgP/l
NH_4^+	0,07	0,04	mgN/l
NO_3^-	13	3,8	mgN/l
NO_2^-	0,02	0,01	mgN/l

As can be seen in Figure 4-5 and Figure 4-6, phosphate was more variable than nitrate in the EBPR system effluent along the studied period. Nevertheless, this variation was never a problem, since, in experiments with green microalgae, the required concentration of phosphorus was 4 mg/l and, as can be seen from Figure 4-5, phosphate has practically never exceeded that level. Therefore, its level has been easily adjusted by adding KH_2PO_4. The same applies to the nitrate. Indeed, its concentration in output from the EPBR system has always been low enough not to affect the downstream experiments.

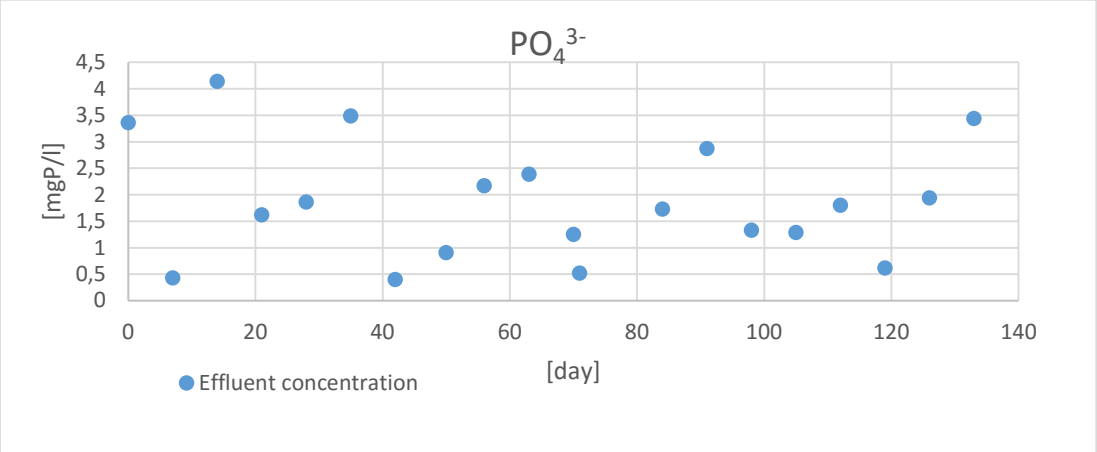

Figure 4-5 Phosphate concentration in EBPR system effluent

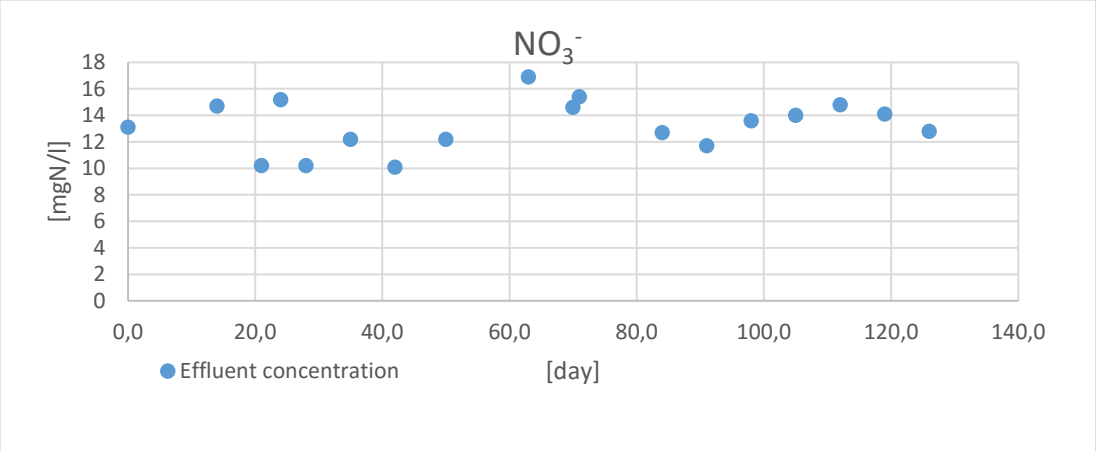

Figure 4-6 Nitrate concentration in EBPR system effluent

4.2 1-L Batch

In the following paragraphs the results from the batch run as described in *Materials and methods - 1-L Batch experiment* are reported.

4.2.1 Preliminary assessment of ASM-A model performance

As previously mentioned, one of the aims of this work was to test and improve the ASM-A model, which was described by Wágner et al. (2016). The model was calibrated initially in Wágner et al. (2016) using synthetic medium, however in this study effluent wastewater was used and it is expected that the parameters would change depending on the growth medium used.

Since in Wágner et al. (2016) the calibration of the m0del was carried out using data related to a mixed culture of *Chlorella sp.* and *Scenedesmus sp.*, a preliminary test on the performance of the model for the new culture, which was a monoculture of *Chlorella sp.*, was needed.

Therefore, the data collected during the 1-L Batch experiment were used to assess the performance of the ASM-A model comparing them with the model prediction. The simulation was run inserting the initial conditions and boundary conditions of this experiment, which are presented in *Materials and methods - 1-L Batch experiment.*

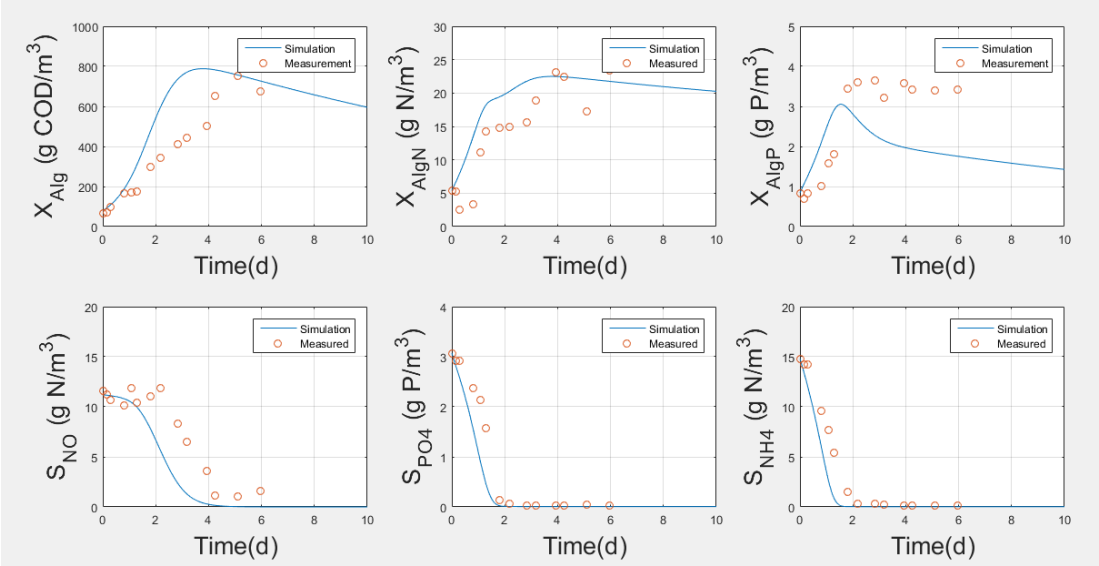

Figure 4-7 Collected data and ASM-A model prediction for 1-L Batch

As expected, the results in Figure 4-7 show a mismatch between the data and the simulation. In particular, the biomass production (XAlg) is overestimated. Nevertheless, this discrepancy could be a consequence of the assumption made on the light intensity in the reactor for this experiment (1-L Bacth). Indeed, the input light intensity to the reactor was not monitored and an average light intensity in the reactor was theoretically calculated and assumed constant along the experiment.

For this reason, the ASM-A model with Wágner et al.(2016) parameters, was in overall considered applicable to assess the settings for the following experiments, e.g. the SRT for the continuous PBRs experiments, as described in *Results and Discussion- Assessment of SRT.*

4.2.2 Implication on N-source

During the analysis of the collected data, an interesting behavior was found. As explained in *State of art - Green microalgae cultivation* , green microalgae have different affinity towards different nitrogen forms. In this contest, only inorganic nitrogen forms were present and the affinity reported in the literature for those is the following:

$$NH_4^+ > NO_3^- > NO_2^-$$

Equation 4-1 General green microalgae affinity with inorganic nitrogen sources

As reported in *Materials and methods - 1-L Batch experiment,* in this experiment the available N-source in the medium was mainly in form of $NH4^+$ and $NO3^-$. In Figure 4-8 the depletion of ammonia and nitrate in the medium is shown and it is clear that the culture has manifested

its preferences consuming firstly $NH4^+$ and secondly $NO3^-$. The culture up took ammonia until it was completely depleted without up taking nitrate, therefore the general uptake of nitrogen resulted to be slowed down in particular during the transition between the two N-sources.

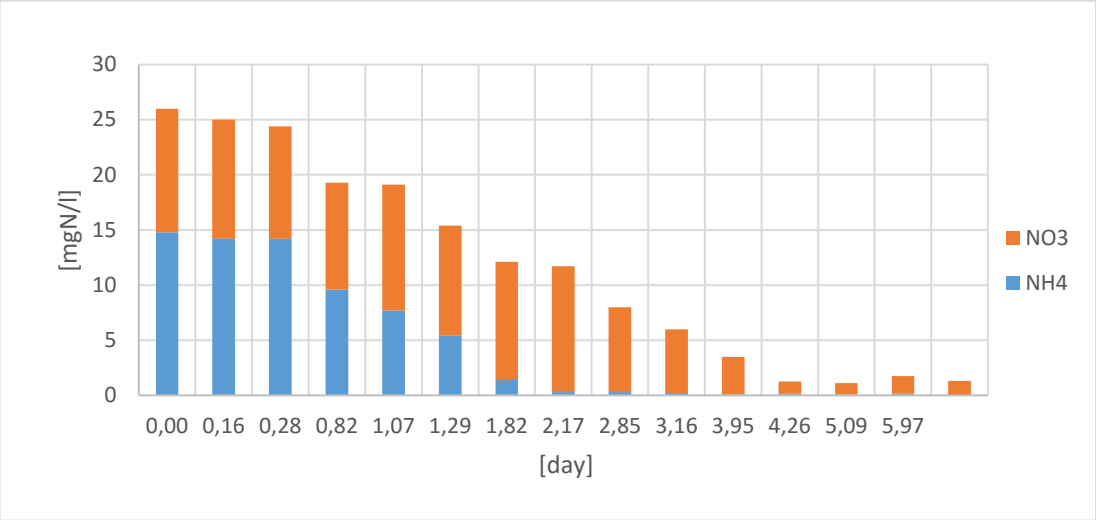

Figure 4-8 Trend of inorganic nitrogen forms in the medium along the experiment

This behavior had influence on the decision to use only one N-source in the following experiments. Indeed, as explained in *TRENS System - EBP2R*, the low SRT set in the EBP2R inhibits the nitrification in the aerobic reactor/phase, therefore only ammonia should be present in the N-stream under optimal conditions and subsequently in the PBRs. Therefore, the ideal condition for the experiments would be having only one N-source: ammonia. Nevertheless, as explained in *Results and Discussion - EBPR system: wastewater pre-treatment*, in the laboratory an EPBR system was implemented, instead of an EBP2R. Therefore, in the pre-treated wastewater the main N-source was $NO3^-$, instead of $NH4^+$. Consequently, to draw closer to the operating conditions of the PBRs in the TRENS system, it was decided to use one sole N-source: $NO3^-$.

Moreover, $NO3^-$ gives advantages in terms of system operation management. Indeed, when it is taken up by algae the pH increases, but it can be controlled through the regulation of the supplied CO2. Instead, when $NH4^+$ is consumed, the pH decreases. Therefore it can work only in waters with high alkalinity.

4.3 Continuous flow PBRs

The experiment described in *Materials and methods - Continuous flow PBRs* was run for 70 days. The data collected for the first 45 days were used to test and improve the ASM-A model.

Instead, the data collected in the following days unfortunately resulted to be not usable, because the cooling system of the reactors did not succeed to maintain 20 °C for a relatively long period and the ASM-A model does not consider the temperature as a variable.
In the following paragraphs, the work on this experiment is reported and the results obtained during the first 45 days are described.

4.3.1 Assessment of SRT

Before starting the experiment, different simulations of the experiment using the ASM-A model were run to assess the feasibility of the experiment and to decide one of the most important parameters: the SRT. The simulations were run only for R2, because it is the one subjected to the changing in the influent nutrients concentrations and therefore it was considered as the critical one. The simulations were set using:

1) the set of parameters calibrated in Wágner et al. (2016);
2) the initial condition expected based on the green microalgae culture in our possession and the typical concentrations in the effluent of the EBPR system, with which the culture would have been diluted to fill the reactors;
3) the sequence of inputs expected for the experiment according to *Materials and methods - Continuous flow PBRs.*

The simulations were run with different SRT, so that an optimal SRT could be identified. The idea was to find the lowest SRT possible that allowed to keep a certain level of biomass in the reactors avoiding algal washout and to reach a good level of nutrients removal.
SRT = 3,5 days was identified as the optimal one. In Figure 4-9 the results of the simulation for R2 with 3,5 days and 1 day as SRT are shown. In the first case the biomass is kept around 500 gCOD/m^3 along the experiment, therefore no washout appears. At the same time, the removal of nitrogen and phosphorus obtained reaches an acceptable level. In the second case, the biomass is too reduce (around 40 gCOD/m3) and consequently the removal of nitrogen and phosphorus is not sufficient.

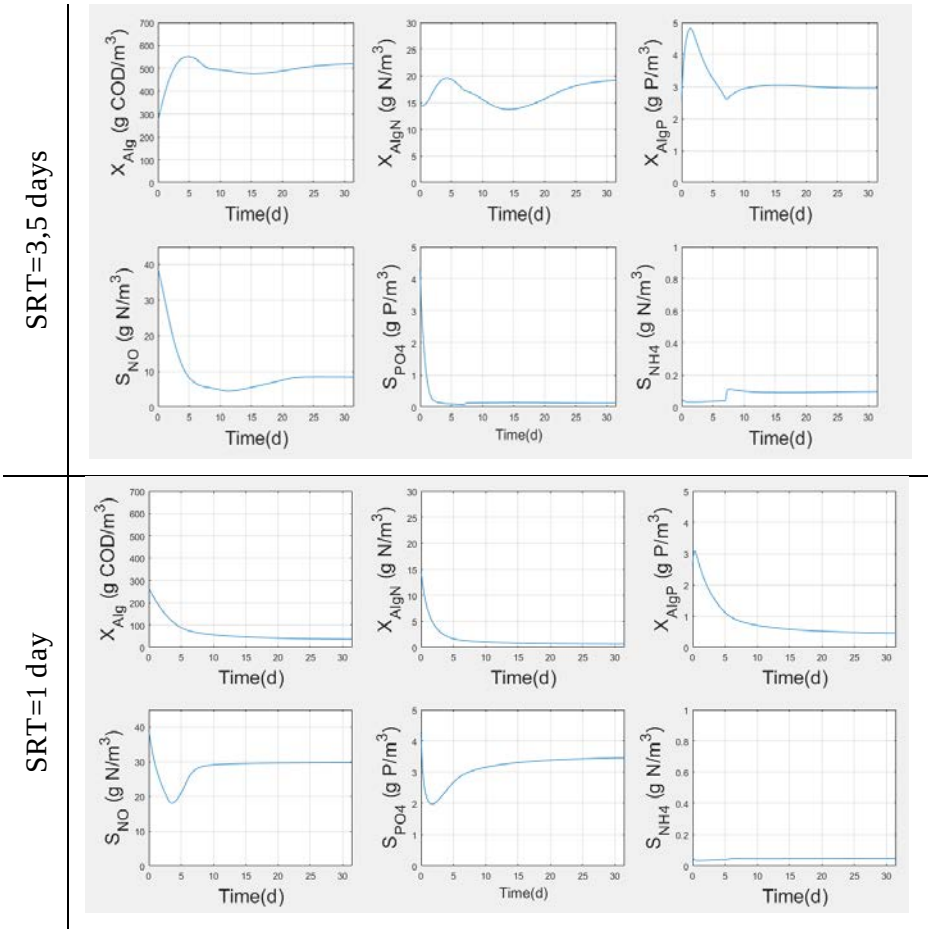

Figure 4-9 Results of the simulation of R2 using SRT=3,5 days (above) and using SRT=1 day (below)

4.3.2 System layout: the problem and the solution

As previously mentioned in *Materials and methods - Continuous flow PBRs* two system layout were tested. Firstly, the experiment was started with the effluent extraction point on the top of the reactors as shown in Figure 4-10.

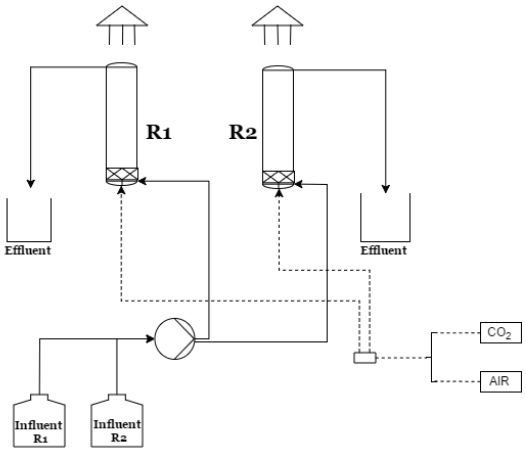

Figure 4-10 System layout 1: Effluent extraction point on the top of the reactor

Using this layout, it was clear that something was not right, because the biomass in the reactors was decreasing, in spite of what was expected based on the simulations previously done. After 15 days, the algae biomass was so reduced and weakened (from 0,1 gTSS/l at Day 1 to 0,02 gTSS/l at Day 15) that other microorganisms (Figure 4-11) contaminated the reactors.

Figure 4-11 Picture of the culture that shows the contamination

Since at that moment the causes were not clear, the experiment was started again with the same setting. In less than 24 hours from the beginning of the experiment, the loss of biomass in both reactors was so pronounced that it was clear that the biomass was washed out from the reactors through the effluent (Table 4-2). In R2, from Day 1 to Day 2 around 0,26 g of biomass was washed out and the same happened in R1. This suggests that SRT and HRT were separated and the biomass was harvested from the top of the reactor through air flotation.

Table 4-2 TSS values in R2 and its effluent at Day 1 and Day 2

	TSS [g/l]	
	Day 1, h=14:00	Day 2, h=09:30
R2	0,220	0,033
Effluent	-	0,805

The cause of this problem was identified in the high airflow, which promoted the floatation of the biomass to the top of the reactors where the extraction point was set.

The designed solution consisted in:

1) Decreasing the airflow as much as possible while maintaining proper mixing;
2) Moving the effluent extraction point from the top to the middle of the reactors (Figure 4-12).

This second system layout was successful and it was used to run the experiment. Its results are presented in the next paragraphs.

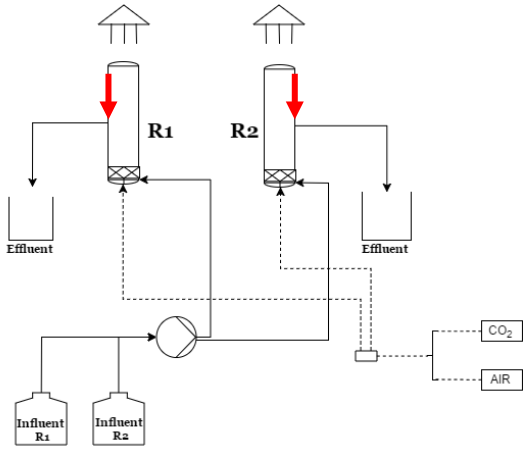

Figure 4-12 System layout 2: Effluent extraction point from the middle of the reactor

4.3.3 Nutrients and biomass

During the experiment, the biomass and the concentrations of the main nutrients in both the solid and liquid the phase were monitored. The main nutrients investigated were nitrogen and phosphorus, since they are the most critical ones for green microalgae growing photoautotrophic, as describe in *State of art - Green microalgae cultivation* . The results obtained from both of the reactors are presented and discussed together in the next paragraphs. Indeed, the idea is to underline the differences between the reference reactor (R1)

and the reactor subjected to the changes described in *Materials and methods - Continuous flow PBRs* (R2).

Biomass

As described in *Materials and methods - Biomass*, the biomass in the two reactors was monitored by measuring the total suspended solids concentration (TSS) and by measuring the optical density (OD) at 750 nm. These two measurements were found to be consistent with each other as shown in Figure 4-13. Since OD shown less scattering than TSS, it has been chosen as the most appropriate parameter to represent the biomass concentration in the reactors.

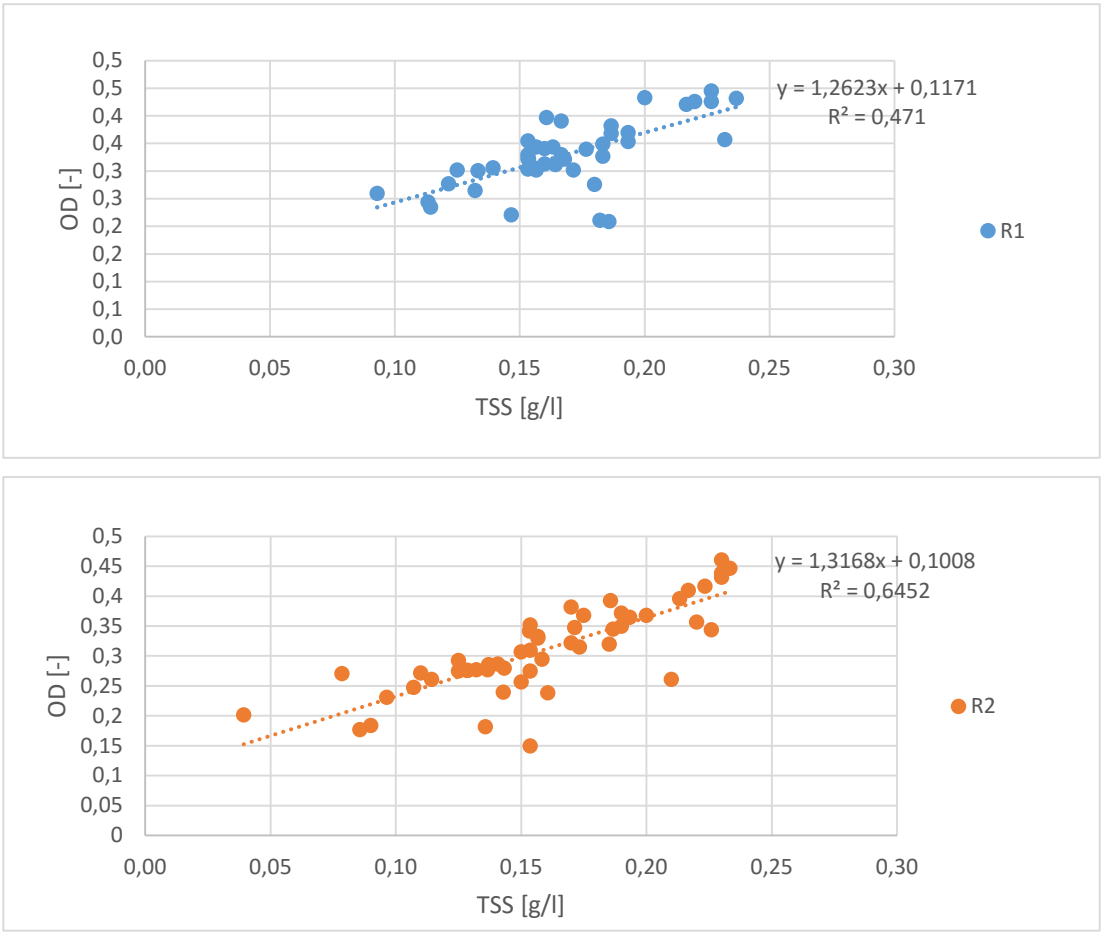

Figure 4-13 Relationship between OD [-] and TSS [g/l] in both reactors

To compare the reactors, it was critical that the two reactors were initialized identically and then run in parallel. To ensure that these conditions were met, among other variables the biomass was monitored. To show the trend of the biomass concentration in the reactors, the

measurements of OD along the experiment in both reactors are reported in Figure 4-14. Despite the biomass changes in the reactors along the experiment, the two reactors were running in parallel in period 1, when they were subjected to the same conditions (average difference around 0,01). A slight gap was manifested during period 2 (average difference 0,05). In particular, R2, under limited nitrogen supply due to the decreasing of N-to-P ratio from 17 molN/molP to 10 molN/molP, showed a lower level of biomass. Despite this, as soon as R2 was subjected again to the same conditions of R1 in period 3, its biomass went back to the same level of R1 after circa 5 days.

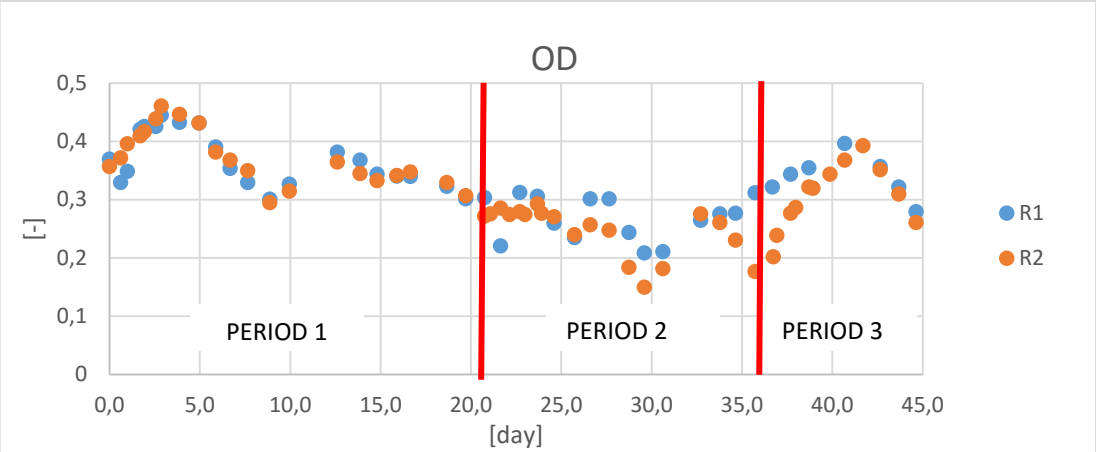

Figure 4-14 OD along the experiment in both reactors

Two conclusions can be draw from the above analysis:

1) Green microalgae have shown the capacity to survive a period of limited nitrogen supply and to go back to the previous equilibrium, when subjected to the same conditions. This aspect may be essential, not only in a WWTP, where the input conditions can easily vary, but also and especially in the TRENS system, where as described in *Background and Motivations - PBR*, the influent to the PBRs regularly suffers of drops in the N-to-P ratio.
2) It seems that a limited supply of nitrogen has only slight consequences on the production of biomass. Anyhow, this aspect should be considered especially when the biomass produced in the PBRs is intended to be harvested for the production of secondary products, for instance biofuel.

Nitrogen

In the PBRs the nitrogen is situated in both the liquid phase and solid phase, i.e. as storage in the green microalgae cells. In the liquid phase, it is present in form of $NH4^{+}$, $NO3^{-}$ and $NO2^{-}$.

As shown in Figure 4-15, in R1 and R2 the levels of nitrate in the effluent and the internal nitrogen quota have remained similar until Period 2 started. During Period 2, the limitation of the influent nitrogen in Reactor 2 affected both the concentration of nitrate in the effluent and the internal nitrogen quota, leading to a visible difference between Reactor 1 and Reactor 2.
The data collected during Period 2 highlighted a remarkable and unexpected result. Before consuming the nitrogen compounds in the surrounding environment, the culture had depleted its nitrogen storage. Only after few days (circa 1 SRT), when the culture got used to the new condition, it increase the consumption of nitrate the nitrite in the medium, increasing its internal nitrogen quota again. According to Benavente-Valés et al. (2016), when green microalgae are subjected to a period of nitrogen starvation, they decrease their activity and they can start using their chlorophyll as nitrogen source. Consequently, as long as they are not used to the new condition, less nitrogen is uptaken from the surrouding environment and the stored nitrogen is consumed. Afterwards, they increase their capacity to uptake nitrogen from the liquid phase consuming almost all the avaiable one, thus they can restore their optimal internal nitrogen quota. During Period 3, the nitrate concentration in Reactor 2 has remained lower than in Reactor 1 for few days (circa 1 SRT) before getting to the same condition of Reactor 1. This may be due to the fact that as soon as the culture has more nitrogen in the medium, it starts consuming a higher quantity of nitrogen than expected, i.e. as R1.
Consequently, the removal of nitrogen reached in Reactor 2 resulted higher than in Reactor 1. Indeed, they reached respectively 81% ± 11,9 and 62% ± 5,5 of nitrogen removal. This aspect is interesting especially in the wastewater treatment field, where higher removal of nitrogen correspond to lower costs. It is also important from a resource recovery perspective, whereby the more nitrogen is stored inside the biomass, the more applicable it is for fertigation.

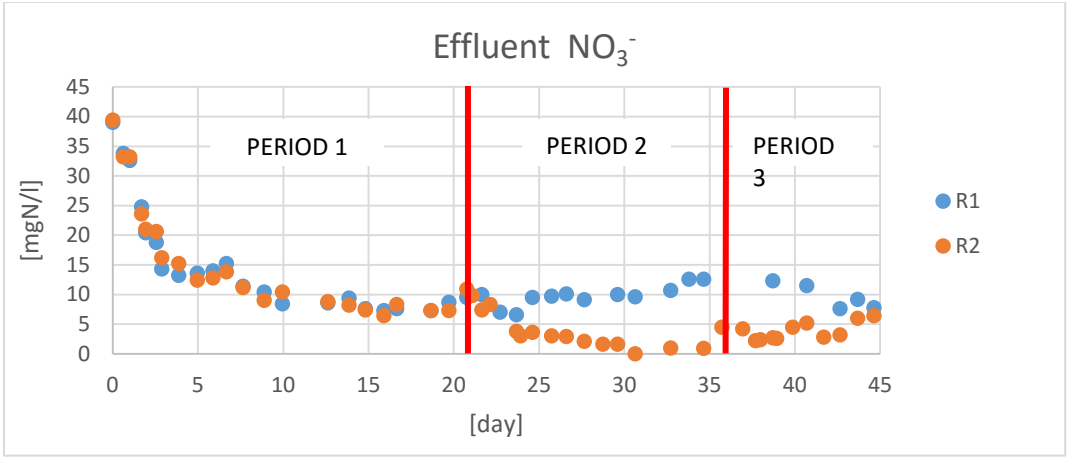

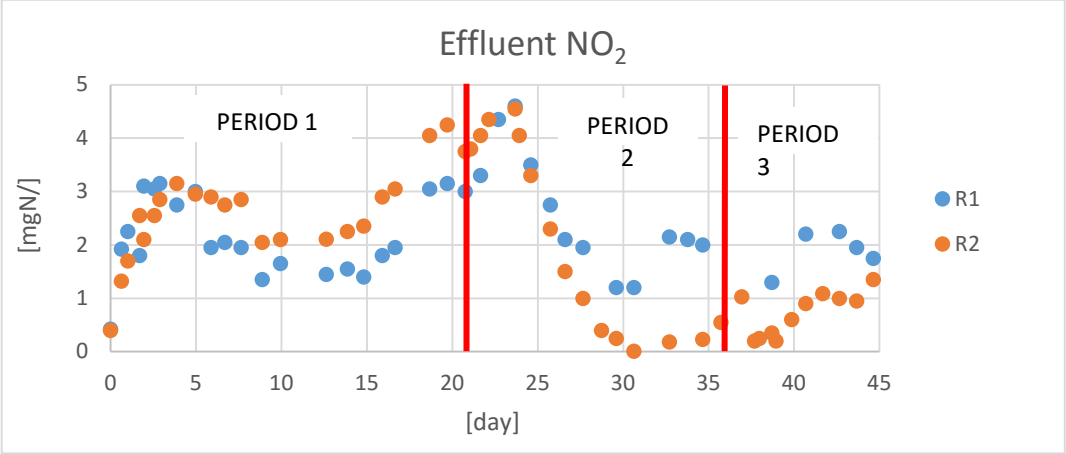
Effluent NO_2
PERIOD 1
PERIOD 2
PERIOD 3
[mgN/]
[day]
R1
R2

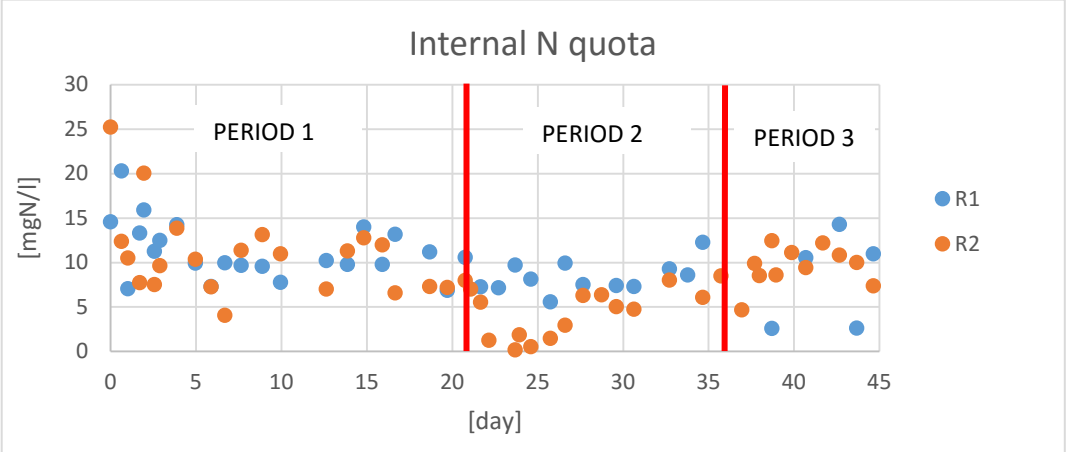
Internal N quota
PERIOD 1
PERIOD 2
PERIOD 3
[mgN/l]
[day]
R1
R2

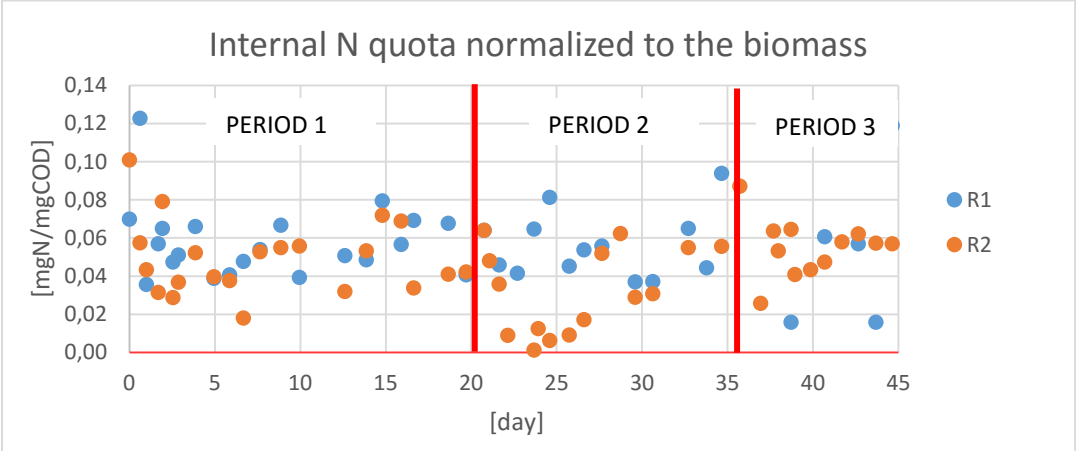
Internal N quota normalized to the biomass
PERIOD 1
PERIOD 2
PERIOD 3
[mgN/mgCOD]
[day]
R1
R2

Figure 4-15 Nitrogen concentration in the liquid phase and in the cells in both reactors along the experiment

Mass balance

The mass balance of the experimental data was checked and a consistent gap was found between the influent nitrogen and the effluent nitrogen.
The most likely cause may be a poor measurement accuracy. Indeed, first of all a minimum of uncertainty in the experimental data has to be always considered.
Secondly, in this case, some concerns have been raised regarding the measurement of the total nitrogen (TN). Indeed, the actual capacity of the method of being able to extract the nitrogen from the green microalgae cells was never ascertained. Since in literature it is reported that is in general difficult to extract proteins and lipids from the green microalgae cells, it could be that this method has the same issues towards components rich in nitrogen.

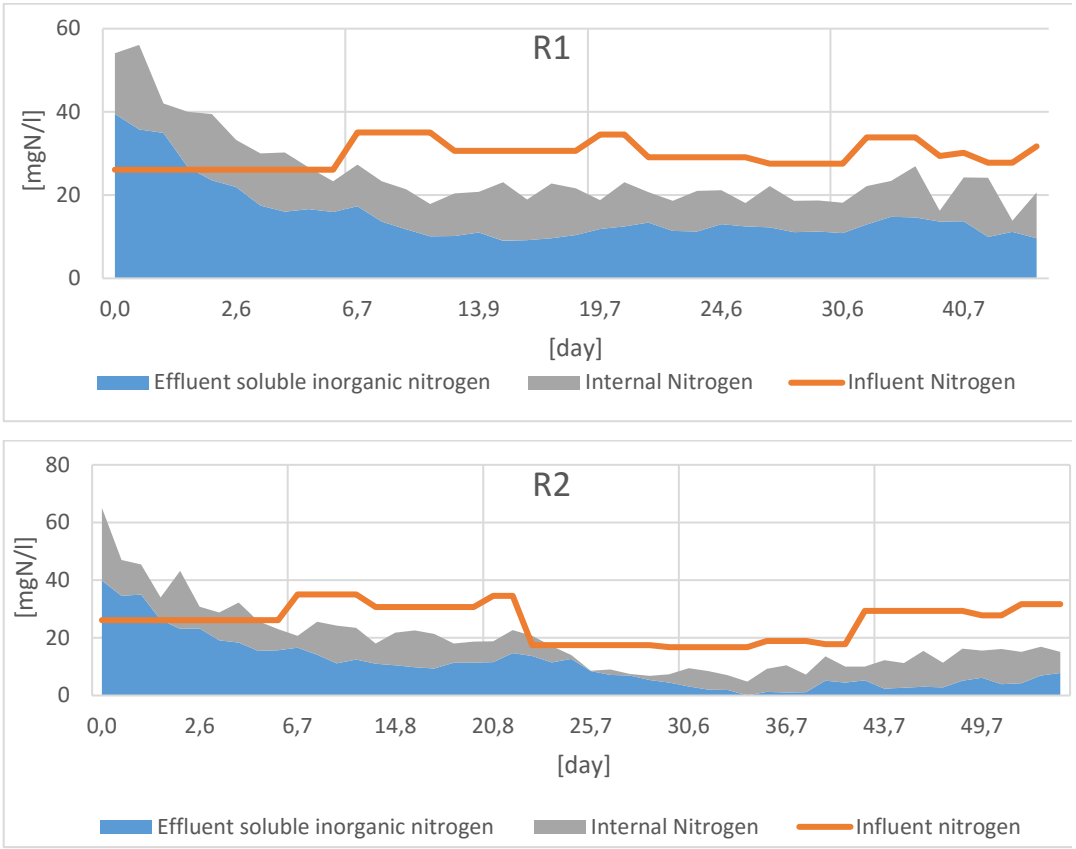

Figure 4-16 Nitrogen mass balance along the experiment for both reactors

Phosphorus

As previously described for the nitrogen, phosphorus was monitored both in the liquid phase, in form of phosphate, and in the green microalgae cells. As show in Figure 4-17, in the two reactors, the level of phosphate in the effluent and the level of the phosphorus in the green microalgae cells have remained similar along the experiment, even during Period 2.

This means that, when green microalgae have less nitrogen in the surrounding environment, the removal of phosphorus is not compromised.

This is another important aspect for the wastewater treatment field, where the variation of the influent in terms of nitrogen content cannot compromise the efficiency of the treatment in its entirety.

In this experiment, the removal of phosphorus reached in both reactors was a little bit higher than 55%. Therefore, an average of 2 mgP/l was removed by green microalgae on an input of around 4 mgP/l.

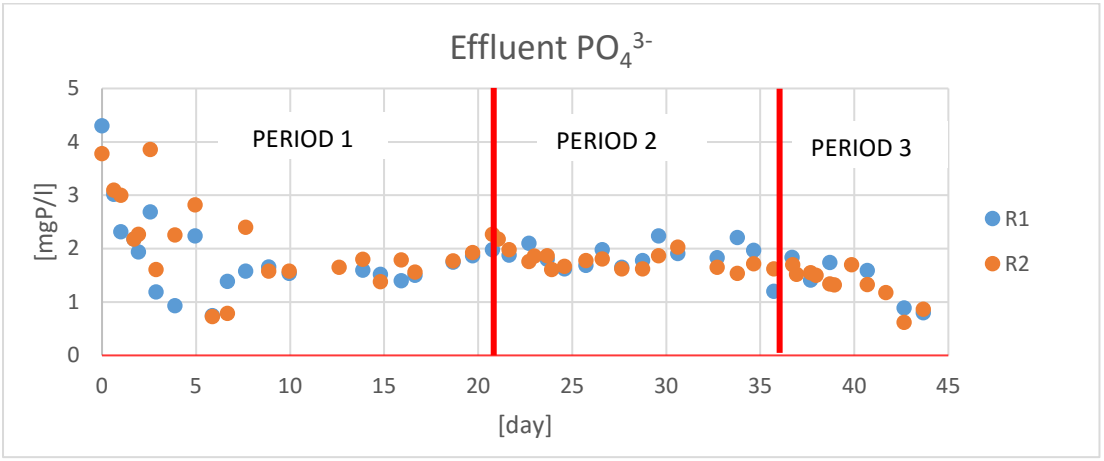

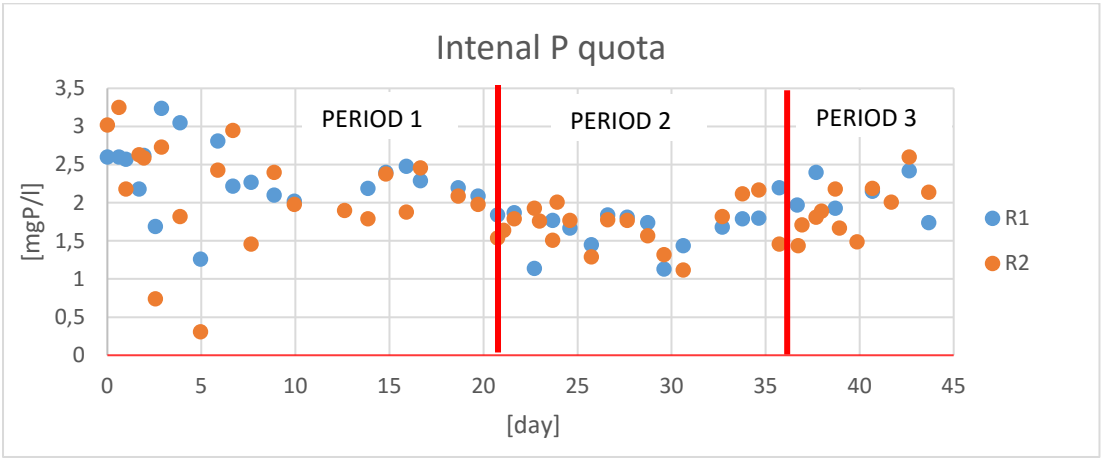

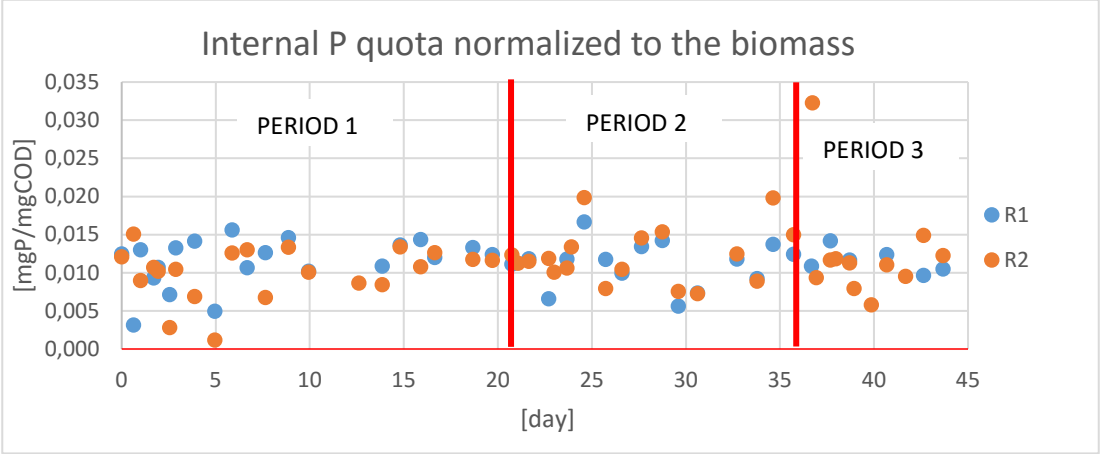

Figure 4-17 Phosphorus concentration in the liquid phase and in the cells in both reactors along the experiment

Mass balance

Differently from the nitrogen case, the overall mass balance for the phosphorus was found to be respected. The error is around 4,3% for both reactors and it is acceptable considering the possible errors occurring during sampling and measurement.

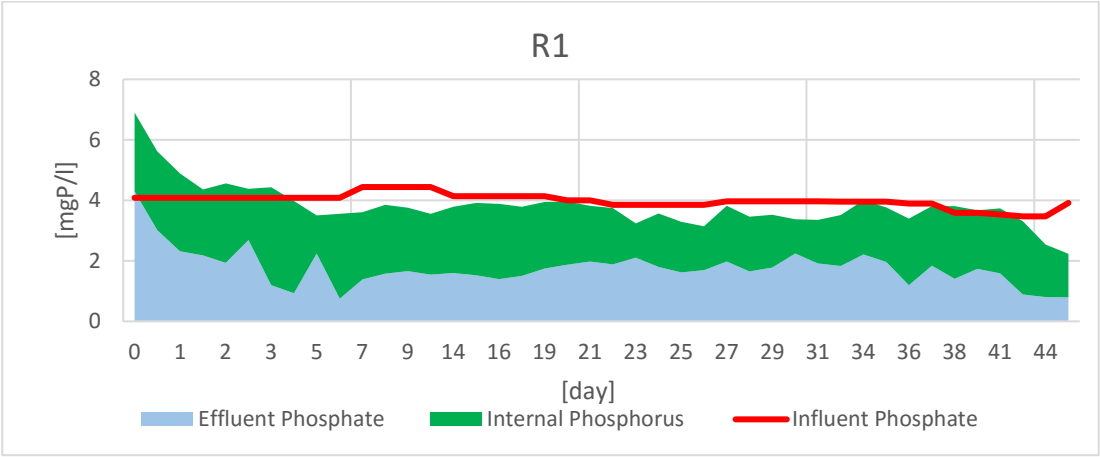

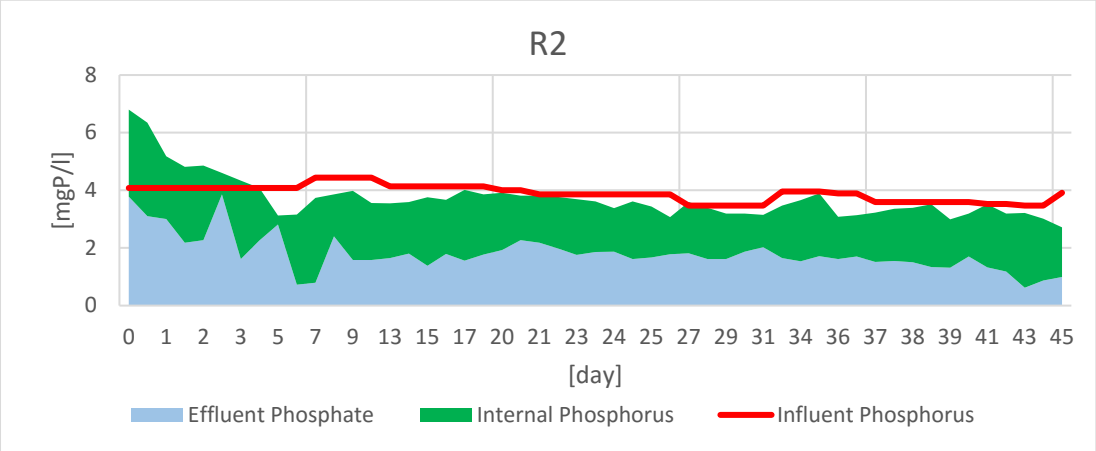

Figure 4-18 Phosphorus mass balance along the experiment for both reactors

4.4 Green microalgae culture history and the nutrients uptake and storage

One of the aim of this work was to verify the existence of a link between the history of the culture and its uptake and storage of nutrients. With this purpose, two batches were run as described in *Materials and methods - 1.2 L s.* The cultures used in these experiments were exposed to the same N-to-P ratio during the experiments, but they had two different histories: one was used to grow in a medium with 17 N-to-P ratio (17-17 Batch), the other was used to grow in a medium with 10 N-to-P ratio (10-17 Batch). To assess the differences in the nutrients uptake and storage in the two cases, two parameters sets where estimated, one for each case, as described in the following paragraphs.

4.4.1 ASM-A MODEL: Parameters estimations

The method Latin Hypercube Sampling based Simplex (LHSS) was used to estimate the kinetic parameters and to assess their identifiability. It is described in details in *Materials and methods - Parameters estimation*, but more informations can be found in Wágner et al.(2016).

17-17 Batch

Before starting the parameters estimation, a simulation of this experiment, using the parameters set given by Wágner et al. (2016), was run to verify the necessity of the parameters estimation itself. As shown in Figure 4-19, the prediction of the model in this case is inaccurate, especially regarding the growth of the biomass, which in turn influences the other variables. The sum of RMSNE resulted equal to 3,60.

Hence, there is a need to find a new set of kinetic parameters.

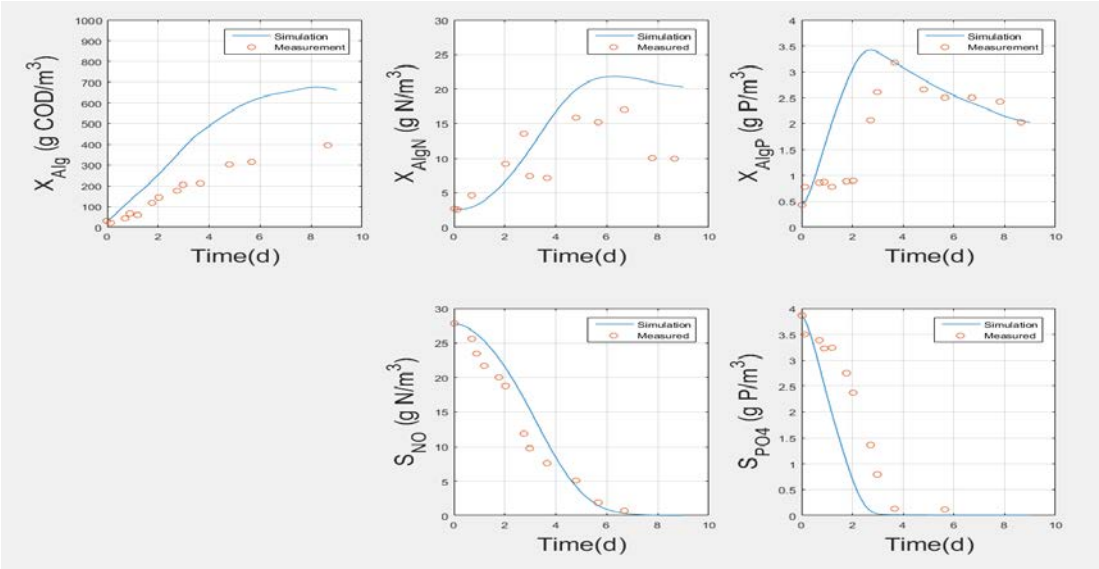

Figure 4-19 Simulation of 17-17 Batch with the set of parameters given by Wágner (2016)

Parameters estimation

The estimated set of parameters is reported in Table 4-3.

Table 4-3 Parameters set estimated for 17-17 Batch and parameters set from Wagner, et al. (2016)

Parameters	**Estimated**		**Wagner, et al. (2016)**
	Mean	**Standard deviation**	**Mean**
$\mu_{A,max}$ (d^{-1})	2,90	0,2965	4,12
$K_{NO,Alg}$ ($gN \cdot m^{-3}$)	13,96	1,4912	12,61
$K_{PO4,Alg}$ ($gP \cdot m^{-3}$)	3,42	1,1887	4,49
$k_{NO,Alg}$ ($gN \cdot g^{1}COD \cdot d^{-1}$)	0,074	0,0135	0,043
$k_{PO4,Alg}$ ($gP \cdot g^{-1}COD \cdot d^{-1}$)	0,075	0,0299	0,16
b_{Alg} (d^{-1})	0,48	0,0225	0,21

The prediction of the model using the new kinetic parameters is shown in Figure 4-20. If these results are compared to the ones shown in Figure 4-19, which were obtained using the parameters set proposed in Wágner et al. (2016), a good improvement can be seen especially regarding the prediction of algal biomass, internal phosphorus quota and phosphate. Moreover, the improvement is quantifiable comparing the sum of RMSNE of the simulations. Indeed, it is reduced from 3,60 to 2,30 giving a Janus coefficient of 0,64.

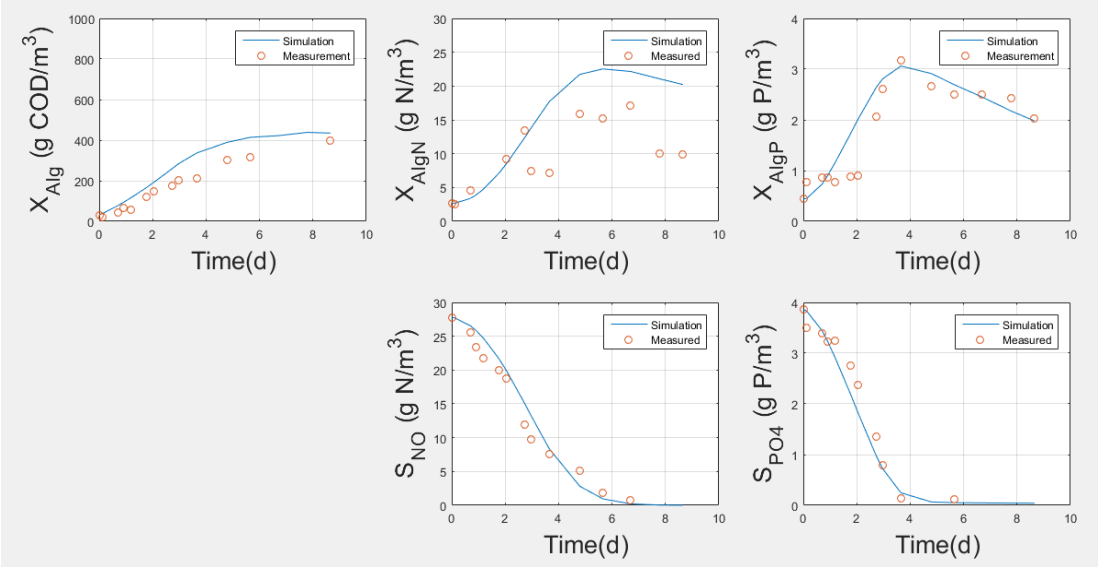

Figure 4-20 Simulation of 17-17 Batch with the estimated parameters set

Identifiability

In accordance with what is described in *Materials and methods - Identifiability analysis*, the identifiability of the parameters was assessed.

The standard deviations reported in Table 4-3 are relatively low considering the respective parameter values and the parameters distribution represented in the histograms in Table 4-4 can be considered narrow. Nevertheless, based on the correlation matrix (Table 4-4) some parameters ($\mu_{A,max}$ and $k_{NO,Alg}$; $\mu_{A,max}$ and $k_{PO4,Alg}$; $K_{PO4,Alg}$ and $k_{PO4,Alg}$) seems to be correlated.

Table 4-4 Parameters distribution and correlation matrix

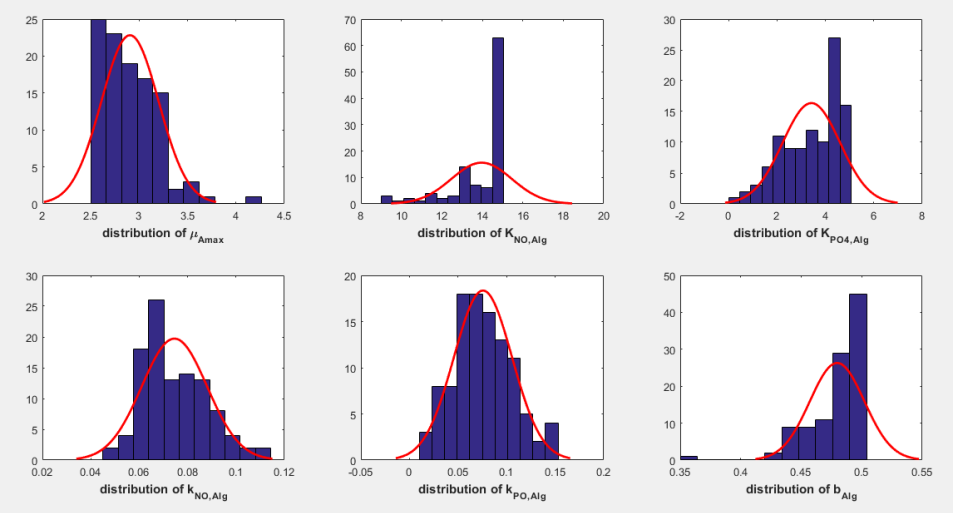

	$\mu_{A,max}$ (d^{-1})	$K_{NO,Alg}$ ($gN \cdot m^{-3}$)	$K_{PO4,Alg}$ ($gP \cdot m^{-3}$)	$k_{NO,Alg}$ ($gN \cdot g^{-1}COD \cdot d^{-1}$)	$k_{PO4,Alg}$ ($gP \cdot g^{-1}COD \cdot d^{-1}$)	b_{Alg} (d^{-1})
$\mu_{A,max}$ (d^{-1})	1					
$K_{NO,Alg}$ ($gN \cdot m^{-3}$)	0,1263	1				
$K_{PO4,Alg}$ ($gP \cdot m^{-3}$)	-0,2424	-0,2906	1			
$k_{NO,Alg}$ ($gN \cdot g^{-1}COD \cdot d^{-1}$)	-0,7337	0,4247	-0,0396	1		
$k_{PO4,Alg}$ ($gP \cdot g^{-1}COD \cdot d^{-1}$)	-0,6719	-0,3477	0,7728	0,3794	1	
b_{Alg} (d^{-1})	-0,0712	0,089	0,3215	0,3102	0,2971	1

To verify the actual presence of a correlation between these parameters, the impact of the parameters variability on the model output was assessed. To this aim, the simulation results using the values of the parameters on the boundaries given by their standard deviations were compared with the simulation results using the mean values of the parameters. The parameters chosen for this purpose were $\mu_{A,max}$ and $k_{PO4,Alg}$. To compare the results, Janus coefficients were calculated and, as reported in Table 4-5, a low variation in the model output was found in each case, because the Janus coefficients were ~ 1. Therefore, the parameters are considered identifiable.

Table 4-5 Janus coefficients used to assess the impact of the parameters variability on the model output

	$\mu_{A,max}$ + sd	$\mu_{A,max}$ - sd	$k_{PO4,Alg}$ + sd	$k_{PO4,Alg}$ - sd
Janus coefficient	1,1680	1,0554	1,0825	1,0647

4.4.2 10-17 Batch

The procedure used for Batch 17-17 was applied verbatim to Batch 10-17.

To assess the need of the parameters estimation, a simulation using the parameters set given by Wágner (2016) was run. From Figure 4-21, it can be seen that the prediction of the model fails in particular regarding the biomass and the phosphate. Therefore, a new set of kinetic parameters needs to be estimated. The sum of RMSNE resulted equal to 2,96.

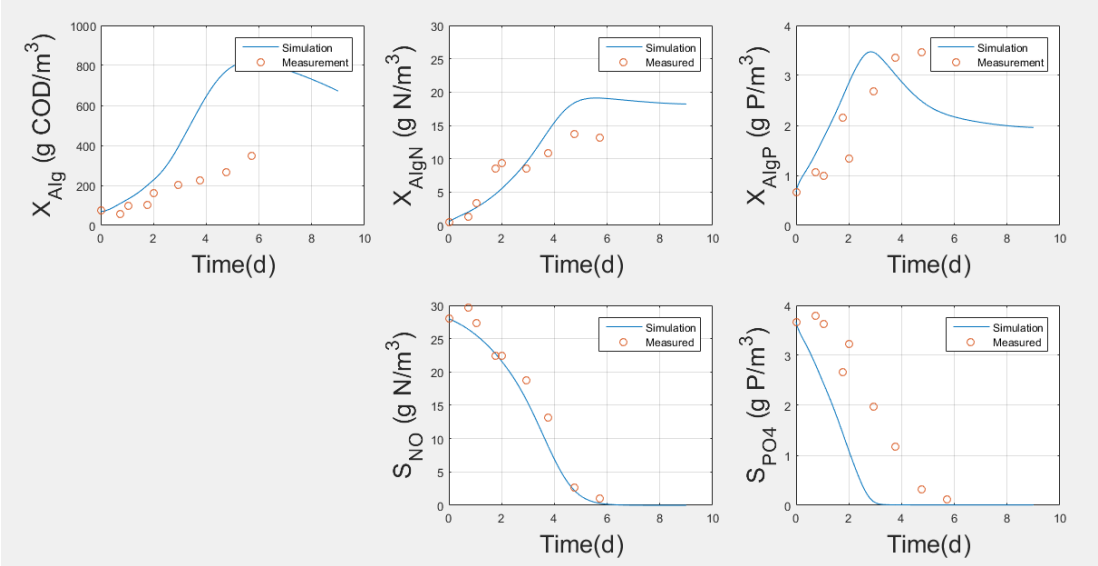

Figure 4-21 Simulation 10-17 Batch with parameters set given by Wágner (2016)

Parameters estimation

The parameters set estimated is reported in Table 4-6.

Table 4-6 Parameters set estimated for 10-17 Batch

Parameters	Estimated		Wagner, et al. (2016)
	Mean	Standard deviation	Mean
$\mu_{A,max}$ (d^{-1})	3,18	0,4365	4,12
$K_{NO,Alg}$ ($gN \cdot m^{-3}$)	12,49	2,7716	12,61
$K_{PO4,Alg}$ ($gP \cdot m^{-3}$)	4,70	0,4770	4,49
$k_{NO,Alg}$ ($gN \cdot g^{1}COD \cdot d^{-1}$)	0,074	0,0144	0,043
$k_{PO4,Alg}$ ($gP \cdot g^{-1}COD \cdot d^{-1}$)	0,042	0,0113	0,16
b_{Alg} (d^{-1})	0,48	0,0187	0,21

The prediction of the model using the new kinetic parameters is shown in Figure 4-22. Comparing these results with the ones shown in Figure 4-21, which were obtained using the parameters set proposed in Wágner (2016), a good improvement can be seen especially regarding the prediction of algal biomass and phosphate. Moreover, the improvement is observable comparing the sum of RMSNE of the simulations. Indeed, it is changed from 2,96 to 1,54 giving a Janus coefficient of 0,52.

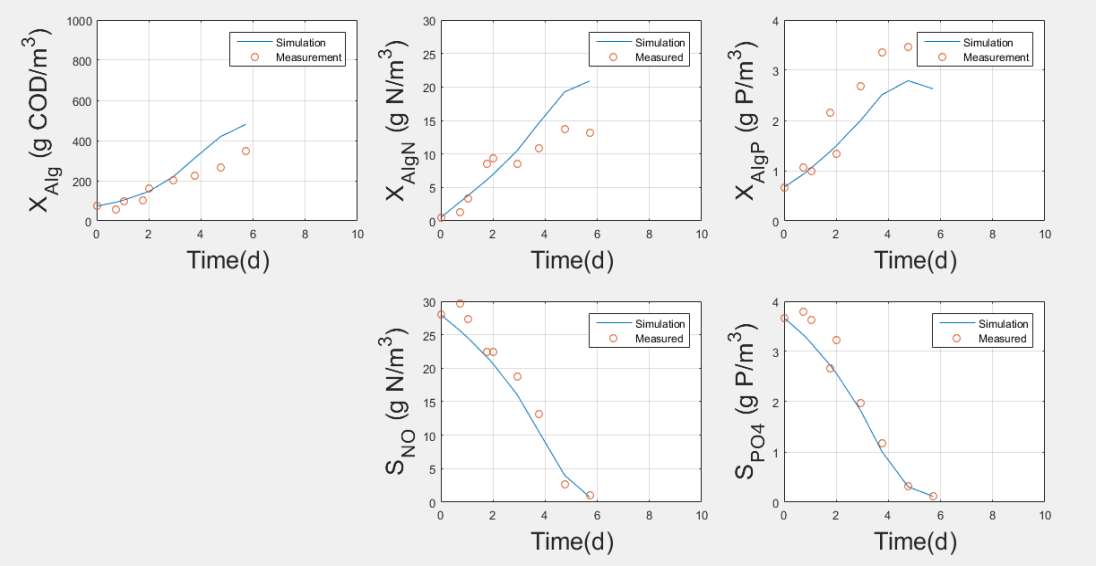

Figure 4-22 Simulation of 10-17 Batch with the estimated parameters set

Identifiability

As done for 17-17 Batch, the identifiability of the parameters was assessed following the method reported in *Materials and methods - Identifiability analysis.* The standard deviations in Table 4-6 are relatively low considering the respective parameter values and the parameters distribution represented in the histograms in Table 4-7 can be considered narrow. Nevertheless, based on the correlation matrix in Table 4-7 some parameters ($\mu_{A,max}$ and $k_{NO,Alg}$; $\mu_{A,max}$ and $k_{PO4,Alg}$; $K_{NO,Alg}$ and $k_{PO4,Alg}$; $K_{PO4,Alg}$ and $k_{PO4,Alg}$) result correlated.

Table 4-7 Parameters distribution and correlation matrix

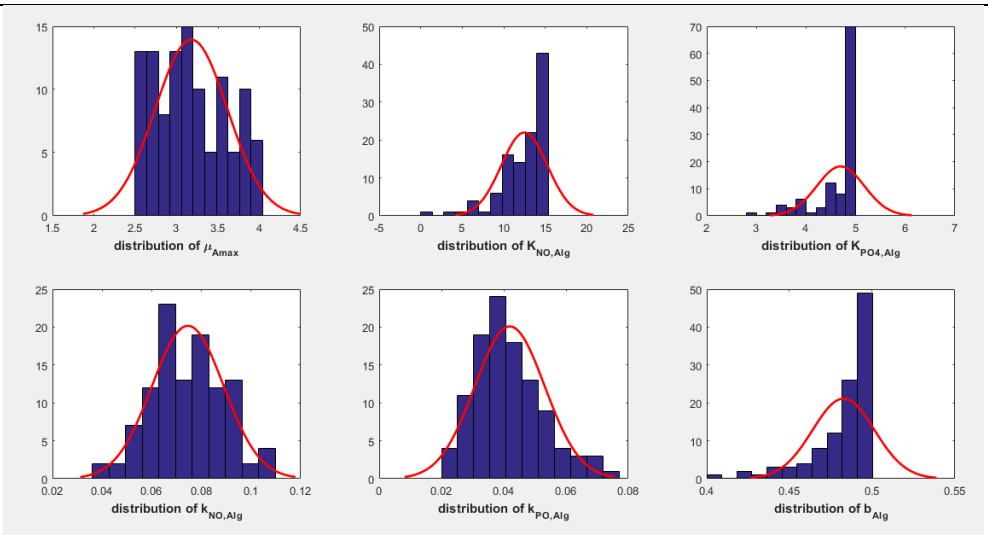

	$\mu_{A,max}$ (d^{-1})	$K_{NO,Alg}$ ($gN \cdot m^{-3}$)	$K_{PO4,Alg}$ ($gP \cdot m^{-3}$)	$k_{NO,Alg}$ ($gN \cdot g^{-1}COD \cdot d^{-1}$)	$k_{PO4,Alg}$ ($gP \cdot g^{-1}COD \cdot d^{-1}$)	b_{Alg} (d^{-1})
$\mu_{A,max}$ (d^{-1})	1	0,1439	-0,136	-0,6659	-0,7657	0,2355
$K_{NO,Alg}$ ($gN \cdot m^{-3}$)	0,1439	1	-0,189	0,5916	-0,3035	0,3201
$K_{PO4,Alg}$ ($gP \cdot m^{-3}$)	-0,136	-0,1892	1	-0,1311	0,5432	0,0651
$k_{NO,Alg}$ ($gN \cdot g^{-1}COD \cdot d^{-1}$)	-0,666	0,5916	-0,131	1	0,3536	0,1552
$k_{PO4,Alg}$ ($gP \cdot g^{-1}COD \cdot d^{-1}$)	-0,766	-0,3035	0,543	0,3536	1	0,0171
b_{Alg} (d^{-1})	0,2355	0,3201	0,065	0,1552	0,0171	1

Equally to what was done for 17-17 Batch, to verify the actual presence of a correlation between these parameters, the impact of the parameters variability on the model output was assessed. The parameters chosen for this purpose were $\mu_{A,max}$, $k_{PO4,Alg}$ and $K_{NO,Alg}$.

The Janus coefficients calculated (Table 4-8) were around 1, therefore, a low variation in the model output was found in each case. Consequently, the parameters are considered identifiable.

Table 4-8 Janus coefficients used to assess the impact of the parameters variability on the model output

	$\mu_{A,max}$ + sd	$\mu_{A,max}$ - sd	$k_{PO4,Alg}$ + sd	$k_{PO4,Alg}$ - sd	$K_{NO,Alg}$ +sd	$K_{NO,Alg}$ -sd
Janus coefficient	1,2724	1,1095	1,0686	1,0421	0,9851	1,1184

Comparison of the results, culture history effects and the average parameters set

Once the estimation was finished, the two parameters sets were compared to assess the presence of a link between the history of the culture and its uptake and storage of nutrients. Based on a qualitative evaluation, the two sets did not show significant differences. Indeed, for each parameter it is possible to observe an overlapping of the variation ranges (Figure 4-23). This means that no significant effect of the history of the culture on the uptake and storage of nutrients was found in these experiments. However, it has to be noted that the framework, where the issue of the effect of the history on the behavior of the culture was first raised (Wágner et al., 2016), was slightly different from the experiments carried out in this work. Indeed, the culture was different. Here a monoculture of *Chlorella sp.* was cultivated, there they had a mixed culture of *Chlorella sp.* and *Scenedesmus sp.*. Therefore, possibly the internal change of the culture composition is a crucial factor for the manifestation of this issue.

Table 4-9 Estimated parameters sets and the average parameters set

Parameters	17-17 Batch		10-17 Batch		Average	
	Mean	Standard deviation	Mean	Standard deviation	Mean	Standard deviation
$\mu_{A,max}$ (d^{-1})	2,90	0,2965	3,18	0,4365	3,04	0,528
$K_{NO,Alg}$ ($gN \cdot m^{-3}$)	13,96	1,4912	12,49	2,7716	13,22	3,147
$K_{PO4,Alg}$ ($gP \cdot m^{-3}$)	3,42	1,1887	4,70	0,4770	4,06	1,281
$k_{NO,Alg}$ ($gN \cdot g^{1}COD \cdot d^{-1}$)	0,074	0,0135	0,074	0,0144	0,074	0,020
$k_{PO4,Alg}$ ($gP \cdot g^{-1}COD \cdot d^{-1}$)	0,075	0,0299	0,042	0,0113	0,059	0,032
b_{Alg} (d^{-1})	0,48	0,0225	0,48	0,0187	0,48	0,029

Considering the relatively low discrepancy between the two sets of parameters estimated, it seemed appropriate to test the operation of the model using an average parameters set, that could potentially fit for both cases. The average parameters set was easily calculated doing an average of the estimated two parameters sets, while the standard deviation were calculating using Equation 4-2. (Table 4-9).

$$SDx_{Av} = \sqrt{SDx_{17-17}^2 + SDx_{10-17}^2}$$

Equation 4-2 Standard deviation for average parameter set calculation

Where:

SD_{AV}= Standard deviation of parameter x of the average parameter set

$SDx_{17\text{-}17}$= Standard deviation of parameter x of the 17-17 Batch parameter set

$SDx_{10\text{-}17}$= Standard deviation of parameter x of the 10-17 Batch parameter set

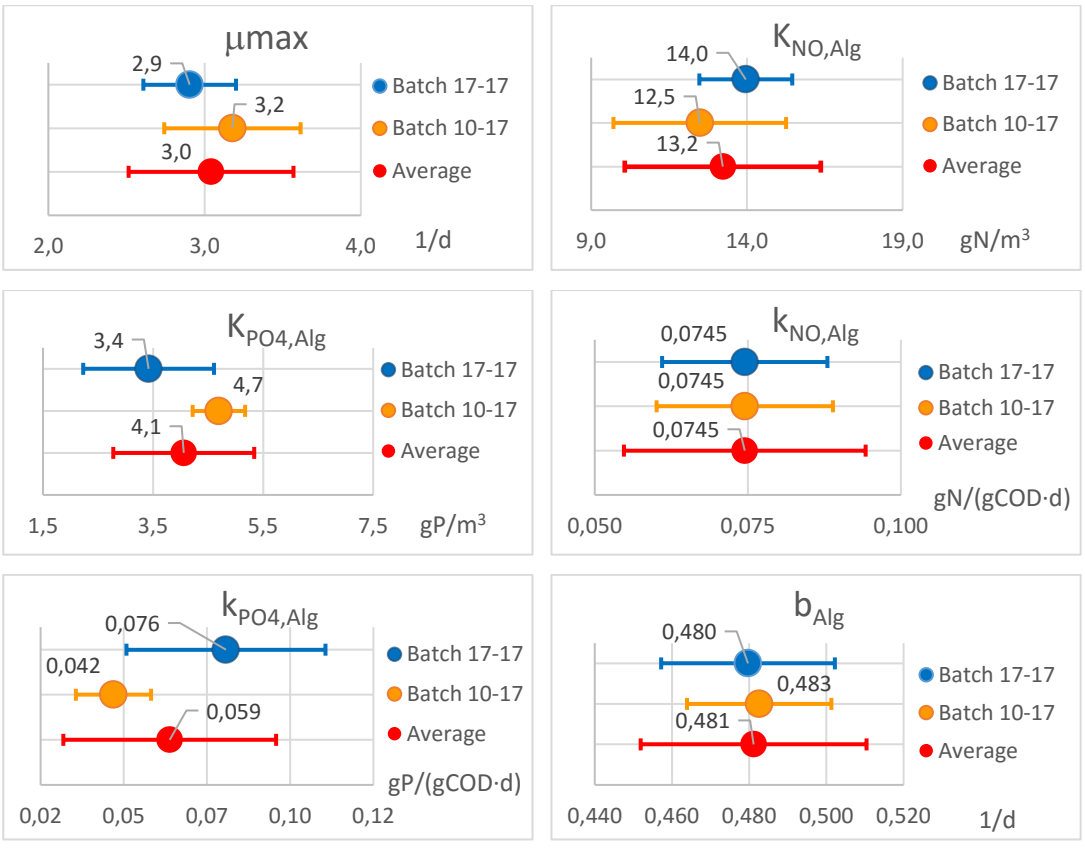

Figure 4-23 Comparison of the variation ranges of the three parameters set involved

To assess the feasibility of the use of the average parameters set, simulations of 17-17 Batch and of 10-17 Batch were run using this new set. Once again, the Janus coefficient was used to

compare the results of these simulations with the simulations previously performed with the parameters sets estimated in this chapter.

Table 4-10 Janus coefficients used to compare the simulations done using the average parameters set and the estimated ones for both 17-17 batch and 10-17 Batch

	17-17 Batch	**10-17 Batch**
Janus coefficient	0,9983	1,0760

From the obtained results (Table 4-10), the average parameters set seems to be applicable in both cases, without compromising the model prediction.

To further verify the accuracy of the model using the average parameters set, Monte Carlo simulations were performed (Figure 4-24 and Figure 4-25). The outcomes shown again the applicability of the average parameters set in both cases.

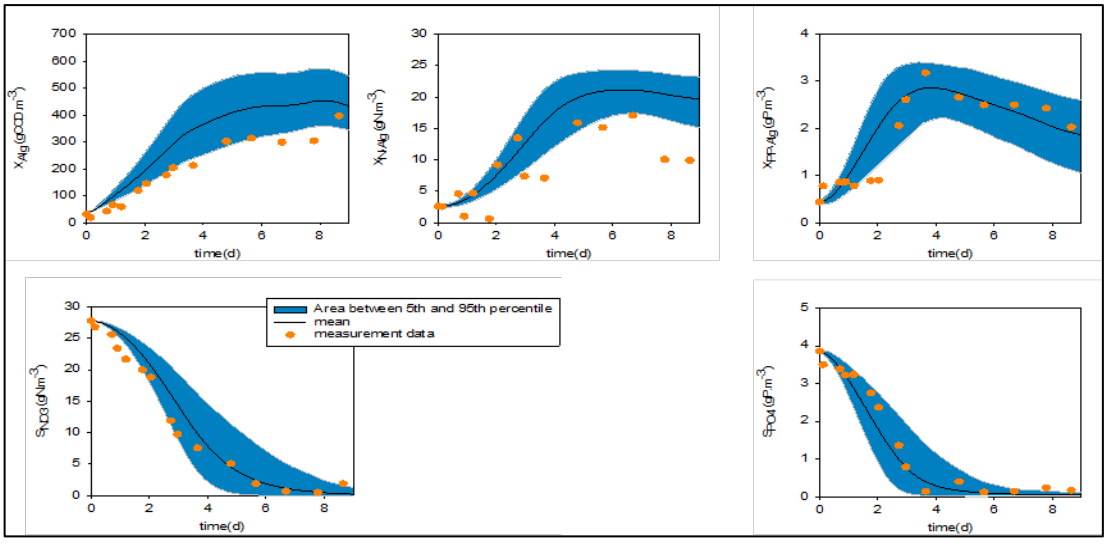

Figure 4-24 Monte Carlo simulation for 17-17 Batch with average parameters set

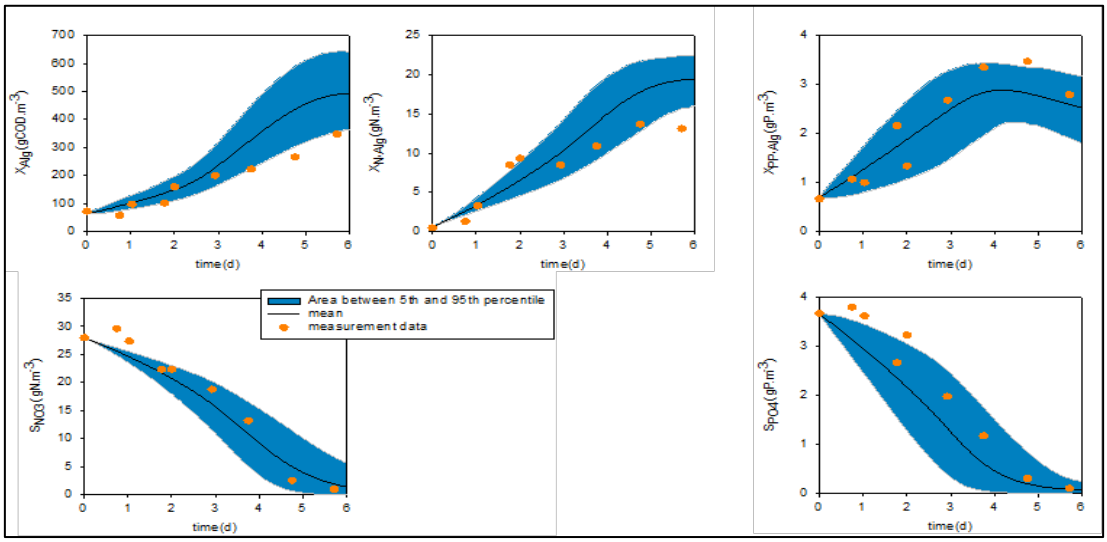

Figure 4-25 Monte Carlo simulation for 10-17 Batch with average parameters set

Validation

The validation of the model with the average parameters set was carried out using the data collected in the first batch experiment described in this work, i.e. the 1-L Batch experiment. Two simulations of this experiment were run: one was run using the parameters set presented by Wágner et al.(2016), the other one using the average parameters set estimated in this study. To compare the results the Janus coefficient was calculated:

$$Janus\ Coefficent\ = 2{,}27$$

This value is higher than the others previously obtained in this chapter, but it is enough close to 1 to ensure the validation of the model. The possible cause of this high value could be the discrepancy between the model's prediction of the soluble phosphate and the collected data. Indeed, the RMSNE is very sensible to the gap between the model prediction and the data, when the data are near to zero. Indeed, it gives more weight to low magnitude values due to the normalization using the experimental data (Hauduc, et al., 2015). About this, see Equation 2-5.

Moreover, as can be seen in Figure 4-26, the trend of the internal phosphorus quota is unexpected, that hardly could have been predicted by the model. The causes of this trend may be errors in the measurements that have compromised the results.

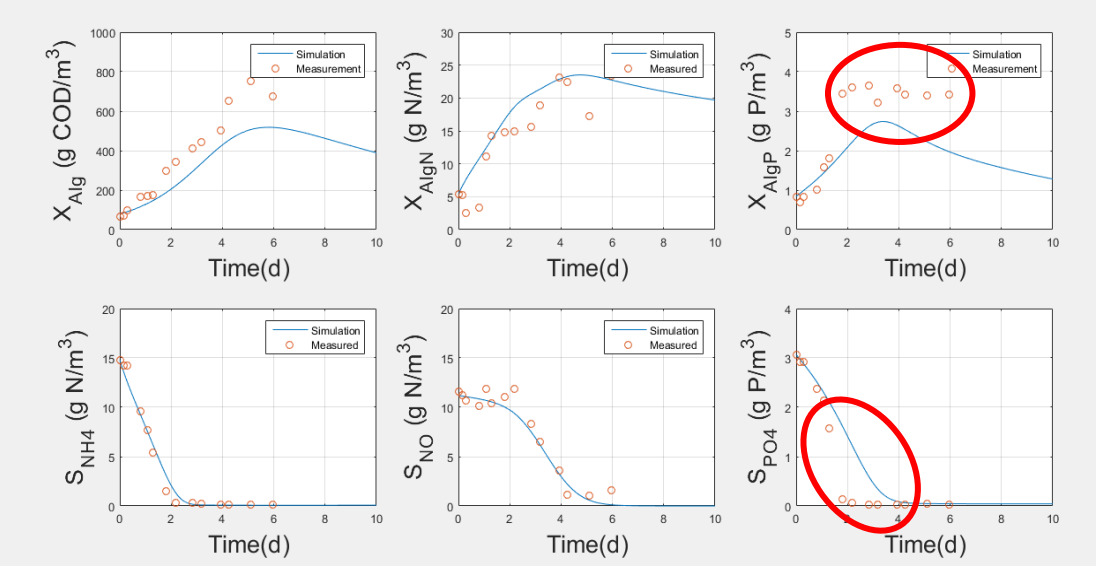

Figure 4-26 Simulation of 1-L Batch using the average parameter set

To further consolidate the validation a Monte Carlo simulations were performed. As can be seen in Figure 4-27, where the results are shown, the observations often either fall out from the area between the 5th and the 95th percentile or on the boundaries of that area. Anyhow, this does not imply the failure of the validation. Indeed, it has to be noticed that for the experiment (1-L Bacth) the input light intensity to the reactor was not monitored, therefore an average light intensity in the reactor was theoretically calculated and assumed constant along the experiment. The effects of this assumption may have caused the underestimation of the biomass production (XAlg) and in turn the underestimation of the phosphorus uptake (SPO4) and storage (XPPAlg).

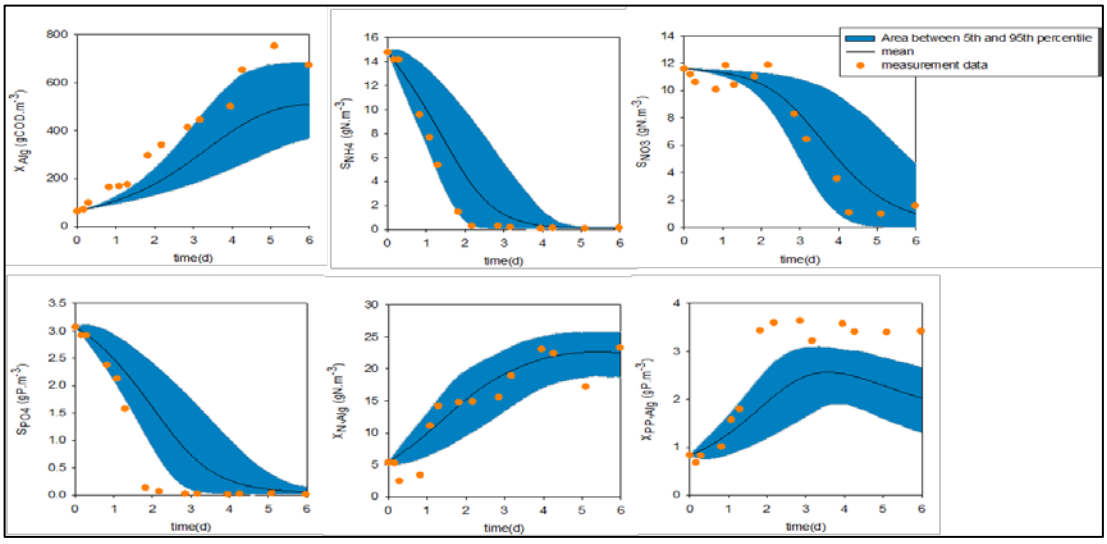

Figure 4-27 Monte Carlo simulation for 1-L Batch with average parameters set

Application of the new parameters set to the continuous PBRs case

The sets of the kinetic parameters estimated in the previous paragraphs were applied with different combinations to simulate the continuous PBRs experiment.

For Reactor 1, which had for the entire experiment an influent N-to-P ratio of 17 molN/molP, the simulations were run using the parameters set from 17-17 Batch and the average parameter set. Instead, for Reactor 2, which had three different influent N-to-P ratio as described in *Materials and methods - Continuous flow PBRs*, different parameters sets within the same simulation were used. One simulation was run using the parameters set from 17-17 Batch for Period 1 and Period 2 and the parameters set from 10-17 Batch for Period 3. The other simulation was run using the average parameters set.

The results are reported respectively in Figure 4-28 and in Figure 4-29. In those figures, the results of the simulations run using the parameters set from Wágner et al.(2016) is reported as well to show the improvements obtained in the model prediction using the new parameters sets.

In both cases, it is clear that a significant improvement is achieved using the new parameters sets instead of the parameters set from Wágner et al. (2016). Moreover, the average parameters set has proven to be the best one for the predictions. These results are interesting, because it means that, once an average parameters set is defined, it is possible to simulate with a good accuracy the trends in the PBR whatever are the conditions which the green microalgae are subjected to.

Despite the good results obtained in both cases, the prediction of the internal nitrogen quota fails at the beginning of Period 2 in R2 when the N-to-P ratio decreased to 10 molN/molP. The simulation does not follow the data (green square) due to the unexpected behavior of the culture in the first days of nitrogen starvation described in *Results and Discussion - Continuous flow PBRs - Nitrogen*, which is not modeled in the ASM-A model.

REACTOR 1
Simulation with the parameters set from Wágner (2016) – RMSNE = 11,97
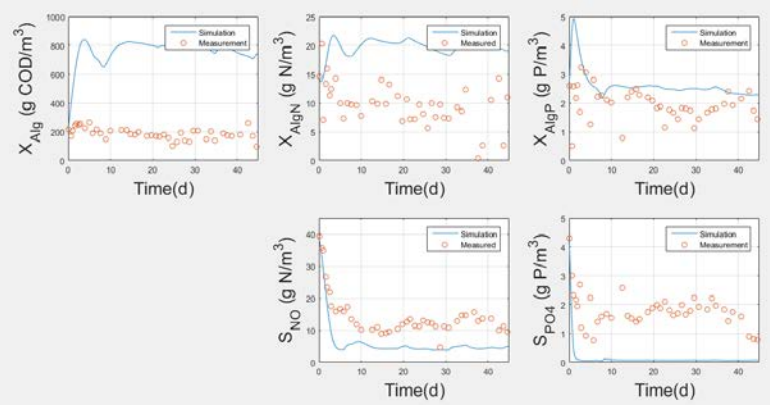
Simulation with the parameters set from 17-17 Batch - RMSNE = 9,13
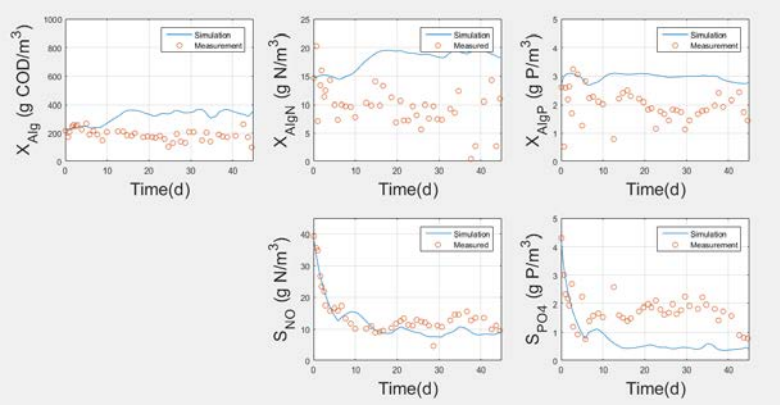
Simulation with the average parameters set - RMSNE = 8,74
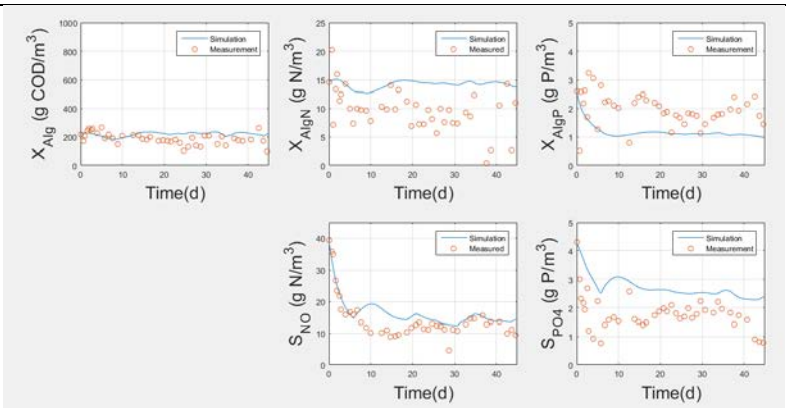

Figure 4-28 Simulations of Reactor 1 with different parameters sets

REACTOR 2

Simulation with the parameters set from Wágner (2016) – RMSNE = 27,32

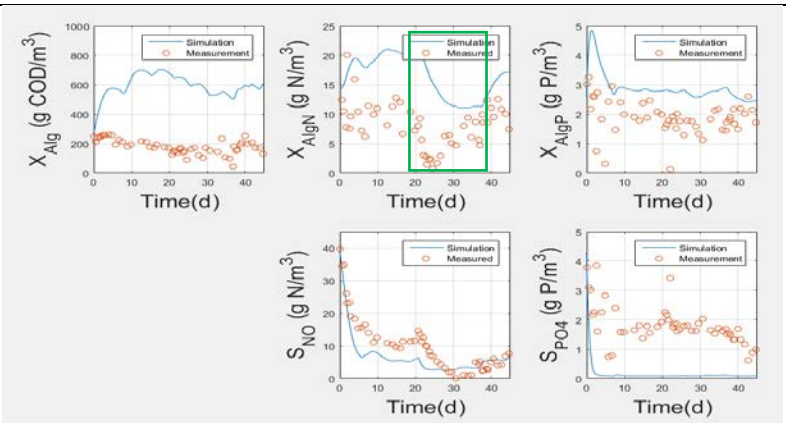

Simulation with:

- **Period 1 and period 2: the parameters set from 17-17 Batch**
- **Period 3: the parameters set from 10-17 Batch**

RMSNE = 23,32

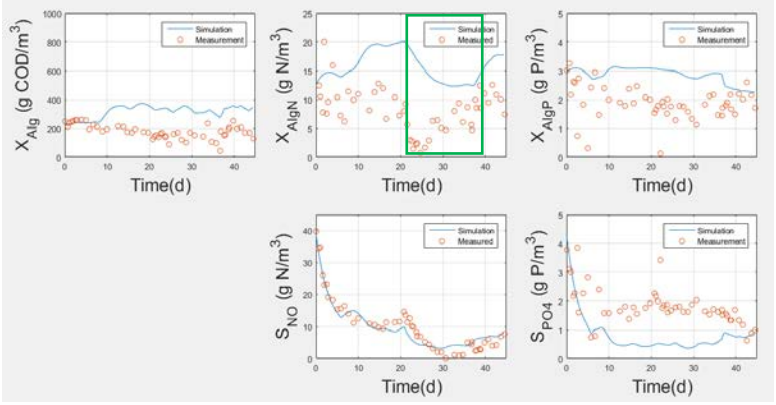

Simulation with the average parameters set - RMSNE = 22,6

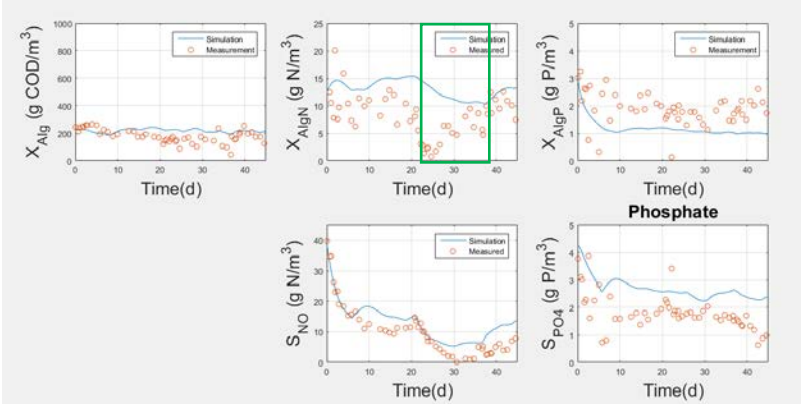

Figure 4-29 Simulations of Reactor 2 with different parameters set

4.5 Images analysis

4.5.1 Development of a new images analysis method

Two cultures were used to develop a new automated image analysis method aimed to quantify the microbial community. The two cultures had different composition:

1. A mixed green microalgae culture containing mostly *Chlorella sp.* and *Scenedesmus sp.* ;
2. A monoculture containing uniquely *Chlorella sp.*.

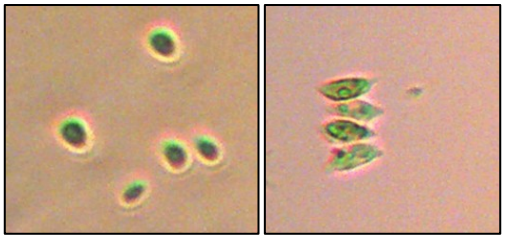

Figure 4-30 On the left a picture of *Chlorella sp.*, on the right a picture of *Scenedesmus sp.*

The different green microalgae types were distinguished according to their morphology, i.e. *Chlorella sp.* (shape: round and small individual cells) and *Scenedesmus sp.* (shape: elongated cells grown in four-cell colonies). As reported in *Materials and methods - Microscopy and image analysis*, images were taken using a Motic AE31 microscope with a magnification of 20x. 60 images were obtained for the mixed culture, two sets of 30 images were instead obtained for the monoculture.

To distinguish between the genera, morphological descriptors (area, diameter or the aspect ratio) of each type were automatically acquired using the image analysis software Image pro plus 7 3D suite (USA). The morphological descriptors are case specific. Same species in different culture may need different morphological descriptors. Therefore, it is suggested to calibrate them every time a new culture is studied. Thanks to this software, the number of cells for each group of green microalgae were easily counted.

In both cases the minimum image number required to yield a representative average cells count was assessed. The minimum number was found as the one for which an additional image gives a margin of improvement of less than 5%.

As shown in Figure 4-31 and Figure 4-32, different results were found for the mixed culture and the monoculture. The minimum number of images necessary to quantify the number of cells in a mixed culture was found to be 17. Instead, the minimum number of images necessary to quantifiy the number of cells in a monoculture was 10.

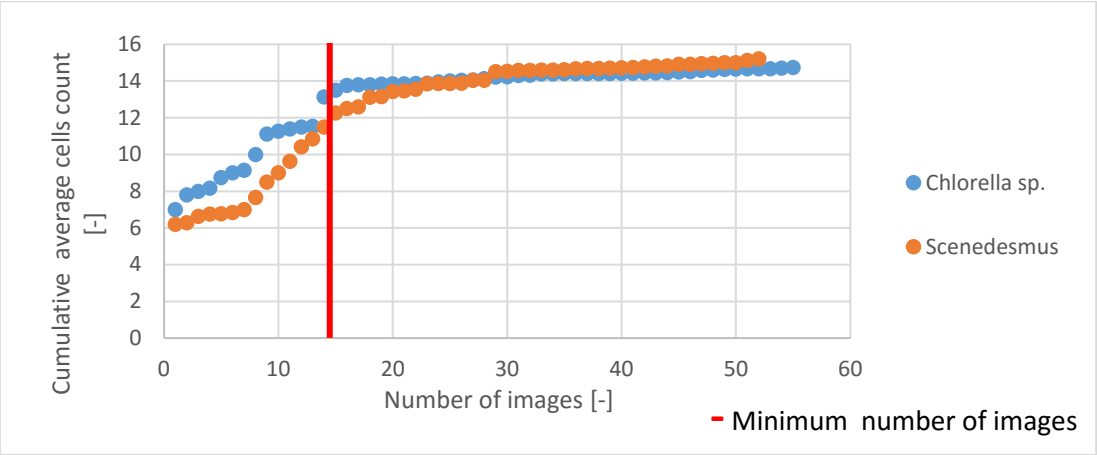

Figure 4-31 Cumulative average cells count for mixed culture of *Chlorella sp.* and *Scenedesmus sp.*

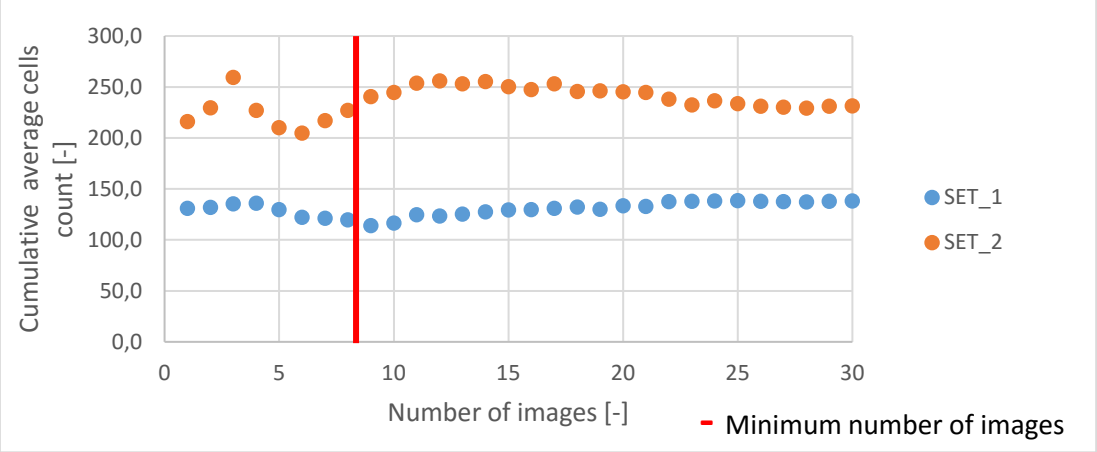

Figure 4-32 Cumulative average cells count for monoculture of *Chlorella sp.*

4.5.2 Application of the new images analysis method to two continuous flow PBRs

The new images analysis method described in the previous paragraph was applied on the main experiment carried out in this work, i.e. the 2 continuous PBRs.

Indeed, one of the goals of this experiment was to assess the effects of the variation of the input N-to-P ratio on the green microalgae culture in terms of composition and unexpected contaminations.

Approximately every second day 10 images were taken for the PBRs and they were analyzed as previously explained.

Only *Chlorella sp*. was found in the reactors for about 45 days, i.e. for the entire length of the experiment. Therefore, the culture did not change and no contamination occurred. This probably means that a healthy culture is strong enough to compete against other potential microorganisms that enter into the PBR through the wastewater, even when it is subject to variation in the N-to-P ratio. This is important when we consider cultivation of microalgae in open systems on wastewater, where culture stability is considered to be an issue.

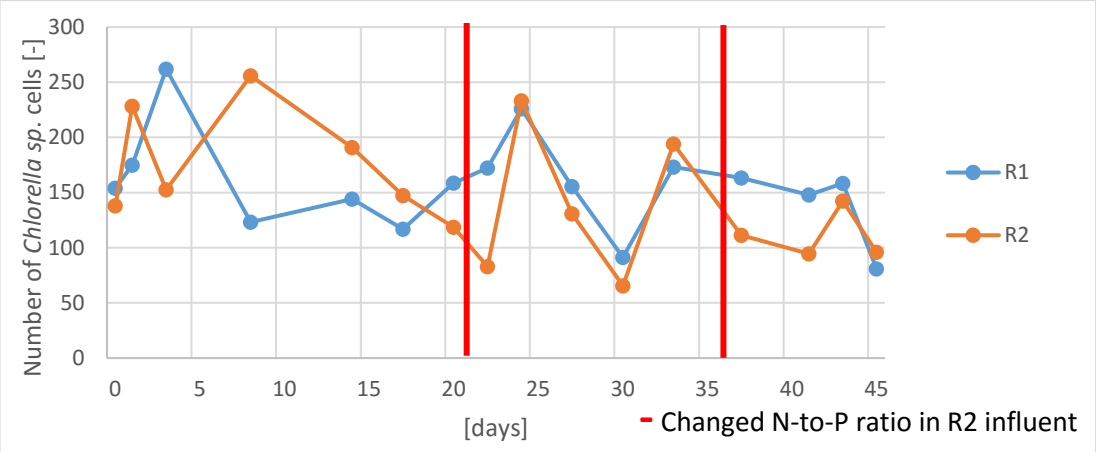

Figure 4-33 Number of *Chlorella sp*. cells along the experiment in R1 and R2

As already highlighted by other parameters for the measurement of the biomass, i.e. TSS and OD, are no significant changes ae observed in the biomass when the N-to-P ratio is changed. Indeed, as shown in Figure 4-33, the number of cells in R1 e R2 remained almost equal during the experiment.

The reliability of the measurement was assessed comparing the OD measurement with the relative number of Chlorella sp. cells found through the new method (Figure 4-34). Although in the plot some scattering is shown, the two measurements can be considered correlated.

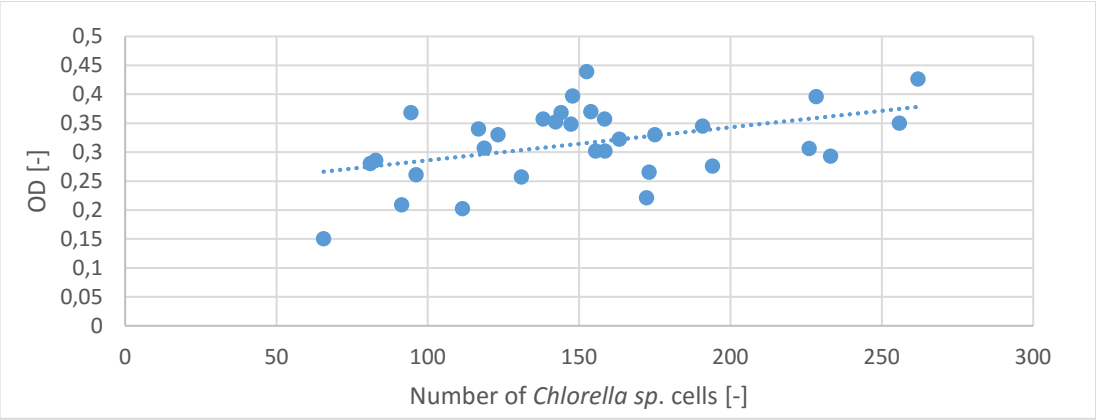

Figure 4-34 OD vs Number of Chlorella sp. cells to assess the reliability of the measurement

Chapter 5
CONCLUSION

During this study, experiments on the cultivation of green microalgae in wastewater were conducted.

1. Starting from the problems pointed out in Valverde-Pérez et al. (2015) about the variation of the medium composition in input to the PBRs in the TRENS, the consequensis on microalgae culture of changings in the influent N-to-P ratio were investigated. The results obtained revealed that the culture stability was not affected. Indeed, the culture composition was maintained and no contaminations occurred. Moreover, microalgae were able to keep a certain level of biomass along the experiment, showing the ability to reestablish it when subjected to limited variations in the N-to-P ratio. Regarding the efficiency of nutrients removal from the wastewater, it was found that the overall nitrogen removal was enhanced when microalgae were subjected to a period of nitrogen limitation. Instead, no effects on the overall phosphorus removal were observed. Finally, the variability of the N-to-P ratio in input to the PBRs reported by Valverde-Pérez et al. (2015) might not compromise the operation of the system.
2. The effects of the culture history on the on the kinetics of microalgae processes were investigated and from this study no relevant influence was found. From the kinetic parameters sets estimated to assess the effects of the culture history, it was possible to obtain an average parameters set, that used in the ASM-A model, gives the best results for prediction of the two continuous flow PBRs run in this work. Therefore, estimating an average parameters set, it may be possible to model a continuous flow PBRs, even if it is subjected to an unstable influent composition in term of nutrients content.
3. The new automated image analysis method developed during this work was tested on the experiments conducted and it was found to be able to identify different microalgae species and to quantify them.

Chapter 6
RECOMMENDATIONS

Based on the work done and the results obtain, few recommendations are here suggested:

1. Further investigating the possibility to enhance the removal of nitrogen exposing the green microalgae culture to cycle of nitrogen starvation in a continuous flow PBR;
2. Studying the effects on the green microalgae culture when it is exposed to phosphorus limitation to assess the possibility to improve its removal as observed for nitrogen;
3. Improving the model prediction when the culture is subjected to nitrogen limitation.
4. Assessing the effects of culture history on the uptake and storage of N and P in case of mixed culture;
5. Investigating the causes of the unexpected gap in the nitrogen mass balance found in the continuous flow PBRs experiment;
6. Testing the new image analysis method on cultures with different microalgae species.

References

[1] Cai , T., Park , S. . Y. & Li, Y., 2013. Nutrient recovery from wastewater streams by microalgae: Status and prospects. *Renewable and Sustainable Energy Reviews,* Volume 19, pp. 360-369.

[2] Christensen, T. B. & Hauggaard-Nielsen, H., 2015. *Circular Economy - A review of the concept and examples of emerging practices.* Sitges, s.n.

[3] Abdel-Raouf, N., Al-Homaidan, A. & Ibraheem, I., 2012. Microalgae and wastewater treatment. *Saudi Journal of Biological Sciences,* Volume 19, pp. 257-275.

[4] Ambrose, R., 2006. *Wasp7 benthic algae-model theory and users guide.* Athens, Georgia: USEPA, Office of research and development.

[5] Apples, L., Baeyens, J., Degrève, J. & Dewil , R., 2008. Principles and potential of the anaerobic digestion of waste-activated sludge. *Progress in Energy and Combustion Science,* Volume 34, pp. 755-781.

[6] Arbib, Z. et al., 2013. Photobiotreatment: Influece of nitrogen and phosphorus ratio in wastewater on growth kinetics of Scenedesmus Obliquus. *International Journal of Phytoremediation,* Volume 15, pp. 774-788.

[7] Arbib, Z. et al., 2013. Photobiotreatment: Influence of Nitrogen and Phosphorus ratio in wastewater on growth kinetics of Scenedesmus Obliquus. *International Journal of Phytoremediation,* Volume 15, pp. 774-788.

[8] Azov, Y., 1982. Effect of pH on Inorganic Carbon Uptake in Algal Cultures. *Applied and Enviromental Microbiology,* 43(6), pp. 1300-1306.

[9] Azov, Y. & Goldman, J., 1982. Free ammonia inhibition of algal photosynthesis in intensive cultures. *Applied and Environmental Microbiology,* 43(4), pp. 735-739.

[10] Benavente-Valés, J. R. et al., 2016. Strategies to enhance the production of photosyntetic pigments and lipids in chlorophycae species. *biotechnology Reports,* Volume 10, pp. 117-125.

[11] Benson, B., Gutierrez-Wing, M. & Rusch, K., 2007. The development of a mechanistic model to investigate the impacts of the light dynamics on algal productivity in a Hydraulically Integrated Serial Turbidostat Algal Reactor (HISTAR). In: s.l.:Aquacultural Engineering, pp. 198-211.

[12] Bernard, O., 2011. Hurdles and challenges for modelling and control of microalgae fo CO2 mitigation and biofuel production. *Journal of Process Control,* Volume 21, pp. 1378-1389.

[13] Beuckles, A., Smolders, E. & Muylaert, K., 2015. Nitrogen availability influences phosphorus removal in microalagae-based wastewater treatment. *Water Research*, Volume 77, pp. 98-106.

[14] Bezzera, R. et al., 2013. Fed-batch cultivation of Arthrospira platensis using carbon dioxide from alcoholic fermentation and urea as carbon and nitrogen sources. *Bioenergy Research*, pp. 1-8.

[15] Boussiba, S., 1989. Ammonia uptake in the alkalophilic cyanobacterium Spirulina platensis. *Plant and Cell Physiology*, 30(2), pp. 303-308.

[16] Boussiba, S. & Gibson, J., 1991. Ammonia translocation in cyanobacteria. *FEMS Microbiology Letters*, 88(1), pp. 1-14.

[17] Broekhuizen, N., Park, J., McBride, G. & Craggs, R., 2012. Modification, calibration and verification of the IWA River Water Quality Model to simulate a pilot-scale high rate algal pond. *Water Research*, Volume 46, pp. 2911-2926.

[18] Brown, L., 1981. World population growth, soil erosion, and food security.. *Science*, 214(4524), pp. 995-1002.

[19] Brussaard, C., Brookes, R., Noordeloos, A. & Riegman, R., 1998. Recovery of nitrogen-starved cultures of the diatom Ditylum brightwellii (Bacillariophyceae) upon nitrogen resupply. *Journal of Experimental Marine Biology and Ecology*, 227(2), pp. 237-250.

[20] Cai, T., Park, S. & Li, Y., 2013. Nutrient recovery from wastewater streamns by microalgae: status and prospects. *Renewable Sustainable Energies Reviewa*, Volume 19, pp. 360-369.

[21] Carballa, M., Regueiro, L. & Lema, J., 2015. Microbial management of anaerobic digestion: exploiting the microbiome-functionality nexus. *Current Opinion in Biotechnlogy*, Volume 33, pp. 103-111.

[22] Carey, R. O. & Migliaccio, K. W., 2009. Contribution of Wastewater Treatment Plant Effluents to Nutrient Dynamics in Aquatic System: A Review. *Environmental Management*, Volume 44, pp. 205-217.

[23] Chi, Z., O'Fallon, J. & Chen, S., 2011. Bicarbonate produced from carbon capture for algae culture. *Trends in Biotechnology*, 29(11), pp. 537-541.

[24] Chi, Z., Zheng, Y., Jiang, A. & Chen, S., 2011. Lipid production by culturing oleaginous yest and algae with wood waste and municipal wastewater un an integrated process. *Applied Biochemestry and Biotechnology*, Volume 165, pp. 442-453.

[25] Choi, H. J. & Lee, S. M., 2015. Effect of the N/P ratio on biomass productivity and nutrient removal from municipal wastewater. *Bioprocess Biosystem Engineering*, 38(4), pp. 761-766.

[26] Cohen, J. E., 1995. Population Growth and Earth's Human Carrying Capacity. *Science*, 269(5222), pp. 341-236.

[27] Colak, O. & Kaya, Z., 1988. A study on the possibilities of biological wastewater treatment using algae. *Doga Biyolji Serisi*, 12(1), pp. 18-29.

[28] CSS, 2015. *U.S. Water Supply and Distribution Factsheet*. s.l.:s.n.

[29] De la Noüe, J. & De Pauw, N., 1988. The potential of microalgal biotechnology. A review of production and uses of microalgae. *Biotechnology Advances,* Volume 6, pp. 725-770.

[30] De Mes, T., Stams, A., Reith, J. & Zeeman, G., 2003. Methane production by anaerobic digestion of wastewater and solid wastes. In: *Bio-methane & Bio-hydrogen*. s.l.:s.n., pp. 58-102.

[31] Decostere, B. et al., 2013. A combined respirometer-titrimeter for the determination of microalgae kinetics: experimental data collection and modelling. *Chemical Engineering Journal,* Volume 222, pp. 85-93.

[32] Doria, E. et al., 2012. Isolation and characterization of a Scenedesmus acutus strain to be used for bioremediation of urban wastewater. *Applied Phycology,* Volume 24, pp. 375-383.

[33] Droop, M., 1973. Some thoughts on nutrient limitation in algae. *Journal of Phycology,* 9(3), pp. 264-272.

[34] Dyhrman, S. & Ruttenberg, K., 2006. Presence and regulation of alkaline phosphatase activity in eukaryotic phytoplankton from the coastal ocean: Implications for dissolved organic phosphorus remineralization. *Limnology and Oceanography,* 51(3), pp. 1381-1390.

[35] Eixler, S., Karsten, U. & Selig, U., 2006. Phosphous storage in Chlorella Vulgaris (Trebouxiophycae, Chlorophyta) cells and its dependence on phosphate supply. *Phycologia,* 45(1), pp. 53-60.

[36] El-Sheek, M. M. & Rady, A. A., 1995. Effect of phosphorus starvation on growth, photosynthesis and some metabolic processess in the unicellular green algae Chlorella kessleri. *Phyton,* Volume 35, pp. 1139-1151.

[37] Evonne, P. & Tang, 1997. Polar cyanobacteria versus green algae for tertiary waster treatment in cool climates. *Journal of Applied Phycology*, Volume 9, pp. 371-381.

[38] Fachet, M., Flassig, R., Rinhko-Struckmann, L. & Sundmacher, K., 2014. A dynamic growth model of Dunaliella salina: Parameter identification and profile likelihood analysis.. *Bioresource Technology*, Volume 173, pp. 21-31.

[39] Fang, L. et al., 2015. Life cycle assessment as development and decision support tool for wastewater resource recovery technlogy. *Waster Research*, Volume 88, pp. 538-459.

[40] FAO, 2016. *FAOSTAT*. [Online] Available at: http://faostat3.fao.org/browse/E/EL/E [Consultato il giorno July 2016].

[41] Flores, E. & Herrero, A., 2005. Nitrogen assimilation and nitrogen control in cyanobacteria. *Biochemical Society Transactions,* 33(1), pp. 164-167.

[42] Flores, E., Herrero, A. & Miguel, G., 1987. Nitrite uptake and its regulation in the cyanobacterium Anacystis nidulans. *Biochimica et Biophysica Acta (BBA),* 896(1), pp. 103-108.

[43] Fuggi, A., 1993. Uptake and assimilation of nitrite in the acidophilic red alga Cyanidium caldarium Geitler. *New Phytologist,* 125(2), pp. 351-360.

[44] Geider, R. J. & La Roche, J., 2002. Redfield revisited: variability of C:N:P in marine microalae and its biochemical basis. *European Journal of Phycology*, Volume 37, pp. 1-17.

[45] Graham, L. & Wilcox, L., 2000. *Algae.* Upper Saddle River, NJ: Prentice Hall.

[46] Grima, J. et al., 1994. A mathematical model for microalgal growth in light-limited chemostat culture. *Journal Chemical Technology and Biotechnology*, Volume 61, pp. 167-173.

[47] Grognard, F., Akhmetzhanov, A. & Bernard, O., 2014. Optimal strategies for biomass productivity maximization in a photobioreactor using natural light. *Automatica,* Volume 50, pp. 359-368.

[48] Guillard, R. & Lorenzen, C., 1972. Yellow-Green algae with chlorophyllide. *Water Science and Technology*, 61(4), pp. 825-839.

[49] Hauduc, H. et al., 2015. Efficiency criteria for environmental model quality assessment: a review and its applications to wastewater treatment. *Environmental modelling and software,* Volume 68, pp. 196-204.

[50] Helton, J. & Davis, F., 2003. Latin hypercube sampling and propagation of uncertainty in analyses of complex systems. *Reliability Engineering and System Safety,* Volume 81, pp. 23-69.

[51] Henze, M. & Comeau, Y., 2008. Wastewater Characterization. In: *Biological Wastewater Treatment: Principles Modelling and Design.* London: IWA Publishing, pp. 33-52.

[52] Henze, M., Gujer, W., Mino, T. & van Loosdrecht, M., 2000. *Activated sludge models ASM1, ASM2, ASM2d and ASM3.* s.l.:IWA Publishing.

[53] Hernandez, J.-P., de-Bashan, L. E. & de-Bashan, Y., 2006. Starvation enhances phosphorus removal from wastewater by the microalga Chlorella spp. coimmobilized with Azospirillum brasilense. *Enzyme and Microbial Technology*, Volume 38, pp. 190-198.

[54] Ispra, 2014. *Rapporto rifiuti Urbani,* Roma: ISPRA - Settore Editoria.

[55] Jeanfils, J., Canisius, M. & Burlion, N., 1993. Effect of high nitrate concentrations on growth and nitrate uptake by free-living and immobilized Chlorella vulgaris cells. *Journal of Applied Phycology*, 5(3), pp. 369-374.

[56] Kadam, K. L., 1997. Power plant flue gas as a source of CO2 for microalgae cultivation: Economic impact of different process options. *Energy Conversion and Managment,* Volume 38, pp. 505-510.

[57] Källqvist, T. & Svenson, A., 2003. Assessment of ammonia toxicity in tests with the microalga, Nephroselmis pyriformis, Chlorophyta. *Water Research,* 37(3), pp. 477-484.

[58] Khin, T. & Annachhatre, A. P., 2004. Novel microbial nitrogen removal process. *Biotechnology Advances,* Volume 22, pp. 519-532.

[59] Larsson, T. & Skogestad, S., 2000. Plantwide control - a review and a new design procedure.. *Journal of Modeling, Identification and Control,* 21(4), pp. 209-240.

[60] Lavoie, A. & De la Noue, J., 1985. Hyperconcentrated cultures of Scenedesmus obliquus. A new approach for wastewater biological tertiary treatment. *Water Research,* Volume 19, pp. 1437-1442.

[61] Lincon, E. & Hill, D., 1980. An integrated microalgae system. *Algae Biomass,* pp. 229-243.

[62] Liu, J. & Vyverman, W., 2014. Differences in nutrient uptake capacity of the benthic filamentous algae Cladophora sp., Klebsormidium sp. and Pseudanabaena sp. under varying N/P conditions. *Bioresource Technology,* Volume 179, pp. 234-242.

[63] Liu, J. & Vyverman, W., 2015. Differences in nutrient uptake capacity of the benthic filamentous algae Cladophora sp., Klebsormidium sp. and Pseudanabaena sp. under varying N/P conditions. *Bioresource Technology,* Volume 179, pp. 234-242.

[64] Li, X., Hu, H.-y., Gan, K. & Sun, Y.-x., 2010. Effects of different nitrogen and phosphorus concentrations on the growth, nutrient uptake, and lipid accumulation of a freshwater microalga Scenedesmus sp.. *Bioresource Technology,* Volume 101, pp. 5494-5500.

[65] Li, Y. et al., 2011. Characterization of microalga Chlorella sp. well adapted to highly concentrated municipal wastewater for nutrient removal and biodiesel production. *Bioresource Technology,* Volume 102, pp. 5138-5144.

[66] Loladze, I. & Elser, J., 2011. The origins of the Redfield Nitrogen-to-Phosphorus ratio are in a homoeostatic protein-to-rRNA ratio. *Ecology Letters,* 14(3), pp. 244-250.

[67] Malerba, A., Connolly, S. & Heimann, K., 2012. Nitrate-nitrite dynamics and phytoplankton growth: formulation and experimental evaluation of a dynamic model. *Linmology and Oceanography,* 57(5), pp. 1555-1571.

[68] Markou, G. & Georgakakis, D., 2011. Cultivation of filamentous cyanobacteria (blue-green algae) in agro-industrial wastes and wastewaters: a review. *Applied Energy,* Volume 88, pp. 3389-3401.

[69] Markou, G., Vandamme, D. & Muylaert, K., 2014. Microalgae and cyanobacterial cultivation: The supply of nutrients. *Water research,* Volume 65, pp. 186-202.

[70] Martin, C., De la Noue, J. & Picard, G., 1985a. Intensive culture of freshwater microalgae on aerated pig manure. *Biomass,* Volume 7, pp. 245-259.

[71] Means, E., 2004. *Water and Wastewater Industry Energy Efficiency: A Reasearch Roadmap,* Sacramento: Awwa REsearch Foundation.

[72] Metcalf&Eddy, I. et al., 2014. *Wastewater Engineering: Treatment and Resource Recovery*. 5th a cura di s.l.:McGraw-Hill's.

[73] Mino, T., van Loosdrecht, M. & Heijen, J., 1998. Microbiology and biochemestry of the enhanced biological phosphate removal process. *Water Research,* 32(11), pp. 3193-3207.

[74] Moawad, S., 1968. Inhibition of coliform bacteria by algal population in micooxidation ponds. *Environmental Health,* Volume 10, pp. 106-112.

[75] Mo, W. & Zhang, Q., 2012. Can municipal wastewater treatment systems be carbon neutral?. *Journal of Environmental Management.*

[76] Mühling, M., Belay, A. & Whitton, B., 2005. Screening Arthrospira (Spirulina) strains for heterotrophy. *Journal of Applied Phycology,* 17(2), pp. 129-135.

[77] Mujtaba, G., Choi, W., Lee, C.-G. & Lee, K., 2012. Lipid production by Chlorella vulgaris after a shift from nutrient rich to nitrogen starvation conditions. *Bioresource Technology,* Volume 123, pp. 279-283.

[78] Mulbry, W., Kondrad, S., Buyer, J. & Luthria, D., 2009. Optimization of an oil extraction. *Journal of the American Oil Chemists' Society,* Volume 101, pp. 3097-3105.

[79] Mulbry, W., Kondrad, S., Pizzaro, C. & Kebede-Westhead, E., 2008. Treatment of dairy manure effluent using freshwater algae: algal productivity and recovery of manure nutrients using pilot-scale algal turf scrubbers. *Bioresource Technology,* Volume 99, pp. 8137-8142.

[80] Mulbry, W., Westhead, E., Pizarro, C. & Sikora, L., 2005. Recycling of manure nutrients: use of algal biomass from diary manure treatment as a slow release fertilizer. *Bioresource Technology,* Volume 96, pp. 451-458.

[81] Mutlu, A., Vangsgaard, A., Sin, G. & Smets, B., 2013. An operational protocol for facilitating star-up of single-stage autotrophic nitrogen-removing reactors based on process stoichiometry. *Water Science and Technology,* 68(3), pp. 514-521.

[82] Muttamara, S., 1996. Wastewater characteristics. *Resources, Conservation and Recycling,* 16(1-4), pp. 145-159.

[83] Napan, K., Teng, L., Quinn, J. & Wood, B., 2015. Impact of heavy metals from flue gass integration with microalgae production. *Algal Research,* Volume 8, pp. 83-88.

[84] Nelder, J. & Mead, R., 1965. A simplex-method for function minimization. *The Computer Journal,* 7(4), pp. 308-313.

[85] Norton, T. A., Melkonian, M. & Andersen, R. A., 1996. Algal biodiversity. *Phycologia,* 35(4), pp. 308-326.

[86] Ortiz-Ospina, E. & Roser, M., 2016. *Our World in Data.* [Online] Available at: https://ourworldindata.org/world-population-growth/

[87] Oswald, W., 1988b. Micro-algae and wastewater treatment. *Microa-algal Biotechnology,* pp. 357-394.

[88] Oswald, W. & Gotaas, H., 1957. Photosynthesis in sewage treatment. *Transactions of the American Society of Civil Engineers,* Volume 122, pp. 73-105.

[89] Park, J. et al., 2010. Ammonia removal from anaerobic digestion effluent of livestock waste using green alga Scenedesmus sp. *Bioresource Technology,* 101(22), pp. 8649-8657.

[90] Pérez-Garcia, O., Escalante, F., De-Bashan, L. & Bashan, Y., 2011. Heterotrophic cultures of microalgae: metabolism and potential products. *Water Research,* Volume 45, pp. 11-36.

[91] Plosz, B. G. & Polesel, F., 2015. *Characterising the Removal of Trace Organic Chemicals in Wastewater - Are we using the Right Tools?*. Singapore, s.n.

[92] Podevin, M., De Francisci, D., Holdt, S. L. & Angelidaki, I., 2015. Effect of nitrogen source and acclimatization on specific growth rates of microalgae determined by a high-throughput in vivo microplate autofluorescence method. *Journal of Applied Phycology,* 27(4), pp. 1415-1423.

[93] Polesel, F., Plosz, B. G. & Trapp, S., 2015. From consumption to harvest: environmental fate prediction of excreted ionizable trace organic chemicals. *Water Research,* Volume 84, pp. 85-98.

[94] Posten, C. & Walter, C., 2012. *Microalgal biotechnology: potential and production*. Berlin: Posten, Clemens; Walter, Christian;.

[95] Powell, N., Shilton, A., Chisti, Y. & Pratt, S., 2009. Towards a luxury uptake process via microalgae – Defining the polyphosphate dynamics. *Water Research,* 43(17), pp. 4207-4213.

[96] Pueschel, C. M. & Korb, R. E., 2001. Storage of nitrogen in the form of protein bodies in the kelp Laminaria solidungula. *Marine Ecology Progress Series,* Volume 218, pp. 107-114.

[97] Rai, L., Gour, J. & Kumar, H., 1981. Phycology and heavy metal pollution. *Biological Reviews,* Volume 56, pp. 99-151.

[98] Randall, C., Barnard, J. & Stensel, H., 1998. *Design and retrofit of wastewater treatment plants for biological nutrient removal.* s.l.:Technomic Publishing Co.

[99] Redfield, A., 1934. On the proportions of organic derivatives in sea water and their relation to the composition of plankton. In: *James Johnstone Memorial Volume.* Liverpool: s.n., pp. 177-192.

[100] Renuka, N. et al., 2013. Evaluation of microalgal consortia for treatment of primary treated sewage effluent and biomass production. *Applied Phycology,* Volume 25, pp. 1529-1537.

[101] Rhee, G.-Y., 1978. Effects of N:P atomic ratios and nitrate limitation on algae growth, cell composition, and nitrate uptake. *Limnology and Oceanography,* 23(1), pp. 10-25.

[102] Ruitz-Martinez, A. et al., 2014. Mixed microalgae culture for ammonium removal in the absence of phosphorus: effect of phosphorus supplementation and process modellin. *Process Biochemistry,* Volume 49, pp. 2249-2257.

[103] Sebastian , S. & Nair, K., 1984. Total removal pf coliforms and E.coli from domestica sewage by high-rate pond mass culture of Scenedesmus obliquus. *Environmental Pollution (Serie A),* Volume 34, pp. 197-206.

[104] Sebog, D., Edgar, T. & Mellichamp, D., 2004. *Process Dynamics and Control.* Seconda edizione a cura di s.l.:John Wiley and Sons Inc..

[105] Seung-Hoon, L. et al., 2013. Increased Microalgae Grwth and Nutrient Removal Using Balanced N:P Ratio in Wastewater. *Journal of Microbiology and Biotechnology,* 23(1), pp. 92-98.

[106] Seyfabadi, J., Ramezanpour, Z. & Khoeyi, Z. A., 2011. Protein, fatty acid and pigment content of Chlorella vulgaris under different light intensities.. *Journal of Applied Phycology*, Volume 23, pp. 721-726.

[107] Shelef, G., Azov, Y., Moraine, R. & Oron , G., 1980. Algal mass production as an integral part of wastewater treatment and reclamation system in algal biomass. *Elsevier*, pp. 163-190.

[108] Sin, G., Mayer, A. & Gernaey, K., 2010. Assessing reliability of cellulose hydrolisis models to support biofuel process design - Identifiability and uncertainty analysis. *Computers and Chemical Engineering*, Volume 34, pp. 1385-1392.

[109] Skogestad, S., 2003. Simple analytic rules for model reduction and PID controller tuning. *Journal of Process Control,* Volume 12, pp. 291-309.

[110] Smith, R. T., Bangert, K., Wilkinson, S. W. & Gilmour, J. D., 2015. Synergistic carbon metabolism in a fast growing mixotrophic freshwater microalgae species Micractinium inermum. *Biomass and Bioenergy*, Volume 82, pp. 73-86.

[111] Sorokin , C. & Krauss, R. W., 1958. The Effects of Light Intensity on the Growth Rates of Green Algae. *Plant Physiology,* 33(2), pp. 109-113.

[112] Spaargaren, D., 1996. The desig of culture media based on the elemental composition of biological material. *Journal of Biotechnology,* 45(2), pp. 97-102.

[113] Spaargeren, D. H., 1996. The design of culture media based on the elemental composition of biological material. *Journal of Biotechnology,* 45(2), pp. 97-102.

[114] Steele, J., 1962. Environmental control of photosynthesis in the sea. *Limnology and Oceanography,* Volume 7, pp. 137-150.

[115] Suttle, C. A. & Harrison, J., 1988. Ammonium and phosphate uptake rates, N:P supply ratios, and evidence for N and P limitation in some oligotrophic lakes. *Limnology and Oceanography,* 33(2), pp. 186-202.

[116] Talbot, P. & De la Noue, J., 1993. Tertiary treatment of wastewater with Phormidium bohneri (Schmidle) under various light ad temperature conditions). *Water Research,* 27(1), pp. 153-159.

[117] Tam, N. & Wong, Y., 1989. Wastewater treatment nutrient removal by Chlorella pyrenoidosa and Scenedesmus sp.. *Enironmental Pollution,* Volume 58, pp. 19-34.

[118] Travieso, L., Sànchez, E., Benitez, F. & Conde, J., 1993. Arthospira sp. intensive cultures for food and biogas purification. *Biotechnology Letters,* 15(10), pp. 1091-1094.

[119] Valverde Pérez, B. et al., 2016. Control structure design for resource recovery using the enhanced biological phosphorus removal and recovery (EBP2R) activated sludge process. *Chemical Engineering Journal,* Volume 296, pp. 447-457.

[120] Valverde-Pérez, B. et al., 2015. *Control Structure Design for an EbP2R Process Operated as a Sequencing Batch Reactor*. s.l.:s.n.

[121] Valverde-Pérez, B., Plosz, B. G. & Smets, B. F., 2015. *Wastewater resource recovery via the Enhanced Biological Phosphorus Removal and Recovery (EBP2R) process coupled with green microalgae cultivation*. Kgs. Lyngby: s.n.

[122] Van Daele, T. et al., 2015. A numerical procedure for model identifiability analysis applie to enzyme kinetics. *Computer Aided Process Engineering,* Volume 37, pp. 575-580.

[123] Van Loosdrecht, M. & Henze, M., 1999. Maintenance, endogeneous respiration, lysis, decay and predation. *Water Science and Technology,* 39(1), pp. 107-117.

[124] Van Wagenen, J., De Francisci, D. & Angelidaki, I., 2015. Comparision of mixotrophic to cyclic autotrophic/heterotrophic growth strategies to optimize productivity of Chlorella sorokiniana. *Journal of Applied Phycology,* Volume 27, pp. 1775-1782.

[125] Van Wagenen, J. et al., 2012. Effects of light and temperature on fatty acid production in Nannochloropsis salina. *Energies,* Volume 5(3), pp. 731-740.

[126] Wagner, D. S. et al., 2016. Towards a consensus-based biokinetic model for green microalgae - The ASM-A. *Water Research,* p. DOI.

[127] Wagner, D. S. et al., 2014. *The effect of light on mixed green micro-algae growth - experimental assessment and modelling*. Lisbon, IWA World Water Congress and Exhibition.

[128] Wang, L. et al., 2010. Cultivation of green algae Chlorella sp. in different wastewaters from municipal wastewater treatment plant. *Applied Biochemestry and Biotechnology,* Volume 162, pp. 1174-1186.

[129] Whitton, R. et al., 2016. Influence of microalgal N and P composition on wastewater nutrient remediation. *Water Research,* Volume 91, pp. 371-378.

[130] Wilkie, A. C. & Mulbry, W. W., 2002. Recovery of dairy manure nutrients by benthic freshwater algae. *Bioresource Technology,* 84(1), pp. 81-91.

[131] Wolf, G., Picioreanu, C. & van Loosdrecht, M., 2007. Kinetic modeling of phototrophic biofilms: the PHOBIA model. *Biotechnology and Bioengineering,* 97(5), pp. 1064-1079.

[132] Yeh, K.-L., Chang, J.-S. & Chen, W.-M., 2010. Effect of light supply and carbon source on cell growth and cellular composition of a newly isolated microalga Chlorella vulgaris ESP-31. *Engineering in Life Sciences,* 10(3), pp. 201-208.

[133] Young, E. B. & Beardall, J., 2003. Photosynthetic function in Dunaliella Tertiolecta (Chlorophyta) during a nitrogen starvation and recovery cycle. *Journal of Phycology*, 39(5), pp. 897-905.

[134] Zhao, S. et al., 2006. Land use change in Asia and the ecological consequences. *Ecological Research*, 21(6), pp. 890-896.